

Bill Davis

NATIONAL ACADEMY OF SCIENCES
NATIONAL RESEARCH COUNCIL
of the
UNITED STATES OF AMERICA

UNITED STATES NATIONAL COMMITTEE
International Union of Radio Science



1978 Spring Meeting
May 15 - 19

Held in conjunction with the

Institute of Electrical and Electronics Engineers
Society of Antennas and Propagation
International Symposium

University of Maryland
College Park, Maryland

Condensed Technical Program
USNC/URSI
15-19 May 1978

MONDAY, 15 MAY

	<u>Room</u>
<u>0900-1200</u>	
B-1 Electromagnetics	0105
B-2 SEM	0109
E-1 Lightning, Spherics and Noise (Joint with F and H)	1105
<u>1330-1700</u>	
B-3 Thin Wires	0105
B-4 Inverse Scattering and Profile Reconstruction	0109
E-2 CCIR Panel Discussion (Joint with F)	1105
F-1 Oceanography	1109
<u>1700</u>	
Commission E Business Meeting	1105
<u>1715</u>	
Commission B Business Meeting	0105

TUESDAY, 16 MAY

<u>0830-1200</u>	
B-5 Scattering	0109
C-1 Impairments to Earth-Satellite Transmission	1101
F-2 Remote Sensing of the Atmosphere from Space	1109
<u>1330-1700</u>	
B-6 Transmission Lines	0109
C-2 System Aspects of Antennas and Dual Polarization Transmission	1101
F-3 Scattering by Random Media and Rough Surfaces (Joint with AP-S and B)	1109
G-1 HF Radio Wave Absorption and Heating Effects	0123
<u>1700</u>	
Commission C Business Meeting	1101
Commission F Business Meeting	0123
Commission H Business Meeting	0123

(continued on inside back cover)

United States National Committee
INTERNATIONAL UNION OF RADIO SCIENCE

PROGRAM AND ABSTRACTS

1978 Spring Meeting

May 15-19

Held Jointly with

ANTENNAS AND PROPAGATION SOCIETY
INSTITUTE OF ELECTRICAL AND ELECTRONICS ENGINEERS

Washington, D.C.

NOTE:

Programs and Abstracts of the USNC/URSI Meetings are available from:

USNC/URSI
National Academy of Sciences
2101 Constitution Avenue, N.W.
Washington, D.C. 20418

at \$2 for meetings prior to 1970, \$3 for 1971-75 meetings, and \$5 for 1976-78 meetings.

The full papers are not published in any collected format; requests for them should be addressed to the authors who may have them published on their own initiative. Please note that these meetings are national and they are not organized by international URSI, nor are the programs available from the international Secretariat.

MEMBERSHIP

United States National Committee INTERNATIONAL UNION OF RADIO SCIENCE

Chairman:

Dr. John V. Evans, Lincoln Laboratory, M.I.T.*

Vice Chairman:

Dr. C. Gordon Little, Environmental Research Labs, NOAA*

Secretary:

Dr. James R. Wait, Environmental Research Labs, NOAA*

Editor:

Dr. Thomas B.A. Senior, University of Michigan

Immediate Past Chairman:

Dr. Francis S. Johnson, University of Texas, Dallas*

Members Representing Societies, Groups and Institutes:

American Astronomical Society	Prof. Gert Westerhout
American Geophysical Union	Dr. Christopher T. Russell
American Meteorological Society	Dr. David Atlas
Institute of Electrical & Electronic Engineering	Dr. Ernst Weber
IEEE Antennas & Propagation Society	Dr. Robert C. Hansen
IEEE Circuits & Systems Society	Dr. Mohammed S. Ghausi
IEEE Information Theory Group	Dr. Jack K. Wolf
Optical Society of America	Dr. Michael K. Barnoski

Liaison Representatives from Government Agencies:

National Science Foundation	Dr. W.K. Klemperer
Department of Commerce	Mr. Alan H. Shapley
National Aeronautics & Space Administration	Dr. Erwin R. Schmerling
Federal Communications Commission	(Vacant)
Office of Telecommunications Policy	Dr. John M. Kelso
Department of Defense	Mr. Emil Paroulek
Dept. of the Army	Mr. Allan W. Anderson
Dept. of the Navy	Dr. Leo Young
Dept. of the Air Force	Mr. Allan C. Schell

Ex-Officio Members:

Chairmen of the USNC-URSI Commissions:

Commission A	Dr. Ramon C. Baird
Commission B	Dr. Thomas A. Senior
Commission C	Dr. William F. Utlaut
Commission D	Dr. Kenneth J. Button
Commission E	Mr. George H. Hagn
Commission F	Dr. A.H. LaGrone
Commission G	Dr. Thomas E. VanZandt
Commission H	Dr. Frederick W. Crawford
Commission J	Dr. K.I. Kellermann

Officers of URSI resident in the United States:
(including Honorary Presidents)

Vice President	Prof. William E. Gordon*
----------------	--------------------------

Chairmen and Vice Chairmen of
Commissions of URSI resident
in the United States:

Chairman of Commission A	Dr. Helmut M. Altschuler
Chairman of Commission J	Prof. Gart Westerhout
Vice Chairman of Commission B	Prof. Leopold B. Felsen
Vice Chairman of Commission E	Mr. George H. Hagn
Vice Chairman of Commission F	Prof. Alan T. Waterman, Jr.
Vice Chairman of Commission H	Dr. Frederick W. Crawford

Foreign Secretary of the U.S.
National Academy of Sciences

Dr. George S. Hammond

Chairman, Office of Physical
Sciences-NRC

Dr. D. Allan Bromley

Honorary Members:

Dr. Harold H. Beverage
Prof. Arthur H. Waynick

NRC Staff Officer

Mr. Richard Y. Dow

* Member of USNC-URSI Executive Committee

DESCRIPTION OF
INTERNATIONAL UNION OF RADIO SCIENCE

The International Union of Radio Science is one of 18 world scientific unions organized under the International Council of Scientific Unions (ICSU). It is commonly designated as URSI (from its French name, Union Radio Scientifique Internationale). Its aims are (1) to promote the scientific study of radio communications, (2) to aid and organize radio research requiring cooperation on an international scale and to encourage the discussion and publication of the results, (3) to facilitate agreement upon common methods of measurement and the standardization of measuring instruments, and (4) to stimulate and to coordinate studies of the scientific aspects of telecommunications using electromagnetic waves, guided and unguided. The International Union itself is an organizational framework to aid in promoting these objectives. The actual technical work is largely done by the National Committees in the various countries.

The officers of the International Union are:

President:	Mr. J. Voge (France)
Immediate Past President:	Sir Granville Beynon (UK)
Vice Presidents:	Prof. W.N. Christiansen (Australia) Prof. W.E. Gordon (USA) Prof. V.V. Migulin (USSR) Prof. F.L.H.M. Stumpers (Netherlands)
Secretary General:	Dr. C.M. Minnis (Belgium)
Honorary Presidents:	B. Decaux (France) W. Dieminger (West Germany) J.A. Ratcliffe (UK) R.L. Smith-Rose (UK)

The Secretary's office and the headquarters of the organization are located at Rue de Nieuwenhove, 81, B-1180 Brussels, Belgium. The Union is supported by contributions (dues) from 36 member countries. Additional funds for symposia and other scientific activities of the Union are provided by ICSU from contributions received for this purpose from UNESCO.

The International Union, as of the XVIII General Assembly held in Lima, Peru, August 1975, has nine bodies called Commissions for centralizing studies in the principal technical fields. The names of the Commissions and the chairmen follow.

- A. Electromagnetic Metrology
Dr. H.M. Altschuler (USA)
- B. Fields and Waves
Prof. J. van Bladel (Belgium)
- C. Signals and Systems
Prof. B. Picinbono (France)
- D. Physical Electronics
Prof. A. Smolinski (Poland)
- E. Interference Environment
Dr. Ya. I. Likhter (USSR)
- F. Wave Phenomena in Nonionized Media
Mr. F. Eklund (Sweden)
- G. Ionospheric Radio
Dr. J.W. King (United Kingdom)
- H. Waves in Plasmas
Dr. R. Gendrin (France)
- J. Radio Astronomy
Prof. G. Westerhout (USA)

Every three years, the International Union holds a meeting called the General Assembly. The next General Assembly, the XIX, will be held in Helsinki, Finland in August, 1978. The Secretariat prepares and distributes the Proceedings of these General Assemblies. The International Union arranges international symposia on specific subjects pertaining to the work of one Commission or to several Commissions. The International Union also cooperates with other Unions in international symposia on subjects of joint interest.

Radio is unique among the fields of scientific work in having a specific adaptability to large-scale international research programs, for many of the phenomena that must be studied are worldwide in extent and yet are in a measure subject to control by experimenters. Exploration of space and the extension of scientific observations to the space environment is dependent on radio for its communication link and at the same time expands the scope of radio research. One of its branches, radio astronomy, involves cosmos-wide phenomena. URSI has in all this a distinct field of usefulness in furnishing a meeting ground for the numerous workers in the manifold aspects of radio research; its meetings and committee activities furnish valuable means of promoting research through exchange of ideas.

Steering Committee:

G. Hyde, Steering Committee Chairman
E. Wolff, Steering Committee Vice-Chairman
L. R. Dod, Secretary to the Steering Committee
R. Lang, Finance Committee Chairman
L. Taylor, Arrangements Committee Chairman
B. Keiser, Registration Committee Chairman
S. DiFonzo, Banquet Committee Chairman
R. Hyde, Family Activities Committee Chairman
A. K. Jordan, Special Events Committee Chairman
W. Kahn, I. Katz, Technical Program Committee Co-Chairmen
A. Atia, Publications Committee Chairman
V. Arens, AP-S Digest
I. Katz, URSI Digest
W. Ament, Government and Industry Committee Chairman
W. English, Publicity Committee Chairman

W. Ament	A. K. Jordan
T. ap Rhys	M. Jordan
V. Arens	W. Kahn
A. Atia	I. Katz
A. Cheung	B. Keiser
W. Destler	J. Lang
D. DiFonzo	R. Lang
S. DiFonzo	D. LeVine
L. R. Dod	M. Schneider
W. English	L. Schwab
G. Hyde	L. Taylor
R. Hyde	

APS/URSI Technical Program Committee: W. Kahn, I. Katz, Co-Chairmen

W. Ament	A. H. LaGrone
T. L. ap Rhys	R. H. Lang
V. R. Arens	D. LeVine
C. I. Beard	R. Mittra
F. W. Crawford	R. Price
W. F. Crowell	L. J. Ricardi
G. A. Deschamps	T. B. A. Senior
W. J. English	J. P. Shelton
L. B. Felsen	M. I. Skolnik
G. H. Hagn	N. A. Spencer
K. J. Harker	C. T. Swift
G. Hyde	W. F. Utlaut
A. K. Jordan	T. E. VanZandt
W. Kahn	W. Wasylkiwskyj
I. Katz	E. A. Wolff
I. W. Kay	L. Young

Editorial Assistants:

A. A. Arens	S. L. Hofmann
R. I. Arens	B. F. Kahn



MONDAY MORNING, 15 MAY, 0830-1200

Commission B Session 1

ELECTROMAGNETICS

Monday A.M., 15 May, Room 0105

Chairman: R. E. Kleinman

University of Delaware, Newark, DE

BI-1 APPLICATION OF THE PLANE WAVE SPECTRUM TO EMP; SHIELDING
0830 EFFECTIVENESS: L. Q. Bowers and E. H. Villaseca, Harris
Electronic Systems Division, Melbourne, FL

The concept of the plane wave expansion technique is ideally suited to relating shielding effectiveness as measured by low-level CW sources in the near field to the shielding effectiveness presented by a shelter to a uniform plane wave. Employing the basic definition of shielding effectiveness put forth by Schelkunoff (1), analytical expressions for SE_D , SE_L , and SE_{EMP} (shielding effectiveness to loops, dipoles and EMP exhibited by a planar metallic wall) can be derived, using the plane wave expansion, regardless of the orientation of the sources. In this way, the validity of a given test procedure can be analyzed by a comparison of theoretical predictions and experimental results.

A description of the method used to obtain analytical expressions for shielding effectiveness will be presented along with specific results for "coaxial" as well as "coplanar" orientations of loops and dipoles. Analytical results for the coaxial configuration of small loop antennas placed on opposite sides of an infinite metallic wall will be shown to give values of shielding effectiveness that closely match the analytical predictions of Bannister (2). Finally, analytical correction factors, which must be added to loop shielding effectiveness measurements and subtracted from dipole measurements to obtain EMP shielding effectiveness, will be presented.

References:

1. Schelkunoff, S. A., Electromagnetic Waves, Van Nostrand, Princeton, N.J. (1943).
2. Bannister, P. R., "New Theoretical Expressions for Predicting Shielding Effectiveness for the Plane Shield Case." IEEE Trans., EMC, Vol. EMC-10, Page 2 (March 1968).

B1-2 COMPUTATIONS OF MODE SCATTERING IN AN IRREGULAR
0850 MULTILAYERED SPHEROIDAL MODEL OF THE EARTH: E. Bahar,
Electrical Engineering Dept., University of Nebraska,
Lincoln, NE

A full wave analysis is used to determine the scattering of radio waves in irregularly shaped spheroidal structures of finite conductivity. (1) The electromagnetic fields are expanded in terms of basis functions that depict the local variations of the structure and exact boundary conditions are imposed.

Maxwell's equations are converted into a set of coupled first order differential equations for the forward and backward traveling local mode amplitudes. Thus it is necessary to accurately determine the loci of the complex roots of the modal equation for spheroidal structures of varying dimensions and electromagnetic parameters. To this end, uniform asymptotic expansions are used to evaluate the spherical Bessel functions over a wide range of complex orders and argument (2), and the modal equation is kept invariant of the scaling factors that are introduced in the computations.

In this work rapid variations in the dimensions of the structures are assumed, thus reflections are not negligible and the irregular structure is characterized by transmission and reflection scattering coefficients, for excitations in both directions.

Since spheroidal models are considered, these results could also be used to determine antipodal effects.

- (1) E. Bahar (1976), Electromagnetic waves in irregular multi-layered spheroidal structures of finite conductivity--Full wave solutions, Radio Science, Vol. 11, No. 2, pp. 137-147.
- (2) F.W.J. Oliver (1954), The asymptotic expansion of Bessel functions of large order. Philos. Trans. Roy. Soc., London, A247, 328-368.

B1-3 AN EQUIVALENT CIRCUIT FOR RADIATION THROUGH SPHERICAL
0910 REGIONS: T. N. Lee and W. K. Kahn, The George
Washington University, Washington, DC

The waveform of radiation from an antenna is constrained by the frequency-transfer characteristics of the space surrounding the antenna. In this paper the radiation from a sphere of radius r_0 enclosing the antenna out to a sphere of radius r is analyzed into conventional spherical (nonuniform) waveguide modes (1,2,3). An equivalent circuit is found for the region between r_0 and the sphere of radius r . The circuit for finite r is believed to be new.

The equivalent circuit has the following form: two lumped constant filters separated by a length of uniform transmission line. In addition, one of the lumped constant filter sections includes one ideal transformer with imaginary turns ratio. The lumped constant sections introduce non-trivial high-pass filter characteristics depending on r_0 and r , exhibiting a maximally flat "delay". The distributed portion of the equivalent circuit contributes a true time delay $(r-r_0)/c$. For $kr_0 > \{n(n+1)\}^{1/2}$ where $k=2\pi/\lambda$ and n is the order of spherical Bessel function of a particular mode, a simple expression is found for the group delay. The network representation yields physical insight into radiation and reception of pulse waveforms.

- (1) L. B. Felsen, "Spherical Transmission Line Theory", M.R.I. Report R-253-5/P.I.B.194, Polytechnic Institute of Brooklyn.
- (2) L. J. Chu, "Physical Limitations of Omni Directional Antennas", J. of Applied Physics, Vol. 19, Dec 1948, pp 1163-1175.
- (3) L. Susman, "Space-Time Directivity of Finite Antennas", PhD Dissertation, Polytechnic Institute of Brooklyn, 1969.

B1-4 THE ELECTRIC FIELD PROBE NEAR A MATERIAL INTERFACE:
0930 G. S. Smith, School of Electrical Engineering, The
Georgia Institute of Technology, Atlanta, GA

In many applications an electric dipole is used as a probe to measure the component of an incident electric field parallel to its axis. When the dipole is located in an inhomogeneous body, such as a geophysical or biological specimen, the response of the probe can change with the position as a result of the variation of the electrical constitutive parameters within the body. The variation in the constitutive parameters may be a slowly varying continuous function of the position or an abrupt change as would occur at a material boundary, such as at a muscle-fat interface in a biological specimen.

In this paper, a theoretical model is formulated to determine the effect the presence of an interface between different media has on the response of a nearby electric field probe. The particular model used is expected to give a "worst case" estimate of the interaction between the probe and the interface. The effect the interface has on the response of the probe is examined as a function of the size of the probe, the insulation on the probe, the load admittance at the terminals of the probe, the dissipation in the surrounding medium and the spacing between the probe and the interface. Experimental apparatus designed to measure the effect the interface has on the response of the probe is described. Theoretical results are shown to be in good agreement with the measured data.

B1-5 SURFACE CURRENTS AND NEAR ZONE FIELDS USING THE T-MATRIX:
1005 V. N. Bringi and T. A. Seliga, Atmospheric Sciences
 Program and Electrical Engineering Dept., The Ohio State
 University, Columbus, OH

Waterman's T-matrix method has been theoretically and numerically investigated by a number of investigators for scattering of acoustic, electromagnetic and elastic waves. The majority of the results thus far have been restricted to calculation of far-zone scattered fields and cross-sections. The T-matrix method, however, can also be used to calculate the induced surface current on perfect conductors without invoking the Rayleigh Hypothesis. The surface current is expanded into a complete set of spherical vector wave functions whose coefficients are obtained by a single matrix inversion. The use of Waterman's method avoids the need to consider the spherical near-zone region surrounding the scatterer. Nevertheless, the coefficients of the vector wave function expansion of such near-zone fields can be obtained by a simple extension of the T-matrix method. Numerical results are presented for the hemispherically capped cylinder and cone configurations.

B1-6 SCATTERING BY A PERFECTLY CONDUCTED SPHERICAL SHELL
 1025 WITH A CIRCULAR APERTURE: T. H. Shumpert and R. K.
 Jones, Electrical Engineering Dept., Auburn University,
 Auburn, AL

In this paper we discuss a method for determination of the scattering behavior of a perfectly conducting spherical shell with a circular aperture. The shell is infinitesimally thin and is illuminated by a time-harmonic plane wave. The E field integral equation is used to produce two coupled integral equations in which the unknowns are the tangential components of the currents on the shell surface. The problem is specialized to the case of a plane wave symmetrically incident upon the aperture for which the ϕ variations of the tangential current components are

$$K_{\theta}(\theta, \phi) = K_1(\theta) \cos \phi \quad \text{and} \quad K_{\phi}(\theta, \phi) = -K_2(\theta) \sin \phi$$

where $K_1(\theta)$ and $K_2(\theta)$ contain the θ variation of K_{θ} and K_{ϕ} respectively. Following the moment method, the shell is divided into N rings and $K_1(\theta)$ and $K_2(\theta)$ are assumed to be constant over each ring. A point-matching technique is then used to cast the integral equation into the form $\bar{V} = \bar{Z} \bar{I}$, where \bar{V} is the excitation matrix, \bar{I} the response matrix, and \bar{Z} the impedance matrix. The elements of the impedance matrix, Z_{mn} , are defined in terms of the geometry of the problem, and numerical techniques for determination of the elements are discussed. The response matrix can then be found by inversion of the impedance matrix and the scattered field may be determined from the surface currents on the shell.

B1-7 IMPROVEMENT OF CONVERGENCE IN MOMENT-METHOD SOLUTIONS
1045 BY THE USE OF INTERPOLANTS: M. J. Hagmann, O. P. Gandhi,
and C. H. Durney, Dept. of Electrical Engineering and
Bioengineering, University of Utah, Salt Lake City, UT

We have developed several procedures in which an interpolant is used to correct solutions obtained using pulse functions as a basis and delta functions for testing. The interpolant is used after the fact to allow for some of the variation of the fields within each cell and thereby increase accuracy and improve convergence. Typically the increase in accuracy is comparable with what would be obtained by doubling the number of cells. Computational expense of using the interpolant is about 1 percent of the cost of the initial numerical solution.

A moment-method solution using a pulse function basis results in a single value representing \vec{E} within each cell. If delta functions are used for testing, then the calculated \vec{E} values are most representative of the cell centers. Experimental tests have shown that the error in \vec{E} calculated for the cell centers is relatively small even when adjacent cells have values which may differ by an order of magnitude. The procedures which we have developed approximate the variation of \vec{E} between the cell centers with a function that is used for computation of SAR (specific absorption rate) with general placement and size of cubical cells.

B1-8 DIFFRACTION OF AN ELECTROMAGNETIC WAVE BY A DIELECTRIC
1105 WEDGE: S. Berntsen, Institute of Electronic Systems,
 Aalborg University Center, Aalborg, Denmark

A new general formalism for diffraction of an electromagnetic wave by a cylinder is developed. If the incident electric field is polarized in the direction of the axis of the scatterer the basic equations of this formalism will have a structure which is very convenient to apply in many cases.

The fundamental new observation of the present theory of two dimensional diffraction problems is that the integral equation representing the scattering problem has a very attractive form, if the basic field to be considered is the field which is zero outside the scatterer, and inside the scatterer coincide with the scattered field.

The convenient representation of the field to be used is the Fourier transform of this field, and the integral equation will be a linear equation in this field.

A large number of two dimensional diffraction problems, involving scatterers with finite extension orthogonal to the axis, will in this representation be formulated as an integral equation in one variable.

The theory is applied to the diffraction of a field by a dielectric wedge. The integral equations for this problem are formulated, and it is shown that the exact solution to the equations will give a field which has the well known optical asymptotic behaviour.

B1-9 ON THE FORMULATION OF SCATTERING PROBLEMS INVOLVING
1125 FINITE PENETRABLE WEDGE STRUCTURES: R. J. Pogorzelski,
TRW Defense and Space Systems Group, Redondo Beach, CA

Recent work on the penetrable wedge geometry has resulted in the construction of a set of functions satisfying the Helmholtz equation in the interior and exterior of the wedge and the boundary conditions on the faces of the wedge as well as appropriate conditions at the edge. The existence of such functions permits one to analyze the scattering of electromagnetic radiation by a variety of related penetrable structures of finite extent. Formulations of several such problems are outlined and example results are given. Several waveguide and lens applications suggest themselves. Various computational considerations are pointed out. In addition, certain aspects of convergence, linear independence, and completeness as they apply to the above problems are addressed.

Present theoretical capabilities are limited to structures of finite extent. The reasons for this are discussed and some rather subtle aspects of the expected form of the infinite wedge solution are exposed. It becomes clear that the infinite wedge is by no means adequately understood as yet despite its theoretical importance. However, the finite geometries described here are theoretically tractable and finite structures are, after all, the only ones encountered in practice.

SEM

Monday A.M., 15 May, Room 0109

Chairman: F. M. Tesche, Science

Applications, Inc., Berkeley, CA

B2-1 IMPEDANCE OF CYLINDRICAL ANTENNA BASED ON SCHELKUNOFF'S
0830 PERTURBATION THEORY: C. T. Tai, Radiation Laboratory,
University of Michigan, Ann Arbor, MI

In a classical paper by Schelkunoff the impedance of a cylindrical antenna was calculated by treating a cylindrical antenna as a non-uniform biconical antenna. In that method the choice of the value of the average characteristic impedance is not unique. This degree of freedom is similar to the one found in the theory of cylindrical antenna based on the integral equation method where the expansion parameter is also not unique.

In this work we have calculated the impedance of a cylindrical antenna using a weighted average characteristic impedance which is different from Schelkunoff's original one. The result shows that as far as the first order solution is concerned the values of the impedance can be significantly different from Schelkunoff's original calculation.

Our aim of this research is to find one weighted average characteristic impedance value such that the resultant antenna impedance will be very close to the one based on the integral equation method. With the aid of this impedance function we can determine its poles in order to ascertain whether or not this set of poles would resemble the pole distribution obtained by Tesche based on the integral equation method. Our preliminary investigation shows that the poles of a cylindrical antenna based on the non-uniform biconical antenna model has two layers instead of many layers as found by Tesche. We are inclined to believe that the pole distribution of a cylindrical antenna may not be unique. Most likely the distribution depends on the modeling or the method of obtaining these poles.

B2-2 SEM AND THE ENTIRE FUNCTION CONTRIBUTION: Capt. J. Barry
 0850 and B. K. Singaraju, Air Force Weapons Laboratory,
 Kirtland, AFB, NM

In the Singularity Expansion Method (SEM), the response current $\vec{J}(\vec{r}, s)$ is expressed in terms of the natural frequencies s_α and the coupling coefficients in addition to an entire function contribution $\vec{W}(s)$ as

$$\vec{J}(\vec{r}, s) = \sum_{\alpha} \frac{\tilde{\eta}_{\alpha}(s) \vec{v}_{\alpha}(\vec{r})}{s - s_{\alpha}} + \vec{W}(\vec{r}, s) \quad (1)$$

where $\vec{v}_{\alpha}(\vec{r})$ is the natural mode associated with s_{α} . It has been shown by some authors that the entire function contribution is zero for certain specific bodies.

In our work, we investigate the conditions under which the entire function contribution is zero. In order to investigate this, we look at the time domain representation of $\vec{J}(\vec{r}, t)$. If the set of functions $e^{s_{\alpha}t}$ forms a complete set in $L_2(0, \infty)$, then any $\vec{J}(\vec{r}, t)$ can be expressed as

$$\vec{J}(\vec{r}, t) = \sum_{\alpha} \vec{A}_{\alpha}(\vec{r}) e^{s_{\alpha}t} \quad \text{Re}(s_{\alpha}) < 0 \quad (2)$$

This implies that the entire function contribution is zero in the frequency domain. We show that the set $e^{s_{\alpha}t} \quad 0 < \alpha < \infty$ forms a complete set iff

$$\sum_{\alpha} \frac{\text{Re}(s_{\alpha})}{1 + |s_{\alpha}|^2} \rightarrow \infty \quad (3)$$

Using this criterion, we investigate various pole distributions in the complex s plane for which equation (3) is satisfied. Two examples of known pole distributions are also discussed. It is clear that even if condition (3) is satisfied, representation of $\vec{J}(\vec{r}, t)$ depends on the coupling vector $\vec{A}_{\alpha}(\vec{r})$. A discussion of the coupling coefficient form based on the pole distribution will also be considered.

- B2-3 ON EXTRAPOLATION OF MEASURED TRANSIENT SKIN CURRENTS TO
0910 NEW EXCITATION CONDITIONS: L. W. Pearson and D. R.
Roberson, Dept. of Electrical Engineering, University
of Kentucky, Lexington, KE

The results of study in the feasibility of extrapolating measured transient data to new excitation conditions by way of the Singularity Expansion Method (SEM) are presented. The SEM description of a scattering object may be derived from a collection of measured data provided certain minimum data sample conditions are met. The vehicle for the extraction is a systematic application of a Prony-type procedure. The authors reported this technique at the January, 1978, URSI meeting.

Considerations about the relationship between limits of extrapolation and the conditions under which initial data is taken are discussed. The notable issues are spectrum of the transient waveforms, the excitation location(s) in the measurement configuration, and spatial sampling frequency.

Numerical results are presented exhibiting the extrapolation of straight-wire scattering data from a localized excitation to plane wave excitation. The effects of spatial excitation variations and of waveform spectrum variations are demonstrated.

- B2-4 THE SINGULARITY EXPANSION METHOD APPLIED TO PERPENDICULAR
0930 CROSSED WIRES OVER A PERFECT GROUND PLANE: T. T. Crow,
M. Kumbale, and C. D. Taylor, Mississippi State University,
Mississippi State, MS

Using the singularity expansion method (SEM) one can determine the time domain scattering characteristics of a conducting object in terms of a summation of damped sinusoids. In the evaluation of the SEM solution the natural frequencies, natural frequencies, natural current modes and coupling coefficients are usually obtained numerically. Here SEM is applied to the study of perpendicular crossed wires oriented parallel to a perfectly conducting ground plane. A numerical solution is developed using the method of moments, and an algorithm based on the Cauchy integral theorem is used to search for the natural frequencies.

A parametric study of the SEM solution is performed to gain insight in the electromagnetic response of aircraft-like objects in proximity to the ground. The natural frequencies and coupling coefficients are considered as various geometrical parameters are varied. Time domain axial currents are also obtained for a unit step electromagnetic pulse incident on the wire configuration.

B2-5 AN ANALYTICAL SINGULARITY EXPANSION METHOD SOLUTION FOR
1005 WIRES IN PROXIMITY TO A PERFECT GROUND: C. D. Taylor
 and V. D. Naik, Mississippi State University, Mississippi
 State, MS

For wire configurations oriented parallel to a conducting ground plane the response to an incident electromagnetic field can be determined by using transmission line theory. Normally to obtain the transient response the singularity expansion method (SEM) requires numerical techniques. However when transmission line theory is used analytical techniques can be utilized in applying SEM.

Considering crossed wires oriented parallel to a perfect ground, transmission line theory is used to obtain the natural frequencies and natural current modes. A comparison with the results obtained by using numerical techniques is made to validate the procedure.

Plane wave illumination and lossy ground plane considerations are also presented.

B2-6 EXPERIMENTALLY DETERMINED TRANSIENT RESPONSES AND NATURAL
1025 FREQUENCIES FOR CONDUCTING STRUCTURES: F. J. Deadrick
and A. J. Poggio, Lawrence Livermore Laboratory, Livermore,
CA

The LLL Transient Electromagnetic Facility has been used to perform a series of experiments involving EM interactions with cylinders, crossed cylinders, and scale models of operational aircraft. The induced surface current and charge densities due to wideband transient pulses of 300 psec duration were measured using probes provided by AFWL. The responses were measured with the bodies in free space and at varying distances from a perfectly ground plane.

The experiments, the associated processing equipment, and the difficulties encountered will be described. The results will be analyzed and it will be shown that the spectral content of the responses is modified and somewhat enhanced by the presence of the ground plane. Also, techniques for defining early time and late time behavior will be presented.

Using the LLL processor PARET which is based on Prony's method, the complex natural resonances of the various bodies have been determined. The migration of the poles as a function of distance to the ground will be illustrated and compared to published theoretical analyses. Comments will be made regarding the nature of the migrations and the phenomena involved.

B2-7 PRONY'S METHOD REVISITED: E. K. Miller, Lawrence
1045 Livermore Laboratory, Livermore, CA

Prony's method belongs to a class of techniques termed "parameter estimators" in system's theory. Parameter estimation is a process for estimating constants which appear in mathematical models of physical phenomena, and may itself be viewed as a subset of system's identification wherein model selection is also an issue. Our interest in Prony's method stems from its utility for obtaining the exponents or poles of data described by exponential series. The effect of noise on parameter estimation in general, and Prony's method in particular, is a problem of central importance. As discussed by many authors, results obtained from Prony processing of noisy data can be severely degraded. Various techniques for reducing noise sensitivity have been studied, including a noise whitening filter and a sliding data window. The latter provides average pole values from the clusters produced by successive window estimates, as well as a means to identify curve-fitting poles.

In this paper we continue to evaluate the sliding window approach by conducting a systematic series of computer experiments on analytically specified transient waveforms. We examine, in particular, propagation of errors through the process by evaluating the accuracy of the input data, the characteristic-equation coefficients and roots, the poles and the residues. Statistical distributions of these quantities are derived for various combinations of input data parameters. We find that averaging the coefficients, rather than the poles, seems generally preferable, in terms of the pole accuracy available from a given number of window iterations. In addition we note that the results presented are obtained using a modest mini-computer (the Commodore PET), demonstrating the relatively undemanding computational requirements of the technique.

B2-8 INVERSION OF ONE-DIMENSIONAL SCATTERING DATA USING
1105 PRONY'S METHOD: D. L. Lager, R. J. Lytle, and E. K.
 Miller, Lawrence Livermore Laboratory, Livermore, CA

A one-dimensional configuration is the simplest geometry to invert, yet has practical application to such problems as scattering from inhomogeneous half-spaces and propagation on non-uniform transmission lines. Whether the medium parameters vary continuously or discretely with position, the problem's numerical description can usually be developed in a finite difference approximation. As such, the scattered and transmitted fields can be represented as exponential series, whose exponents are related to the electrical thicknesses of the layers which comprise the model. If the exponents or poles are derivable from field data, then the inverse problem is formally solvable.

In this paper we consider application of Prony's method, a procedure for obtaining the poles of exponential signals, to such one-dimensional problems. Analysis of both time-domain and frequency-domain data is studied. The effects of the medium characteristics, number of layers, number of data samples, and other factors are examined. We conclude that Prony's method has merit for certain classes of one-dimensional inverse problems.

B2-9 THE NOISE INDUCED STATISTICAL BEHAVIOR OF THE EIGENVALUE
1125 STRUCTURE OF THE PRONY MATRIX: G. J. Scrivner, Computer
Corporation, Albuquerque, NM

Prony's algorithm provides a method of extracting system singularities directly from transient response data. The implementation of the algorithm combined with a least squares criterion results in a matrix equation from whose solution vector the system singularities can be obtained. The importance of the eigenvalue structure of this matrix and its perturbation due to noise in the transient response data has been recognized by Van Blaricum and Mitra [1975] and Scrivner [1976]. The analytic expressions obtained in both of these prior investigations for the expected value of noise perturbed eigenvalues consistently over estimate the effect observed in Monte Carlo experiments. This behavior is explained by the contribution of term which results if second order Rayleigh-Schrodinger perturbation theory is utilized. Performance of the expected value operation on this second order term results in a term of magnitude comparable to the first order contribution. The previous analytic expressions are shown to encompass only the contribution of the first order term. Thus, this paper briefly summarizes the pertinent parts of the previous investigations, points out the deficiencies, and presents several new and stronger theoretical results supported by appropriate numerical experiments.

LIGHTNING, SPHERICS AND NOISE

Monday A.M., 15 May, Room 1105

Chairman: G. H. Hagn, Stanford

Research Institute, Arlington, VA

E1-1 THE GENERATION OF LIGHTNING BY COSMIC RAYS: J. W.
0900 Follin, Jr., E. P. Gray, and K. Yu, Applied Physics
 Laboratory, Johns Hopkins University, Laurel, MD

A new theory has been proposed for the generation of lightning, which postulates an intimate connection between that phenomenon and cosmic rays. The proposed scenario is as follows. A large cosmic ray soft air shower, comprising about 10^4 electrons and having an energy of about 10^{14} eV, ionizes some of the molecules in a thundercloud. The resulting secondary electrons are accelerated downward in the ambient electric field of the cloud and thus start an electron avalanche which concentrates several coulombs of charge near the base of the cloud. This charge moves to the ground in steps of varying size along the stepped leader. Each step is the result of a further, much smaller electron avalanche, triggered by a cosmic ray muon. The secondary electrons it produces will avalanche sufficiently near the charge, stopping when they get far enough away. Once the charge has migrated to the tip of the step, a new muon triggers another step. After the stepped leader reaches the ground, a high-current return stroke grounds part of the cloud and produces an intense electric field. There, new electron avalanches can be triggered by much smaller soft air showers, comprising only about 10^2 electrons and having an energy of about 10^{12} eV. These produce the multiple strokes usually observed. Evidence for this theory will be presented, as will some model calculations for the electron avalanche. Some of the consequences of the theory will be discussed.

- E1-2 THE INFLUENCE OF TORTUOSITY ON THE SPECTRUM OF RADIATION
0930 FROM LIGHTNING RETURN STROKES: D. M. Le Vine and R.
Meneghini, NASA/Goddard Space Flight Center, Greenbelt, MD

The effects of channel tortuosity on the fields radiated from lightning return strokes is being studied using a computer generated, piecewise linear representation for the channel. The fields radiated from each element are calculated using the solution for an arbitrarily oriented current filament located over a conducting plane and driven by a traveling current wave. As a check on the model, the temporal shape of radiated electric field waveforms are compared with measurements made on Florida lightning. The model produces electric field waveforms which are in reasonable agreement with observations when commonly accepted choices are made for the current waveform and velocity of propagation along the channel.

The spectrum of electric fields, computed with this simulation for an observer on the surface, is dominated at low frequencies by the channel-observer geometry and at high frequencies by the current waveform. At intermediate frequencies (e.g., about 100 kHz to 100 MHz), tortuosity has a pronounced effect. Reasonable choices of tortuosity produce spectra qualitatively in agreement with reported measurements, whereas the spectrum of electric fields radiated from a long straight channel, with the same current waveform and orientation, does not agree as well with experiment.

- E1-3 SFERIC BURST RATES AND TORNADIC ACTIVITY: R. L. Johnson,
1000 Southwest Research Institute, San Antonia, TX

During the spring 1977 thunderstorm season, sferic data were collected from 9 storm systems occurring in the Texas-Louisiana area. The sensor was a crossed baseline interferometer located in San Antonio, Texas. Sferic activity was characterized by azimuthal angle of arrival and was recorded in histogram form, providing a visual presentation of sferic count versus direction of arrival. Effective range of the sensor was found to be approximately 650 km with individual cell discrimination possible to distances of 120 km. The storm data were monitored for 43 hours at a receiver frequency of 2 MHz. During the observation period, three occurrences of tornadoes were reported and two of these were confirmed as hook echoes on NWS radar. In each case the sferic burst rates exhibit a period of relative inactivity followed by an abrupt enhancement of sferic activity in association with the tornado.

- E1-4 EFFECTS OF GEOMAGNETIC DISTURBANCES ON MAN-MADE SYSTEMS
1045 IN BOREAL/AURORAL REGIONS OF CENTRAL CANADA: W. M.
 Boerner, W. R. Goddard and D. A. Woodford, AEM Special
 Studies Group, University of Manitoba, Winnipeg, Canada

The rapidly increasing energy demands of central latitudinal U.S. regions will require the development of large scale energy reclamation and transportation/transmission systems far into the auroral regions where abundant untapped hydro-electric and also petrol resources are available. These man-made systems suffer rather severe disturbances from geomagnetically induced currents which effects are still not fully understood. A brief survey of major disturbances of SIC effects on pipelines, electric power transmission and communication systems in Central Canadian regions will be given and analyzed with the aim to isolate specific phenomena which require further coordinated ground-based, air-borne, balloon and satellite experiments for proper interpretation. Similarly, sources of man-made noise within boreal/auroral regions will be specified which cause undesired interaction with the magnetosphere as for example the power-line induced VLF chorus resulting from harmonics of 60Hz radiated from unbalanced power transmission systems.

- E1-5 A STUDY OF LATITUDINAL PROPERTIES OF POLAR VLF HISS AND
1115 EMISSION OBSERVED BY SATELLITE: T. Yoshino, University
 of Electro-Communications, Tokyo, Japan; T. Matsuo,
 Faculty of E.E., Kyoto University, Kyoto, Japan; and
 H. Fukunishi, National Inst. of Polar Research, Tokyo,
 Japan

A Japanese satellite tracking and data telemetry facility was constructed at Syowa Station in Antarctica in March 1976. Data have been received from the ISIS-1 and 2 spacecraft and combined with simultaneous ground-based and rocket-borne observations. We have succeeded in obtaining such simultaneous three-dimensional data in active aurora break-ups on three days.

In this paper we show an example of the dynamic spectrum of latitudinal properties of wide-band VLF hiss and emissions in the winter. We also found that in the region of the auroral oval VLF saucer emissions suddenly appeared and the VLF hiss disappeared gradually when there was an active aurora over the Syowa Station. In the region between the auroral oval and the plasma pause the VLF emission mode changes to the chorus type and after crossing the plasma pause region many whistler mode waves appeared. Proton and Helium ion whistler waves were frequently observed on the high latitude side of the plasma pause.

MONDAY AFTERNOON, 15 MAY, 1330-1700

Commission B Session 3

THIN WIRES

Monday, P.M., 15 May, Room 0105

Chairman: D. C. Chang

University of Colorado, Boulder, CO

- B3-1 A NEW FORMULATION FOR THE ANALYSIS OF THIN-WIRE
1330 STRUCTURES: C. M. Butler and D. R. Wilton, University
of Mississippi, University, MS

A new integro-differential equation for thin-wire structures is presented and discussed. By means of the equivalence of two differential operations upon Green's functions, the usual electric field integro-differential equation for non-parallel thin wires is transformed into a form which possesses only the harmonic differential operator--no mixed partial derivatives. This special form is particularly amenable to testing in the moment method procedure with either piecewise sinusoidal or piecewise linear functions, or, if desired, it can be converted directly to a Hallen-type integral equation. The resulting Hallen equation and that which follows from the linear and sinusoidal testing involve only single integrations which are simple to perform numerically. Lossy and loaded wires can be handled readily and the exact kernel causes no difficulty. The various equations of this method are quite general and are independent of the basis set chosen. Included as special cases are the piecewise linear and sinusoidal Galerkin methods. Wire structures have been analyzed by means of various forms of this technique. The solution convergence rate is extremely high and implementation is simple.

$$\frac{\partial^2}{\partial u \partial v} \frac{e^{-jkd}}{D} = - \left(k^2 + \frac{\partial^2}{\partial u^2} \right) \left[\frac{\mu_0 \cdot e^{-jkd}}{\sqrt{u^2 + v^2} D} \right]$$

$$D = \sqrt{u^2 + v^2 + w^2}$$

B3-2 A HYBRID TECHNIQUE FOR COMBINING THE MOMENT METHOD
1355 TREATMENT OF WIRE ANTENNAS WITH THE GTD FOR CURVED
SURFACES: E. P. Ekelman, Jr. and G. A. Thiele, The
Ohio State University ElectroScience Laboratory,
Columbus, OH

The problem of interest is a wire antenna structure arbitrarily oriented on or arbitrarily near a curved surface. The hybrid technique represents the antenna structure with a moment method formulation, setting up the matrix equation $[Z'](I')=(V)$ where $[Z']=[Z]+[\Delta Z]$ and $[\Delta Z]$ is the modification of the free space impedance matrix $[Z]$ to account for the effect of the curved surface. $[\Delta Z]$ is calculated with the aid of the GTD for curved surfaces.

Specifically, the problems of a dipole parallel or perpendicular to a perfectly conducting circular cylinder are analyzed and the input impedance compared with results found from the exact eigen solution or the use of image theory. The results show excellent agreement for dipoles arbitrarily close to the curved surface and for small ($r_c=\lambda/4$) radii or curvature. This favorable behavior of the solution for small distances and small radii of curvature was not initially expected due to the approximations inherent in the GTD but was subsequently obtained when it was noticed that incident field from the wire segments could be separated into spherical waves originating from well-defined points on the wire segments thereby permitting values of the incident field with no radial component to be obtained at the specular points on the surface. Results for dipole input impedance will be shown for various cylinder radii and dipole to surface distances from near zero to one wavelength.

B3-3 CURRENT INDUCED ON SINGLE AND CROSSED ELECTRICALLY
 1420 SHORT AND THIN TUBES BY A NORMALLY INCIDENT, PLANE
 ELECTROMAGNETIC WAVE: R. W. P. King, D. J. Blejer,
 and B. H. Sandler, Gordon McKay Laboratory, Harvard
 University, Cambridge, MA

The currents induced in electrically thin conducting tubes are evaluated from the general solution of the coupled integral equations derived by C. C. Kao in the form of transverse Fourier components. It is shown that on a single cylinder of length $2h$ and radius a in a normally incident, F-polarized field with wave number k the rotationally symmetric zero-order term dominates for $ka < 0.1$ and increases in magnitude as ka is reduced but only when $kh > 1$. Under these conditions, supplemented with the inequality $a \ll h$, thin-cylinder theory is valid. The relatively small first-order term produces small departures from rotational symmetry that increase or decrease the current on the illuminated side depending on the condition of axial resonance and the location of the cross section in the standing-wave pattern. As kh is reduced so that $ka < kh \ll 1$, the rotationally symmetric part of the axial current decreases and becomes negligible compared to the first-order current which is proportional to $\cos \theta$. Thin-cylinder theory is then no longer useful.

When two electrically thin tubes intersect, thin-wire theory and junction conditions determine only the rotationally symmetric part of the axial currents in the arms. These dominate only when the arms of the cross are not electrically short. The first-order, nonrotationally symmetric components of the axial current and the transverse currents can be determined from the incident magnetic field. They dominate when the arms of the cross are electrically short. The significance of the surface currents and charges on aircraft illuminated by an electromagnetic wave or pulse at low frequencies is pointed out.

- B3-4 CURRENT INDUCED IN A THIN, INFINITELY LONG WIRE
1445 EMBEDDED IN A LOSSY INTERFACE BY A PLANE WAVE:
J. N. Brittingham, Lawrence Livermore Laboratory,
Livermore, CA, and F. V. Schultz, Purdue University,
West Lafayette, IN

Recently a method was developed by one of the authors [A New Series Solution for the Electric Fields From A Long, Thin Wire On An Interface, J. N. Brittingham, IEEE-APS, International Symposium, Stanford, California, June 1977] to evaluate the fields from a line source on a lossy interface when the field-points are on the interface. This procedure provide an accurate and numerical efficient method to calculate the fields from such a problem. Since this method isolates the singular behavior of the fields as the field-points approach the source-point, it provides a good procedure to numerically evaluate the self-term in a thin wire model of a wire on the interface.

In this paper we use this new series solution, along with the thin wire theory, to find the current on a thin wire embedded in a lossy interface. A plane wave incidences the wire from the free space side of the interface. In this study the electrical parameter, frequency, earth's dielectric constant, earth's conductivity and wave size, will be allowed to vary. The effects of the angle of incidence and the polarization of the incident-plane are studied also.

- B3-5 HORIZONTAL ANTENNA AND HORIZONTAL GROUND SCREEN NEAR A
 1525 HALF-SPACE: J. N. Brittingham, E. K. Miller, and J. T. Okada, Lawrence Livermore Laboratory, Livermore, CA

Two recent developments [A Bi-Variate Interpolation Approach for Efficiently and Accurately Modeling Near a Half-Space, J. N. Brittingham, E. K. Miller, J. T. Okada, IEEE-APS, International Symposium, Stanford, California, June 1977] and [A New Series Solution for Sommerfeld Integrals in a Two Media Problem, J. N. Brittingham and J. T. Okada, URSI, National Radio Science Meeting, January 1978] provide an accurate and numerically efficient method to evaluate Sommerfeld integrals. These new procedures, along with a moment method solution, are used to study a center fed horizontal antenna over a finite-length, horizontal ground screen near a half-space. To study the effects of an antenna and screen we have calculated the antenna's input impedance and the radiation pattern. The parameters that are varied in the study are the antenna's height, screen length and wire spacing.

- B3-6 CHARACTERIZATION OF THE TRANSIENT FAR-FIELD RESPONSE
 1550 OF THIN-WIRE ANTENNAS: J. A. Landt, Los Alamos Scientific Laboratory, Los Alamos, NM

Many concepts have been developed for the frequency domain analysis of antennas. These concepts include the well known parameters: gain, directivity, polarization, efficiency, impedance, and bandwidth. These parameters permit evaluation of antenna performance in communitation and conventional radar systems. Design goals for antennas used for transient application may not be well defined by these conventional parameters. Typically, one may desire a specific far-field (or near-field) temporal and spatial behavior, or perhaps to maximize total radiated energy, or alternately to obtain a radiated signal of a particular bandwidth. In this paper, antenna transient performance is evaluated using time-domain concepts as well as extensions of frequency domain concepts. These include time varying antenna gain, measures of signal fidelity, and over-all energy gain (or directivity). The transient performance of several antenna types (dipole, log periodic) are investigated. Several pulse shaping techniques are also evaluated. These studies illustrate that the antenna is an integral part of the pulse shaping network and demonstrate some of the capabilities and limitations of various antenna types.

B3-7 THE USE OF TAPERING TO REDUCE THE OFF-NORMAL BACKSCATTER
 1615 FROM A LINE SCATTERING FEATURE: K. M. Mitzner, Aircraft
 Group, Northrop Corp., Hawthorne, CA

For a straight line scattering feature such as a long wire or an edge, the envelope of the backscatter radar cross section decreases roughly as $\sin^{-2}\theta$ when we increase the angle θ between the direction of incidence and the normal to the scattering line.

It is often desirable to sharpen the scattering pattern by making the envelope drop off faster. This can be done by tapering the scattering properties of the line near its ends, either by shaping or by using absorber materials.

This paper examines the question of how much can in principle be accomplished by tapering over a distance d at each end of the line. It is shown from very basic considerations that the parameter $q = 4(d/\lambda)\sin\theta$ must be approximately 1 or greater to give significant reductions in the envelope at wavelength λ and angle θ . As an example, if the field scattered per unit length of line is tapered linearly to zero, the result is 13.5 Db or more envelope reduction for all λ and θ for which $q \geq 1.64$. This result takes advantage of the resonance curve nature of the dependence of the envelope reduction on q .

B3-8 INTERNAL EMP COUPLING TO A COMPOSITE AIRCRAFT: R. A.
 1640 Perala, K. M. Lee, and R. B. Cook, Mission Research
 Corp., Albuquerque, NM

In this paper, results are presented for internal EMP Coupling to an Advanced Design Composite Aircraft (ADCA). The ADCA is a conceptual aircraft whose skin is fabricated out of significant portions of graphite-epoxy composite material. Numerical results obtained for externally induced currents and charges (external coupling) are used to find the internal electromagnetic fields by making use of the surface transfer impedances. These internal fields are then used to excite the cables inside the aircraft. Both short circuit currents and open circuit voltages are calculated by time domain finite-difference techniques. The response so calculated from skin diffusion for a composite aircraft are compared to those experimentally observed on metallic aircraft. From the relative magnitude of these levels with respect to the levels induced via other POEs, a judgement is thereby made of the significance of diffusion coupling versus aperture coupling.

INVERSE SCATTERING AND PROFILE RECONSTRUCTION

Monday, P.M., 15 May, Room 0109

Chairman: A. K. Jordan, Naval

Research Laboratory, Washington, DC

B4-1 THE EXACT INVERSE SCATTERING INTEGRAL EQUATION APPLIED
1330 TO CONFORMAL SYNTHESIS: N. N. Bojarski, Newport Beach,
CA

Uniqueness aspects of my exact inverse scattering integral equation (1973) are discussed briefly.

Distinct methods of solution of this integral equation for the inverse source problem, inverse scattering problem, and synthesis problem are presented and discussed.

The integral equation for the synthesis problem is recast into a form suitable for conformal synthesis (i.e., for the case of the radiation or scattering sources being confined to a given surface, vis-a-vis a volume).

Numerical results are shown for the case of synthesized excitations resulting in rectangular beams radiated by right circular cylinders.

B4-2 NUMERICAL STUDIES OF THE EFFECTS OF NOISE AND SPATIAL
1350 BANDLIMITING ON SOURCE RECONSTRUCTIONS OBTAINED USING
THE BOJARSKI EXACT INVERSE SCATTERING THEORY: W. R.
Stone, Megatek Corp., San Diego, CA; and Dept. of
Applied Physics and Information Sciences, University
of California, San Diego, CA

N. N. Bojarski has presented an exact solution to the general inverse scattering problem. The uniqueness of this solution has been proven by Bleistein and Cohen, and by Stone. The effect of incomplete knowledge of the boundary values (i.e., bandlimiting in the spatial frequency domain) has been examined by Bojarski, by Bleistein, and by Mager. [For the purposes of this paper, the inverse scattering problem is taken to be the determination of the source term in the wave equation, given values for the fields over a boundary surface.]

This paper addresses two practical aspects of the application of the Bojarski solution: The effect of noise in the recorded data, and the effect of incomplete knowledge of the boundary values. These effects are demonstrated via simple numerical examples. These examples apply an iterative formulation of the Bojarski solution to the reconstruction of radiating sources and refractive index inhomogeneities from complex scalar field data recorded over a linear, sampled aperture. The results are applicable to reconstructions from data recorded with planar arrays. The effect of incorporating a priori information which is often available in real life (e.g., the maximum and minimum spatial extent, or refractive index variation, of an inhomogeneity) into the solution is also examined. Finally, the implications of these results for the processing of experimental data taken with the Holographic Radio Camera (J. Atmos. Terr. Phys. 38, 583-92, 1976) are discussed.

- B4-3 AN INTERDISCIPLINARY APPROACH TO ELECTROMAGNETIC INVERSE
1410 SCATTERING USING RADON TRANSFORM THEORY: Y. Das and
W. M. Boerner, Dept. of Electrical Engineering, University
of Manitoba, Winnipeg, Canada

It is known that the cross-sectional area of a target as a function of the distance along the line of sight can be estimated from its backscattered electromagnetic ramp response signature, which in turn can be approximately synthesized by using a 10:1 frequency bandwidth in the target's low resonance range. Thus the determination of the target shape and size using the ramp response signature is reduced to the geometrical problem of reconstructing a body from its cross-sectional areas (*Kennaugh-Cosgriff-Moffat*). This problem is most naturally tackled by employing the theory of Radon transforms, because it is known that for the characteristic function, γ of a three-dimensional body, the values of its Radon transform are given by the appropriate cross-sectional areas of the body. In particular it is shown that the *Kennaugh-Moffat* and the *Bojarski-Lewis* inverse theories, both derived from the physical optics approximation, represent a Radon transform pair. Well-known results in the theory of Radon transforms are used and two of the reconstruction algorithms (the convolution and the simultaneous iterative reconstruction technique) are used to recover the three-dimensional shapes of spherical and prolate spheroidal scatterers.

- B4-4 A DIRECT TIME DOMAIN APPROACH TO INVERSE SCATTERING:
1430 C. L. Bennett and H. Mieras, Sperry Research Center,
Sudbury, MA

The inverse scattering problem consists of determining the geometry of a scattering body when only the field incident on the body and the field scattered by the body are known. Much work on solving this problem in the frequency domain has been carried out. Recently, the inverse problem has been formulated as an inversion of a space-time integral equation that provides an exact relationship between the target ramp response and the target geometry for the rotationally symmetric scattering problem. An iterative solution technique was developed for solving this integral equation numerically on a digital computer. This paper describes a new, direct time domain solution procedure for this integral equation that is carried out by simply "marching on in time" the numerical representation of the integral equation. This new procedure yields the complete target geometry after one pass and does not require the multiple iterations needed for the previous time domain solution procedure. Results computed using this new technique are presented and discussed for a sphere, a sphere capped cylinder, and a flat-end sphere-cap cylinder.

B4-5 NAVAL VESSEL IDENTIFICATION BY RADAR: D. L. Moffatt
1505 and C. M. Rhoads, The Ohio State University ElectroScience
Laboratory, Columbus, OH

It has been shown [1,2] that predictor-correlator processing of transient response data using excitation invariant target parameters can be used for successful identification of aircraft and other free space objects. The identification of naval vessels from active radar data is a more perverse problem because of the large electrical size of the targets and the natural presence of an interfering sea medium. In this paper it is shown that naval vessels can be correctly identified using the concept of substructure resonances. With this approach discrete, multiple frequency scattering data spanning hull lengths of roughly 6.0 to 21.2 wavelengths are utilized. Therefore, at least a factor of five increase in the frequencies previously needed for identification are realized.

Representative multiple frequency complex scattering data on five classes of naval vessels will be shown with emphasis on interpolating complex $\sin(x)/x$ fits of the measurements. From these data both conventional ramp responses and a new matched filter-type response using only amplitude data are synthesized. Based on matched filter responses and quasi-invariant target descriptors, successful vessel identification will be demonstrated. It is emphasized that the results are obtained using real radar data where noise is inherently present.

Some initial results on the direct extraction of excitation invariant target descriptors using encapsulated source-receiver configurations and conventional TDR measurements will also be given. These results are confined at present to classical target shapes and very simple models.

REFERENCES

- [1] D.L. Moffatt and R.K. Mains, "Detection and Discrimination of Radar Targets," IEEE Trans. Antennas Propag., Vol. AP-23, No. 3, May 1975, pp. 358-367.
- [2] C.W. Chuang and D.L. Moffatt, "Natural Resonances of Radar Targets Via Prony's Method and Target Discrimination," IEEE Trans. Aerospace and Electronic Sys., Vol. AES-12, No. 5, September 1976, pp. 583-589.

B4-6 PENCIL-OF-FUNCTION METHOD: A COMPLETELY NEW APPROACH TO
1525 SYSTEM IDENTIFICATION: T. K. Sarkar, Gordon McKay
Laboratory, Harvard University, Cambridge, MA; J. Nebat
and D. D. Weiner, Dept. of Electrical Engineering,
Syracuse University, Syracuse, NY; and V. K. Jain, Dept.
of Electrical Engineering, University of South Florida,
Tampa, FL

The objective of this paper is to demonstrate that stable, reliable, consistent and accurate results in the identification of a system by poles and residues from a measured finite length, input-output record can be achieved by the pencil-of-function method. Numerical results will be presented to support this objective.

[For details please see Scientific Report No. 2 on Air Force Contract F33615-77-C-2059, Air Force Weapons Laboratory, December 1977.]

B4-7 DIELECTRIC PROFILE RECONSTRUCTION FROM MEASURED REFLECTION
1545 COEFFICIENT DATA -- PRELIMINARY RESULTS: K. E. Melick and
E. L. Coffey, III, Physical Science Laboratory, New Mexico
State University, Las Cruces, NM

An efficient operator-interactive method for reconstructing dielectric constant profiles from pseudo-measured data is discussed. Continuous dielectric profiles may be determined, eliminating the usual constraint of layering. The dielectric constant profile of the medium is varied until the calculated reflection coefficient converges to the measured data at all frequencies in the measured spectrum.

To implement the method, many thousands of reflection coefficient calculations are required. Hence an efficient method of solving linear second order differential equations with nonconstant coefficients is needed. Analog/hybrid computer techniques supply such a method. A single differential equation may be solved on a hybrid computer in less than 1 msec., so that reflection coefficients at 50 frequencies may be determined in about 60 msec., including computer overhead. One thousand simulations require only 1 minute. To encourage rapid convergence the computer operator dynamically adjusts the dielectric profile for a best match with the measured data.

Results will be presented for several reflection coefficient spectra to illustrate the efficiency of the method and also to demonstrate the effects of small errors which may occur in the reconstruction process.

B4-8 PROFILE RECONSTRUCTION FOR REFLECTION COEFFICIENTS WITH
1605 ANGULAR SPECTRA: S. Ahn and A. K. Jordan, Naval Research
Laboratory, Washington, DC

The profile reconstruction method, which the authors have previously used (Ahn & Jordan, IEEE Trans. Ant. & Prop., AP-24, 879-882; 1976), is extended to consider reflection coefficients, $r(k)$, where the wave number is a function of incidence angle, $k=k_0 \cos\theta$. The profile of permittivity of an inhomogeneous dielectric region is reconstructed from the analytic representation of the reflection coefficient. The interesting case of a reflection coefficient with discrete and continuous spectra is considered, since the discrete spectrum in this instance corresponds to a surface-wave mode on the dielectric interface. A specific $r(k)$ is considered with two poles in the lower half of the k -plane (these represent the continuous spectrum) and one pole in the upper half-plane (this represents the discrete spectrum). The analytic properties of the reflection coefficient are related to the scattered and the surface modes. The reconstruction method is used to obtain profiles for an inhomogeneous plasma region with a specified dispersion relation, and an inhomogeneous dielectric region with an implicit dispersion relation. Previous examples, which considered only normal incidence, are related to the present analysis for oblique incidence.

B4-9 INVERSE PROBLEM FOR A VIBRATING SPHERICALLY SYMMETRIC BODY:
1625 V. Barcilon, Dept. of Geophysical Sciences, University of
Chicago, Chicago, IL

This paper deals with an aspect of the general problem of inferring the structure of a vibrating body from a knowledge of its normal modes. The specific problem under consideration is the reconstruction of the density of a spherically symmetric liquid ball solely from natural frequency data. This study contrasts with other recent studies of inverse problems for vibrating systems in that (i) the body is 3-D but admits a certain symmetry and (ii) impulse response data containing amplitude information are not supplied. These two features are also present in the geophysical problem of inferring the internal structure of the earth.

Given two frequency spectra associated with angular numbers 0 and 1, it is shown that a one parameter family of densities can be constructed which are all compatible with the data. The same result holds for the pair of spectra associated with angular numbers 0 and 2. If q is the difference between the angular numbers of a given pair of spectra, then it is conjectured that the family of densities compatible with the data increases as $[q]$ increases, where $[q/2]$ denotes the largest integer smaller or equal to $q/2$.

PANEL DISCUSSION OF U.S. CCIR ACTIVITIES
FOR THE XIVth PLENARY ASSEMBLY AND 1979 WARC

Monday P.M., 15 May, Room 1105

Chairman: S. E. Probst, Office of

Telecommunications Policy, Washington, DC

Panelists

H. G. Kimball, OTP	Introduction
	<u>Study Group</u>
W. F. Utlaut, O.T.	1
E. L. Eaton, NASA	2
T. DeHass, ITS	3
J. B. Potts, COMSAT	4
H. T. Dougherty, ITS	5
C. M. Rush, ITS	6
H. Fosque, NASA	7
H. Blaker, Rockwell Int.	8
H. E. Wepler, AT&T	9
N. McNaughton, FCC	10,11

The International Radio Consultative Committee (CCIR) provides an International forum for the development of technical criteria affecting the manner in which Administrations of the world use and share the radio spectrum.

As an active participant in this forum, the United States has a national organization that generally parallels the international structure. The national organization, operating under the sponsorship of the State Department consists of a number of Study groups each of which have specific orientation toward one or more facets of this complex spectrum sharing and usage topic.

In this year, 1978, the CCIR completes another cycle of its ongoing review, revision and update of its basic body of published literature. The XIVth Plenary Assembly of the CCIR is scheduled to begin on June 6th in Kyoto, Japan and will conclude on June 23rd. During that meeting the CCIR will officially celebrate its 50th anniversary.

Two stages of preparatory meetings, in 1976, 1977 and early 1978, have been held in Geneva, Switzerland to develop the reports and recommendations to be placed before the Plenary for approval.

Commission E Session 2 (Joint with Commission F)

An unusual aspect of the next cycle (which will lead to XVth Plenary Assembly) is that a World Administrative Radio Conference (WARC) will be held in Geneva in the fall of 1979 with the broad objective of reviewing the Rules and Regulations of the International Telecommunications Union (ITU) in order to bring them up-to-date and to structure them to meet the needs of the world community for perhaps the next two decades. This is the first such general conference in twenty years although several specialized conferences have been held in the interim.

As it has in past conferences, the CCIR will play an important role in this 1979 WARC. In particular, a Special Preparatory Meeting (SPM) of the CCIR is scheduled for the fall of 1978. The objective of the SPM is to provide a technical report on radio spectrum sharing and usage matters as advice and guidance to the delegates of the 1979 WARC.

This Panel Session will provide the members of URSI an overview of the US CCIR activities leading up to both XIVth Plenary and the SPM. The Panel Session will be moderated by Mr. S.E. Probst, Assistant Director for Frequency Management, Office of Telecommunications Policy.

An overview of the United States Preparatory activities for the SPM and the WARC will be given by Mr. Harold G. Kimball, Spectrum Management Staff, Office of Telecommunications, Department of Commerce.

Each of the ten US Study Group chairmen will then provide a review of their Study Group's programs and initiatives. The US Study Group chairmen and their affiliations are:

- | | |
|--|--|
| Study Group 1 - Spectrum Utilization and Monitoring
Dr. William F. Utlaut, Institute of Telecommunications Sciences, Dept of Commerce | Study Group 6-Ionospheric Propagation
Dr. Charles M. Rush, Institute for Telecommunication Sciences
Dept of Commerce |
| Study Group 2 - Space Research and Radioastronomy
Mr. Elbert L. Eaton, Chief, Communications and Frequency Management, NASA | Study Group 7-Standard Frequency and Time Signal Services
Mr. Hugh Fosque, NASA |
| Study Group 3 - Fixed Services below 30 MHz
US Study Group-inactive
Mr. Ted DeHass-ITS, Acting International Chairman - SG 3 | Study Group 8-Mobile Services
Mr. Herb Blaker, Rockwell Int'l |
| Study Group 4 - Fixed Satellite Service
Mr. James B. Potts, Asst Vice President, COMSAT | Study Group 9-Fixed Services Using Radio Relay Systems
Mr. H.E. Weppler, AT&T |
| Study Group 5 - Propagation in Non-Ionized Media
Dr. Harold T. Daugherty, Institute of Telecommunication Sciences, Dept of Commerce | Study Group 10-Broadcasting Svc (Sound)
Study Group 11-Broadcasting Svc (TV)
Mr. Neal McNaughten, FCC |

OCEANOGRAPHY

Monday, P.M., 15 May, Room 1109

Chairman: W. L. Jones, NASA/Langley

Research Center, Hampton, VA

F1-1 THE MODULATION OF SHORT GRAVITY WAVES BY LARGER SCALE
1330 PERIODIC FLOWS - A SECOND ORDER THEORY: G. R. Valenzuela
and J. W. Wright, Naval Research Laboratory, Washington, DC

Keller and Wright's (1975) linear relaxation time model for the microwave scattering and hydrodynamic straining of wind-waves by longer gravity waves has been found adequate to interpret measured modulations of short gravity wind-wave spectra for U_0/C (ratio of orbital velocity to long gravity wave phase speed) up to 0.07 or 0.08 for air friction velocities u_* as large as 30 or 40 cm/sec (moderate wind speeds) for a long gravity wave of 0.575 Hz. Recently Plant et al (1977) find in coastal measurements that the first order relaxation model also predicts the general features of the modulation of centimetric wind-waves by shoaling waves, but not the anomalously large modulations observed when the shallow water wave speed coincides with the wind speed of 4.5 to 6.5 m/sec.

In this work a higher order theory is developed to investigate the modulation of short gravity wind-waves by longer scale flows in an attempt to reconcile the experimental measurements and theory. Explicit results will be given for the second order contributions.

F1-2 SURFACE TRUTH FOR EVALUATING REMOTE MICROWAVE SENSORS OF
1355 OCEAN WAVE FIELDS: WEST COAST EXPERIMENT: J. W. Wright
and W. J. Plant, Naval Research Laboratory, Washington,
DC; and W. L. Jones, NASA/Langley Research Center, Hampton,
VA

Microwave radars will be a principal remote sensor in satellite oceanography. These radars can sense large ocean waves at viewing angles away from nadir because the large waves modulate the short gravity-capillary waves, the predominant microwave scatterers. A CW Doppler radar operated at short range is an effective wave probe for measuring these modulations. The frequency modulation of the microwave signal is due to the orbital speed; the amplitude modulation is due to the modulation of the scattering cross-section. Cross-correlation of signals derived from the frequency and amplitude modulations respectively yields the modulation transfer function which governs, e.g. the wave contrast in radar images of ocean waves.

We measured modulation transfer functions at 9.375 and 1.5 GHz for vertical polarization, depression angles near 40° and winds up to 11 m/sec, in 18 meters of water off Mission Beach, CA during the West Coast Experiment, March 1977. The measurements show that X-band radar can provide strong wave images at low winds though the dependence of the modulations on the wind might decrease the reliability of quantitative determinations of wave height from the imagery. The 1.5 GHz modulations exhibit a desirably weaker dependence on the wind but are still strong enough to produce good imagery.

Fl-3 THE EFFECTS OF ORBITAL MOTION ON THE DISTORTION OF RADAR
 1420 IMAGES ON THE OCEAN: C. T. Swift, NASA/Langley Research
 Center, Hampton, VA (on leave at NOAA/WPL, Boulder, CO),
 and C. L. Rufenach, NOAA, Wave Propagation Laboratory,
 Boulder, CO

A Synthetic Aperture Radar (SAR) develops high resolution two-dimensional images of the earth surface by time-Doppler processing of the return signal. The Doppler history is produced by the motion of the radar and the Doppler frequency is consequently a linear function of time. Along track resolution is then developed by passing the signal through a matched filter. This signal processing is equivalent to generating a synthetic aperture of length $2vT$, where v is the forward velocity of the radar and T is the required integration time. The resultant ground resolution is $\lambda h/2vT$, where λ is the electromagnetic wavelength and h is the altitude of the radar. Cross-track resolution is developed by transmitting pulses of width τ , and recording the time history of the back-scattered signal.

If the target is stationary, all parameters are known a priori, and the signal processing is straight-forward. However, if the target is in motion, Raney⁽¹⁾ has shown that severe defocussing and image displacement can occur if the target is accelerating and/or in constant motion. In order to generalize Raney's results to the imaging of the ocean surface, a large ocean wave was assumed to propagate through a uniform scattering surface. Such scattering would approximately occur if the radar viewing angle is sufficiently far away from nadir so that Bragg scattering dominates. The shape of the large wave was assumed to be a trochoid, which is the simplest model of a wave that supports "orbital" particle motion; i.e., each elementary particle moves in a circle with tangential velocity $a\omega$, where a is the wave amplitude and ω is the radian frequency.

With no motion, the resultant image would be "grey" because of the assumed uniform cross section. However, this is not the case when the scatters are in motion. Because of the varying radial acceleration as seen by the radar, only those scatters near the zero crossings are imaged. Other points along the wave are defocussed resulting from an increasing value of the radial acceleration. Although a sharp image is formed at the zero crossing, displacement occurs because the radial velocity is maximum. Furthermore, the displacement alternates between a forward and backward image shift due to sign changes in the direction of the radial velocity component. Parametric calculations are presented as a function of $a\omega$, and the results are related to the physical characteristics of the ocean waves.

(1) Raney, R. K., "Synthetic Aperture Imaging Radar and Moving Targets", IEEE Trans. on Aerospace and Electronic Systems, Vol. AES-7, May, 1971. pp 499-505.

- F1-4 MEASUREMENT OF DIRECTIONAL GRAVITY WAVE SPECTRA USING A
 1445 MULTIPLEXED DUAL-FREQUENCY MICROWAVE RADAR: D. L. Schuler,
 Naval Research Laboratory, Washington, DC

A technique has been developed, using a dual-frequency radar operating at L-band, which permits remote measurements to be made on directional gravity wave "modulation" spectra. The modulation spectra sensed by the radar and the actual gravity wave spectra appear to be closely related. Past measurements using dual-frequency radars operating first at X-band and later at L-band have not been totally satisfactory because of the long data-acquisition time required for both Doppler processing and signal averaging. Measurements have been made recently using a more highly evolved L-band radar system which is capable of making multiplexed measurements on 50 transmitted frequency pairs in only 5 ms. Multiplexing of the radar data makes possible 1) more accurate measurements of gravity wave spectra since the data is interleaved throughout the entire data acquisition period, and, 2) allows more averaging to be performed during the time interval for which the wave system may reasonably be considered as being stationary. In particular, we have used a frequency synthesizer (capable of switching frequencies in 20 μ s) programmed remotely by a set of frequencies stored by an EPROM, to provide a multiplexed output which is then upconverted to L-band. Examples of wave spectra obtained from measurements made at our experimental site on the Chesapeake Bay will be provided. Data will also be presented which gives the dependence of the fractional modulation, $M(k)$, sensed by the radar as a function of surface wind speed. The relative insensitivity of $M(k)$ with wind speed indicates that radar data taken when the surface wind speed is not known will still yield meaningful wave spectra.

- F1-5 THE SURFACE CONTOUR RADAR, AN INSTRUMENT FOR MEASURING
 1525 OCEAN DIRECTIONAL WAVE SPECTRA: J. E. Kenney, A. E.
 Uliana, Naval Research Laboratory, Washington, DC and
 E. J. Walsh, NASA/Wallops Flight Center, Wallops Island, VA

This paper describes an airborne beam-limited 8.6 millimeter radar with selectable range resolutions of 0.15, 0.3, 0.61, 1.52 meters. The radar is designed to produce a three-dimensional map of the ocean surface. It employs digital pulse compression and frequency diversity with the two frequencies separated far enough to be decorrelated on the sea surface. The system is computer controlled and uses a mechanically-scanned antenna and software range tracking. It produces a real-time, false-color coded elevation map of the surface. The transmit antenna produces a 1.2° pencil beam while receive antenna has a 1.2 x 40° fan beam. By varying the aircraft altitude, the radar can adjust its swath width to equal seven times the dominant ocean wavelength (λ) and the along track resolution to 0.2 λ with data point spacing of 0.1 λ .

- F1-6 SIMULTANEOUS OPEN OCEAN MEASUREMENTS OF SEA SURFACE
1540 ELEVATION AND MICROWAVE BACKSCATTER AT K_A BAND FOR VARIOUS
INCIDENCE ANGLES AND WIND DIRECTIONS: E. J. Walsh, NASA/
Wallops Flight Center, Wallops Island, VA and J. E. Kenney,
Naval Research Laboratory, Washington, DC

This paper deals with measurements taken by an airborne nadir-looking beam-limited 8.6 mm radar with 0.15 m range resolution which scans laterally within $\pm 15^\circ$ of the perpendicular to the aircraft wings. The radar simultaneously produces perfectly registered patterns of the sea surface elevations and relative microwave backscatter. Data will be presented which was taken while the aircraft was in a 15° bank so that the incidence angle varied between 0° and 27° from the vertical and varied through the upwind, crosswind and downwind directions as the aircraft turned in a circle.

- F1-7 ANALYSIS OF A COMPACT HF ANTENNA TECHNIQUE FOR MEASURING
1610 COASTAL WAVEHEIGHT DIRECTIONAL SPECTRA: D. E. Barrick,
Wave Propagation Laboratory, NOAA, Boulder, CO and B. J.
Lipa, Center for Radar Astronomy, Stanford University,
Stanford, CA

There is an increasing need to measure directional wavefields in coastal waters. Low-powered automated shore-based stations are desired having compact, unobtrusive antenna systems; this precludes the use of conventional, narrow-beam long antenna arrays previously employed at HF. A novel receiving antenna system is being tested that uses two electrically small crossed loops and a vertical monopole to form a broad cardioid pattern. This beam is scanned in azimuth by the receiver processing software. The natural angular basis expansion for both the wavefield directional spectrum and the received sea-echo spectrum is the Fourier series. To second order, one obtains a nonlinear integral equation relating the matrix of the desired frequency-dependent Fourier coefficients of the wavefield to the measured second-order Doppler frequency-dependent Fourier coefficients. An accompanying paper presents the method for inverting this system.

From the zeroth coefficient vs wave frequency, one obtains the nondirectional spectrum; the sum of the squares of these coefficients yields the mean-square waveheight. For wind-driven seas, one can obtain the mean wave direction and the directional spread factor for each desired band of wave frequencies. It is also shown that swell arriving from two directions at the same wave frequency can be resolved with this technique.

Commission B Session 3

- B3-5 HORIZONTAL ANTENNA AND HORIZONTAL GROUND SCREEN NEAR A
1525 HALF-SPACE: J. N. Brittingham, E. K. Miller, and J. T.
Okada, Lawrence Livermore Laboratory, Livermore, CA

Two recent developments [A Bi-Variate Interpolation Approach for Efficiently and Accurately Modeling Near a Half-Space, J. N. Brittingham, E. K. Miller, J. T. Okada, IEEE-APS, International Symposium, Stanford, California, June 1977] and [A New Series Solution for Sommerfeld Integrals in a Two Media Problem, J. N. Brittingham and J. T. Okada, URSI, National Radio Science Meeting, January 1978] provide an accurate and numerically efficient method to evaluate Sommerfeld integrals. These new procedures, along with a moment method solution, are used to study a center fed horizontal antenna over a finite-length, horizontal ground screen near a half-space. To study the effects of an antenna and screen we have calculated the antenna's input impedance and the radiation pattern. The parameters that are varied in the study are the antenna's height, screen length and wire spacing.

- B3-6 CHARACTERIZATION OF THE TRANSIENT FAR-FIELD RESPONSE
1550 OF THIN-WIRE ANTENNAS: J. A. Landt, Los Alamos
Scientific Laboratory, Los Alamos, NM

Many concepts have been developed for the frequency domain analysis of antennas. These concepts include the well known parameters: gain, directivity, polarization, efficiency, impedance, and bandwidth. These parameters permit evaluation of antenna performance in communication and conventional radar systems. Design goals for antennas used for transient application may not be well defined by these conventional parameters. Typically, one may desire a specific far-field (or near-field) temporal and spatial behavior, or perhaps to maximize total radiated energy, or alternately to obtain a radiated signal of a particular bandwidth. In this paper, antenna transient performance is evaluated using time-domain concepts as well as extensions of frequency domain concepts. These include time varying antenna gain, measures of signal fidelity, and overall energy gain (or directivity). The transient performance of several antenna types (dipole, log periodic) are investigated. Several pulse shaping techniques are also evaluated. These studies illustrate that the antenna is an integral part of the pulse shaping network and demonstrate some of the capabilities and limitations of various antenna types.

B3-7 THE USE OF TAPERING TO REDUCE THE OFF-NORMAL BACKSCATTER
 1615 FROM A LINE SCATTERING FEATURE: K. M. Mitzner, Aircraft
 Group, Northrop Corp., Hawthorne, CA

For a straight line scattering feature such as a long wire or an edge, the envelope of the backscatter radar cross section decreases roughly as $\sin^{-2}\theta$ when we increase the angle θ between the direction of incidence and the normal to the scattering line.

It is often desirable to sharpen the scattering pattern by making the envelope drop off faster. This can be done by tapering the scattering properties of the line near its ends, either by shaping or by using absorber materials.

This paper examines the question of how much can in principle be accomplished by tapering over a distance d at each end of the line. It is shown from very basic considerations that the parameter $q = 4(d/\lambda)\sin\theta$ must be approximately 1 or greater to give significant reductions in the envelope at wavelength λ and angle θ . As an example, if the field scattered per unit length of line is tapered linearly to zero, the result is 13.5 Db or more envelope reduction for all λ and θ for which $q \geq 1.64$. This result takes advantage of the resonance curve nature of the dependence of the envelope reduction on q .

B3-8 INTERNAL EMP COUPLING TO A COMPOSITE AIRCRAFT: R. A.
 1640 Perala, K. M. Lee, and R. B. Cook, Mission Research
 Corp., Albuquerque, NM

In this paper, results are presented for internal EMP Coupling to an Advanced Design Composite Aircraft (ADCA). The ADCA is a conceptual aircraft whose skin is fabricated out of significant portions of graphite-epoxy composite material. Numerical results obtained for externally induced currents and charges (external coupling) are used to find the internal electromagnetic fields by making use of the surface transfer impedances. These internal fields are then used to excite the cables inside the aircraft. Both short circuit currents and open circuit voltages are calculated by time domain finite-difference techniques. The response so calculated from skin diffusion for a composite aircraft are compared to those experimentally observed on metallic aircraft. From the relative magnitude of these levels with respect to the levels induced via other POEs, a judgement is thereby made of the significance of diffusion coupling versus aperture coupling.

Commission B Session 4

INVERSE SCATTERING AND PROFILE RECONSTRUCTION

Monday, P.M., 15 May, Room 0109

Chairman: A. K. Jordan, Naval

Research Laboratory, Washington, DC

B4-1 THE EXACT INVERSE SCATTERING INTEGRAL EQUATION APPLIED
1330 TO CONFORMAL SYNTHESIS: N. N. Bojarski, Newport Beach,
CA

Uniqueness aspects of my exact inverse scattering integral equation (1973) are discussed briefly.

Distinct methods of solution of this integral equation for the inverse source problem, inverse scattering problem, and synthesis problem are presented and discussed.

The integral equation for the synthesis problem is recast into a form suitable for conformal synthesis (i.e., for the case of the radiation or scattering sources being confined to a given surface, vis-a-vis a volume).

Numerical results are shown for the case of synthesized excitations resulting in rectangular beams radiated by right circular cylinders.

B4-2
1350 NUMERICAL STUDIES OF THE EFFECTS OF NOISE AND SPATIAL
BANDLIMITING ON SOURCE RECONSTRUCTIONS OBTAINED USING
THE BOJARSKI EXACT INVERSE SCATTERING THEORY: W. R.
Stone, Megatek Corp., San Diego, CA; and Dept. of
Applied Physics and Information Sciences, University
of California, San Diego, CA

N. N. Bojarski has presented an exact solution to the general inverse scattering problem. The uniqueness of this solution has been proven by Bleistein and Cohen, and by Stone. The effect of incomplete knowledge of the boundary values (i.e., bandlimiting in the spatial frequency domain) has been examined by Bojarski, by Bleistein, and by Mager. [For the purposes of this paper, the inverse scattering problem is taken to be the determination of the source term in the wave equation, given values for the fields over a boundary surface.]

This paper addresses two practical aspects of the application of the Bojarski solution: The effect of noise in the recorded data, and the effect of incomplete knowledge of the boundary values. These effects are demonstrated via simple numerical examples. These examples apply an iterative formulation of the Bojarski solution to the reconstruction of radiating sources and refractive index inhomogeneities from complex scalar field data recorded over a linear, sampled aperture. The results are applicable to reconstructions from data recorded with planar arrays. The effect of incorporating a priori information which is often available in real life (e.g., the maximum and minimum spatial extent, or refractive index variation, of an inhomogeneity) into the solution is also examined. Finally, the implications of these results for the processing of experimental data taken with the Holographic Radio Camera (J. Atmos. Terr. Phys. 38, 583-92, 1976) are discussed.

- B4-3 AN INTERDISCIPLINARY APPROACH TO ELECTROMAGNETIC INVERSE
 1410 SCATTERING USING RADON TRANSFORM THEORY: Y. Das and
 W. M. Boerner, Dept. of Electrical Engineering, University
 of Manitoba, Winnipeg, Canada

It is known that the cross-sectional area of a target as a function of the distance along the line of sight can be estimated from its backscattered electromagnetic ramp response signature, which in turn can be approximately synthesized by using a 10:1 frequency bandwidth in the target's low resonance range. Thus the determination of the target shape and size using the ramp response signature is reduced to the geometrical problem of reconstructing a body from its cross-sectional areas (*Kennaugh-Cosgriff-Moffat*). This problem is most naturally tackled by employing the theory of Radon transforms, because it is known that for the characteristic function, γ of a three-dimensional body, the values of its Radon transform are given by the appropriate cross-sectional areas of the body. In particular it is shown that the Kennaugh-Moffat and the Bojarski-Lewis inverse theories, both derived from the physical optics approximation, represent a Radon transform pair. Well-known results in the theory of Radon transforms are used and two of the reconstruction algorithms (the convolution and the simultaneous iterative reconstruction technique) are used to recover the three-dimensional shapes of spherical and prolate spheroidal scatterers.

- B4-4 A DIRECT TIME DOMAIN APPROACH TO INVERSE SCATTERING:
 1430 C. L. Bennett and H. Mieras, Sperry Research Center,
 Sudbury, MA

The inverse scattering problem consists of determining the geometry of a scattering body when only the field incident on the body and the field scattered by the body are known. Much work on solving this problem in the frequency domain has been carried out. Recently, the inverse problem has been formulated as an inversion of a space-time integral equation that provides an exact relationship between the target ramp response and the target geometry for the rotationally symmetric scattering problem. An iterative solution technique was developed for solving this integral equation numerically on a digital computer. This paper describes a new, direct time domain solution procedure for this integral equation that is carried out by simply "marching on in time" the numerical representation of the integral equation. This new procedure yields the complete target geometry after one pass and does not require the multiple iterations needed for the previous time domain solution procedure. Results computed using this new technique are presented and discussed for a sphere, a sphere capped cylinder, and a flat-end sphere-cap cylinder.

B4-5 NAVAL VESSEL IDENTIFICATION BY RADAR: D. L. Moffatt
1505 and C. M. Rhoads, The Ohio State University ElectroScience
Laboratory, Columbus, OH

It has been shown [1,2] that predictor-correlator processing of transient response data using excitation invariant target parameters can be used for successful identification of aircraft and other free space objects. The identification of naval vessels from active radar data is a more perverse problem because of the large electrical size of the targets and the natural presence of an interfering sea medium. In this paper it is shown that naval vessels can be correctly identified using the concept of substructure resonances. With this approach discrete, multiple frequency scattering data spanning hull lengths of roughly 6.0 to 21.2 wavelengths are utilized. Therefore, at least a factor of five increase in the frequencies previously needed for identification are realized.

Representative multiple frequency complex scattering data on five classes of naval vessels will be shown with emphasis on interpolating complex $\sin(x)/x$ fits of the measurements. From these data both conventional ramp responses and a new matched filter-type response using only amplitude data are synthesized. Based on matched filter responses and quasi-invariant target descriptors, successful vessel identification will be demonstrated. It is emphasized that the results are obtained using real radar data where noise is inherently present.

Some initial results on the direct extraction of excitation invariant target descriptors using encapsulated source-receiver configurations and conventional TDR measurements will also be given. These results are confined at present to classical target shapes and very simple models.

REFERENCES

- [1] D.L. Moffatt and R.K. Mains, "Detection and Discrimination of Radar Targets," IEEE Trans. Antennas Propag., Vol. AP-23, No. 3, May 1975, pp. 358-367.
- [2] C.W. Chuang and D.L. Moffatt, "Natural Resonances of Radar Targets Via Prony's Method and Target Discrimination," IEEE Trans. Aerospace and Electronic Sys., Vol. AES-12, No. 5, September 1976, pp. 583-589.

B4-6 PENCIL-OF-FUNCTION METHOD: A COMPLETELY NEW APPROACH TO
1525 SYSTEM IDENTIFICATION: T. K. Sarkar, Gordon McKay
Laboratory, Harvard University, Cambridge, MA; J. Nebat
and D. D. Weiner, Dept. of Electrical Engineering,
Syracuse University, Syracuse, NY; and V. K. Jain, Dept.
of Electrical Engineering, University of South Florida,
Tampa, FL

The objective of this paper is to demonstrate that stable, reliable, consistent and accurate results in the identification of a system by poles and residues from a measured finite length, input-output record can be achieved by the pencil-of-function method. Numerical results will be presented to support this objective.

[For details please see Scientific Report No. 2 on Air Force Contract F33615-77-C-2059, Air Force Weapons Laboratory, December 1977.]

B4-7 DIELECTRIC PROFILE RECONSTRUCTION FROM MEASURED REFLECTION
1545 COEFFICIENT DATA -- PRELIMINARY RESULTS: K. E. Melick and
E. L. Coffey, III, Physical Science Laboratory, New Mexico
State University, Las Cruces, NM

An efficient operator-interactive method for reconstructing dielectric constant profiles from pseudo-measured data is discussed. Continuous dielectric profiles may be determined, eliminating the usual constraint of layering. The dielectric constant profile of the medium is varied until the calculated reflection coefficient converges to the measured data at all frequencies in the measured spectrum.

To implement the method, many thousands of reflection coefficient calculations are required. Hence an efficient method of solving linear second order differential equations with nonconstant coefficients is needed. Analog/hybrid computer techniques supply such a method. A single differential equation may be solved on a hybrid computer in less than 1 msec., so that reflection coefficients at 50 frequencies may be determined in about 60 msec., including computer overhead. One thousand simulations require only 1 minute. To encourage rapid convergence the computer operator dynamically adjusts the dielectric profile for a best match with the measured data.

Results will be presented for several reflection coefficient spectra to illustrate the efficiency of the method and also to demonstrate the effects of small errors which may occur in the reconstruction process.

B4-8 PROFILE RECONSTRUCTION FOR REFLECTION COEFFICIENTS WITH
1605 ANGULAR SPECTRA: S. Ahn and A. K. Jordan, Naval Research
Laboratory, Washington, DC

The profile reconstruction method, which the authors have previously used (Ahn & Jordan, IEEE Trans. Ant. & Prop., AP-24, 879-882; 1976), is extended to consider reflection coefficients, $r(k)$, where the wave number is a function of incidence angle, $k=k_0 \cos\theta$. The profile of permittivity of an inhomogeneous dielectric region is reconstructed from the analytic representation of the reflection coefficient. The interesting case of a reflection coefficient with discrete and continuous spectra is considered, since the discrete spectrum in this instance corresponds to a surface-wave mode on the dielectric interface. A specific $r(k)$ is considered with two poles in the lower half of the k -plane (these represent the continuous spectrum) and one pole in the upper half-plane (this represents the discrete spectrum). The analytic properties of the reflection coefficient are related to the scattered and the surface modes. The reconstruction method is used to obtain profiles for an inhomogeneous plasma region with a specified dispersion relation, and an inhomogeneous dielectric region with an implicit dispersion relation. Previous examples, which considered only normal incidence, are related to the present analysis for oblique incidence.

B4-9 INVERSE PROBLEM FOR A VIBRATING SPHERICALLY SYMMETRIC BODY:
1625 V. Barcilon, Dept. of Geophysical Sciences, University of
Chicago, Chicago, IL

This paper deals with an aspect of the general problem of inferring the structure of a vibrating body from a knowledge of its normal modes. The specific problem under consideration is the reconstruction of the density of a spherically symmetric liquid ball solely from natural frequency data. This study contrasts with other recent studies of inverse problems for vibrating systems in that (i) the body is 3-D but admits a certain symmetry and (ii) impulse response data containing amplitude information are not supplied. These two features are also present in the geophysical problem of inferring the internal structure of the earth.

Given two frequency spectra associated with angular numbers 0 and 1, it is shown that a one parameter family of densities can be constructed which are all compatible with the data. The same result holds for the pair of spectra associated with angular numbers 0 and 2. If q is the difference between the angular numbers of a given pair of spectra, then it is conjectured that the family of densities compatible with the data increases as $[q]$ increases, where $[q/2]$ denotes the largest integer smaller or equal to $q/2$.

Commission E Session 2 (Joint with Commission F)

PANEL DISCUSSION OF U.S. CCIR ACTIVITIES
FOR THE XIVth PLENARY ASSEMBLY AND 1979 WARC

Monday P.M., 15 May, Room 1105

Chairman: S. E. Probst, Office of
Telecommunications Policy, Washington, DC

Panelists

	Introduction
	<u>Study Group</u>
H. G. Kimball, OTP	
W. F. Utlaut, O.T.	1
E. L. Eaton, NASA	2
T. DeHass, ITS	3
J. B. Potts, COMSAT	4
H. T. Dougherty, ITS	5
C. M. Rush, ITS	6
H. Fosque, NASA	7
H. Blaker, Rockwell Int.	8
H. E. Wepler, AT&T	9
N. McNaughton, FCC	10,11

The International Radio Consultative Committee (CCIR) provides an International forum for the development of technical criteria affecting the manner in which Administrations of the world use and share the radio spectrum.

As an active participant in this forum, the United States has a national organization that generally parallels the international structure. The national organization, operating under the sponsorship of the State Department consists of a number of Study groups each of which have specific orientation toward one or more facets of this complex spectrum sharing and usage topic.

In this year, 1978, the CCIR completes another cycle of its ongoing review, revision and update of its basic body of published literature. The XIVth Plenary Assembly of the CCIR is scheduled to begin on June 6th in Kyoto, Japan and will conclude on June 23rd. During that meeting the CCIR will officially celebrate its 50th anniversary.

Two stages of preparatory meetings, in 1976, 1977 and early 1978, have been held in Geneva, Switzerland to develop the reports and recommendations to be placed before the Plenary for approval.

Commission E Session 2 (Joint with Commission F)

An unusual aspect of the next cycle (which will lead to XVth Plenary Assembly) is that a World Administrative Radio Conference (WARC) will be held in Geneva in the fall of 1979 with the broad objective of reviewing the Rules and Regulations of the International Telecommunications Union (ITU) in order to bring them up-to-date and to structure them to meet the needs of the world community for perhaps the next two decades. This is the first such general conference in twenty years although several specialized conferences have been held in the interim.

As it has in past conferences, the CCIR will play an important role in this 1979 WARC. In particular, a Special Preparatory Meeting (SPM) of the CCIR is scheduled for the fall of 1978. The objective of the SPM is to provide a technical report on radio spectrum sharing and usage matters as advice and guidance to the delegates of the 1979 WARC.

This Panel Session will provide the members of URSI an overview of the US CCIR activities leading up to both XIVth Plenary and the SPM. The Panel Session will be moderated by Mr. S.E. Probst, Assistant Director for Frequency Management, Office of Telecommunications Policy.

An overview of the United States Preparatory activities for the SPM and the WARC will be given by Mr. Harold G. Kimball, Spectrum Management Staff, Office of Telecommunications, Department of Commerce.

Each of the ten US Study Group chairmen will then provide a review of their Study Group's programs and initiatives. The US Study Group chairmen and their affiliations are:

- | | |
|--|--|
| Study Group 1 - Spectrum Utilization and Monitoring
Dr. William F. Utlaut, Institute of Telecommunications Sciences, Dept of Commerce | Study Group 6-Ionospheric Propagation
Dr. Charles M. Rush, Institute for Telecommunication Sciences
Dept of Commerce |
| Study Group 2 - Space Research and Radioastronomy
Mr. Elbert L. Eaton, Chief, Communications and Frequency Management, NASA | Study Group 7-Standard Frequency and Time Signal Services
Mr. Hugh Fosque, NASA |
| Study Group 3 - Fixed Services below 30 MHz
US Study Group-inactive
Mr. Ted DeHass-ITS, Acting International Chairman - SG 3 | Study Group 8-Mobile Services
Mr. Herb Blaker, Rockwell Int'l |
| Study Group 4 - Fixed Satellite Service
Mr. James B. Potts, Asst Vice President, COMSAT | Study Group 9-Fixed Services Using Radio Relay Systems
Mr. H.E. Weppler, AT&T |
| Study Group 5 - Propagation in Non-Ionized Media
Dr. Harold T. Daugherty, Institute of Telecommunication Sciences, Dept of Commerce | Study Group 10-Broadcasting Svc(Sound)
Study Group 11-Broadcasting Svc(TV)
Mr. Neal McNaughten, FCC |

OCEANOGRAPHY

Monday, P.M., 15 May, Room 1109

Chairman: W. L. Jones, NASA/Langley

Research Center, Hampton, VA

F1-1 THE MODULATION OF SHORT GRAVITY WAVES BY LARGER SCALE
1330 PERIODIC FLOWS - A SECOND ORDER THEORY: G. R. Valenzuela
and J. W. Wright, Naval Research Laboratory, Washington, DC

Keller and Wright's (1975) linear relaxation time model for the microwave scattering and hydrodynamic straining of wind-waves by longer gravity waves has been found adequate to interpret measured modulations of short gravity wind-wave spectra for U_0/C (ratio of orbital velocity to long gravity wave phase speed) up to 0.07 or 0.08 for air friction velocities u_* as large as 30 or 40 cm/sec (moderate wind speeds) for a long gravity wave of 0.575 Hz. Recently Plant et al (1977) find in coastal measurements that the first order relaxation model also predicts the general features of the modulation of centimetric wind-waves by shoaling waves, but not the anomalously large modulations observed when the shallow water wave speed coincides with the wind speed of 4.5 to 6.5 m/sec.

In this work a higher order theory is developed to investigate the modulation of short gravity wind-waves by longer scale flows in an attempt to reconcile the experimental measurements and theory. Explicit results will be given for the second order contributions.

F1-2 SURFACE TRUTH FOR EVALUATING REMOTE MICROWAVE SENSORS OF
1355 OCEAN WAVE FIELDS: WEST COAST EXPERIMENT: J. W. Wright
and W. J. Plant, Naval Research Laboratory, Washington,
DC; and W. L. Jones, NASA/Langley Research Center, Hampton,
VA

Microwave radars will be a principal remote sensor in satellite oceanography. These radars can sense large ocean waves at viewing angles away from nadir because the large waves modulate the short gravity-capillary waves, the predominant microwave scatterers. A CW Doppler radar operated at short range is an effective wave probe for measuring these modulations. The frequency modulation of the microwave signal is due to the orbital speed; the amplitude modulation is due to the modulation of the scattering cross-section. Cross-correlation of signals derived from the frequency and amplitude modulations respectively yields the modulation transfer function which governs, e.g. the wave contrast in radar images of ocean waves.

We measured modulation transfer functions at 9.375 and 1.5 GHz for vertical polarization, depression angles near 40° and winds up to 11 m/sec, in 18 meters of water off Mission Beach, CA during the West Coast Experiment, March 1977. The measurements show that X-band radar can provide strong wave images at low winds though the dependence of the modulations on the wind might decrease the reliability of quantitative determinations of wave height from the imagery. The 1.5 GHz modulations exhibit a desirably weaker dependence on the wind but are still strong enough to produce good imagery.

- F1-3 THE EFFECTS OF ORBITAL MOTION ON THE DISTORTION OF RADAR
 1420 IMAGES ON THE OCEAN: C. T. Swift, NASA/Langley Research
 Center, Hampton, VA (on leave at NOAA/WPL, Boulder, CO),
 and C. L. Rufenach, NOAA, Wave Propagation Laboratory,
 Boulder, CO

A Synthetic Aperture Radar (SAR) develops high resolution two-dimensional images of the earth surface by time-Doppler processing of the return signal. The Doppler history is produced by the motion of the radar and the Doppler frequency is consequently a linear function of time. Along track resolution is then developed by passing the signal through a matched filter. This signal processing is equivalent to generating a synthetic aperture of length $2vT$, where v is the forward velocity of the radar and T is the required integration time. The resultant ground resolution is $\lambda h/2vT$, where λ is the electromagnetic wavelength and h is the altitude of the radar. Cross-track resolution is developed by transmitting pulses of width τ , and recording the time history of the back-scattered signal.

If the target is stationary, all parameters are known a priori, and the signal processing is straight-forward. However, if the target is in motion, Raney⁽¹⁾ has shown that severe defocussing and image displacement can occur if the target is accelerating and/or in constant motion. In order to generalize Raney's results to the imaging of the ocean surface, a large ocean wave was assumed to propagate through a uniform scattering surface. Such scattering would approximately occur if the radar viewing angle is sufficiently far away from nadir so that Bragg scattering dominates. The shape of the large wave was assumed to be a trochoid, which is the simplest model of a wave that supports "orbital" particle motion; i.e., each elementary particle moves in a circle with tangential velocity $a\omega$, where a is the wave amplitude and ω is the radian frequency.

With no motion, the resultant image would be "grey" because of the assumed uniform cross section. However, this is not the case when the scatters are in motion. Because of the varying radial acceleration as seen by the radar, only those scatters near the zero crossings are imaged. Other points along the wave are defocussed resulting from an increasing value of the radial acceleration. Although a sharp image is formed at the zero crossing, displacement occurs because the radial velocity is maximum. Furthermore, the displacement alternates between a forward and backward image shift due to sign changes in the direction of the radial velocity component. Parametric calculations are presented as a function of $a\omega$, and the results are related to the physical characteristics of the ocean waves.

(1) Raney, R. K., "Synthetic Aperture Imaging Radar and Moving Targets", IEEE Trans. on Aerospace and Electronic Systems, Vol. AES-7, May, 1971. pp 499-505.

- F1-4 MEASUREMENT OF DIRECTIONAL GRAVITY WAVE SPECTRA USING A
 1445 MULTIPLEXED DUAL-FREQUENCY MICROWAVE RADAR: D. L. Schuler,
 Naval Research Laboratory, Washington, DC

A technique has been developed, using a dual-frequency radar operating at L-band, which permits remote measurements to be made on directional gravity wave "modulation" spectra. The modulation spectra sensed by the radar and the actual gravity wave spectra appear to be closely related. Past measurements using dual-frequency radars operating first at X-band and later at L-band have not been totally satisfactory because of the long data-acquisition time required for both Doppler processing and signal averaging. Measurements have been made recently using a more highly evolved L-band radar system which is capable of making multiplexed measurements on 50 transmitted frequency pairs in only 5 ms. Multiplexing of the radar data makes possible 1) more accurate measurements of gravity wave spectra since the data is interleaved throughout the entire data acquisition period, and, 2) allows more averaging to be performed during the time interval for which the wave system may reasonably be considered as being stationary. In particular, we have used a frequency synthesizer (capable of switching frequencies in 20 μ s) programmed remotely by a set of frequencies stored by an EPROM, to provide a multiplexed output which is then upconverted to L-band. Examples of wave spectra obtained from measurements made at our experimental site on the Chesapeake Bay will be provided. Data will also be presented which gives the dependence of the fractional modulation, $M(k)$, sensed by the radar as a function of surface wind speed. The relative insensitivity of $M(k)$ with wind speed indicates that radar data taken when the surface wind speed is not known will still yield meaningful wave spectra.

- F1-5 THE SURFACE CONTOUR RADAR, AN INSTRUMENT FOR MEASURING
 1525 OCEAN DIRECTIONAL WAVE SPECTRA: J. E. Kenney, A. E.
 Uliana, Naval Research Laboratory, Washington, DC and
 E. J. Walsh, NASA/Wallops Flight Center, Wallops Island, VA

This paper describes an airborne beam-limited 8.6 millimeter radar with selectable range resolutions of 0.15, 0.3, 0.61, 1.52 meters. The radar is designed to produce a three-dimensional map of the ocean surface. It employs digital pulse compression and frequency diversity with the two frequencies separated far enough to be decorrelated on the sea surface. The system is computer controlled and uses a mechanically-scanned antenna and software range tracking. It produces a real-time, false-color coded elevation map of the surface. The transmit antenna produces a 1.2° pencil beam while receive antenna has a 1.2 x 40° fan beam. By varying the aircraft altitude, the radar can adjust its swath width to equal seven times the dominant ocean wavelength (λ) and the along track resolution to 0.2 λ with data point spacing of 0.1 λ .

- F1-6 SIMULTANEOUS OPEN OCEAN MEASUREMENTS OF SEA SURFACE
1540 ELEVATION AND MICROWAVE BACKSCATTER AT K_A BAND FOR VARIOUS
INCIDENCE ANGLES AND WIND DIRECTIONS: E. J. Walsh, NASA/
Wallops Flight Center, Wallops Island, VA and J. E. Kenney,
Naval Research Laboratory, Washington, DC

This paper deals with measurements taken by an airborne nadir-looking beam-limited 8.6 mm radar with 0.15 m range resolution which scans laterally within $\pm 15^\circ$ of the perpendicular to the aircraft wings. The radar simultaneously produces perfectly registered patterns of the sea surface elevations and relative microwave backscatter. Data will be presented which was taken while the aircraft was in a 15° bank so that the incidence angle varied between 0° and 27° from the vertical and varied through the upwind, crosswind and downwind directions as the aircraft turned in a circle.

- F1-7 ANALYSIS OF A COMPACT HF ANTENNA TECHNIQUE FOR MEASURING
1610 COASTAL WAVEHEIGHT DIRECTIONAL SPECTRA: D. E. Barrick,
Wave Propagation Laboratory, NOAA, Boulder, CO and B. J.
Lipa, Center for Radar Astronomy, Stanford University,
Stanford, CA

There is an increasing need to measure directional wavefields in coastal waters. Low-powered automated shore-based stations are desired having compact, unobtrusive antenna systems; this precludes the use of conventional, narrow-beam long antenna arrays previously employed at HF. A novel receiving antenna system is being tested that uses two electrically small crossed loops and a vertical monopole to form a broad cardioid pattern. This beam is scanned in azimuth by the receiver processing software. The natural angular basis expansion for both the wavefield directional spectrum and the received sea-echo spectrum is the Fourier series. To second order, one obtains a nonlinear integral equation relating the matrix of the desired frequency-dependent Fourier coefficients of the wavefield to the measured second-order Doppler frequency-dependent Fourier coefficients. An accompanying paper presents the method for inverting this system.

From the zeroth coefficient vs wave frequency, one obtains the nondirectional spectrum; the sum of the squares of these coefficients yields the mean-square waveheight. For wind-driven seas, one can obtain the mean wave direction and the directional spread factor for each desired band of wave frequencies. It is also shown that swell arriving from two directions at the same wave frequency can be resolved with this technique.

F1-8
1625 FREQUENCY-DEPENDENT DIRECTIONAL COEFFICIENTS FOR OCEAN WAVE SPECTRA FROM HF SEA-ECHO: B. J. Lipa, Center for Radar Astronomy, Stanford University, Stanford, CA and D. E. Barrick, Wave Propagation Laboratory, NOAA, Boulder, CO

We describe a general method which has been developed to derive the directional ocean wave spectrum from the Doppler spectrum of HF radar backscattered from the sea surface. The second order spectrum is normalized by the first to eliminate unknown path losses and system gains and then inverted to give Fourier moments of the ocean wave spectrum as a function of sea wavelength. In this method, no assumptions are made on the form of the ocean spectrum; it therefore represents an improvement on a previous method in which the spectrum was separated into a wavelength-independent directional factor and an amplitude factor (Lipa 1977, 1978). The present method applies to arbitrary antenna patterns; we discuss application to simulated data from two systems (a) a narrow beam antenna (e.g., a skywave radar) (b) a broad beam antenna which may be rotated in azimuth (described in the preceding paper).

System (a) provides only the even moments of the ocean wave spectrum because of right-left symmetry while both even and odd moments are available from system (b). Zero, first and second order moments are obtainable from a single radar observation with accuracy dependent on the sample size. For a 100-sample average we show that typical confidence limits are 10% for the zero and first order moments are 50% for the second order moments.

Lipa, B.J., 1977, Radio Science, 12, 425.

Lipa, B.J., 1978, J. of Geophys. Res., in press.

FL-9 RADAR SEA CLUTTER MODEL: M. M. Horst, F. B. Dyer, and
1645 M. T. Tuley, Engineering Experiment Station, Georgia
Institute of Technology, Atlanta, GA

Accurate prediction of the performance of a radar system depends upon accurate models of not only the target and radar, but also the background signals. For a surface search radar operating over the ocean, the background signal interfering most with the target return is often sea clutter. Although descriptions of both amplitude distribution shapes and temporal behavior of sea return are required for a complete model, perhaps the most generally useful statistic in a sea clutter model is average cross section per unit area, σ^0 . Over the past ten years, investigators at Georgia Tech have evolved a deterministic parametric model for σ^0 as a function of radar wavelength and polarization, angle of incidence at the radar cell, sea state, and aspect angle between antenna boresight and the wind/sea vector. Georgia Tech's basic sea clutter model has currently been validated over a frequency range of 3-18 GHz for incidence angles from grazing to 15° , average wave heights up to twelve feet, and HH and VV polarizations. Within these domains, the model predicts σ^0 within 5 dB. Recent efforts, based on extremely limited supporting data, have extended the model down to 400 MHz and up to 95 GHz, but further measurements are needed for complete validation.

TUESDAY MORNING, 16 MAY, 0830-1200

Commission B Session 5

SCATTERING

Tuesday A.M., 16 May, Room 0109

Chairman: S. W. Lee, Electrical Engineering

Dept., University of Illinois, Urbana, IL

B5-1 ELECTROMAGNETIC SCATTERING FROM BURIED INHOMOGENEITIES -
0830 A GENERAL THREE DIMENSIONAL FORMALISM: G. Kristensson,
 Institute of Theoretical Physics, Fack, S-402 20
 Göteborg 5, Sweden

In this work we present an extension to electromagnetic fields of the previously - in the scalar field case - developed transition matrix formalism for an infinite surface with a buried inhomogeneity. Green's theorem together with appropriate expansions of the Green's functions and the surface fields are the foundations of the formalism. We choose for the finite inhomogeneity an expansion of the Green's function in spherical vector-waves, but for the infinite surface the plane waves are more suitable. These different expansions of the Green's function also indicate a natural way to expand the fields. The transformation between spherical and plane wave representation is an important technical tool for obtaining the basic equations. The elimination of the surface fields introduces integral and matrix inverses, which contain the mutual coupling and multiple scattering effects of the ground and the buried obstacle. The basic equations have an immediate analogy to the finite scattering case, and the interpretation of the equations is very similar. In the special case of a flat interface the integral inverses degenerate to simple algebraic relations and one obtains a matrix equation which is solved numerically by iteration. Some numerical results will be presented for a plane interface and some simple buried inhomogeneities.

B5-2 BOUNDARY FORMULATIONS FOR SCATTERING FROM HOMOGENEOUS
0855 MATERIAL BODIES: R. F. Harrington and J. R. Mautz,
Dept. of Electrical and Computer Engineering, Syracuse
University, Syracuse, NY

The problem of electromagnetic scattering from a homogeneous material body can be formulated in terms of equivalent electric and magnetic currents over the surface which defines the body. Application of boundary conditions leads to four simultaneous surface integro-differential equations to be satisfied by the unknown equivalent currents. This set of four equations can be reduced to a coupled pair of equations in many different ways by taking linear combinations of the original equations. One linear combination leads to the formulation discussed by Poggio and Miller [1], another linear combination leads to Müller's formulation [2]. Other formulations will be discussed.

The two formulations [1,2] have been solved by the method of moments for dielectric bodies of revolution, and a general computer program is available [3]. Numerical computations will be given for plane-wave scattering from dielectric spheres and from a finite dielectric cylinder. It is shown that the solution is unique for a large class of formulations which include those of [1] and [2].

- [1] A. J. Poggio and E. K. Miller, "Integral Equation Solutions of Three-dimensional Scattering Problems," Chap. 4 of Computer Techniques for Electromagnetics, edited by R. Mittra, Pergamon Press, 1973.
- [2] C. Müller, Foundations of the Mathematical Theory of Electromagnetic Waves, Springer-Verlag, 1969, p. 301.
- [2] J. R. Mautz and R. F. Harrington, "Electromagnetic Scattering from a Homogeneous Body of Revolution," Report TR-77-10, ECE Dept., Syracuse University, November 1977.

- B5-3 ELECTROMAGNETIC SCATTERING BY INHOMOGENEOUS DIELECTRIC
0920 BODIES: D. Y. Wang and P. W. Barber, Dept. of
Bioengineering, University of Utah, Salt Lake City, UT

One of the major limitations to investigating the scattering of electromagnetic waves by three-dimensional dielectric objects is the lack of theoretical techniques for handling complex bodies. In this paper, the Extended Boundary Condition Method is applied to three-dimensional electromagnetic scattering problems involving non-spherical, multilayered, dielectric bodies. The theoretical formulation is reviewed and the capabilities and practical limitations of the method are discussed.

Numerical results show excellent agreement with the Mie theory solution for the multilayered sphere. Furthermore, a built-in test is used to continually check the validity of the numerical results. Calculations of the angular scattering characteristics and the scattering, absorption and extinction efficiencies for oriented multilayered prolate spheroids are presented and the influence of the layers on the overall scattering characteristics is described. The method has application in such diverse areas as investigating the propagation of microwaves through rain and studying the light scattering properties of small chemical and biological particles.

- B5-4 ON THE CONCEPT OF SCATTERER INVISIBILITY:
0945 N. G. Alexopoulos, Dept. of Electrical Sciences and
Engineering, University of California, Los Angeles, CA;
N. K. Uzunoglu, Dept. of Electrical Engineering, National
Technical University of Athens, Athens 147, Greece; and
O. M. Stafsudd, Dept. of Electrical Sciences and
Engineering, University of California, Los Angeles, CA

The concept of scatterer invisibility is discussed by considering the extinction cross-section of scattering objects such as particles and fibers. It is shown, e.g., that the extinction cross section of active particles is zero at discrete frequencies. This implies that in media where such particles are suspended there can be no observation of phase shifts, attenuation or amplification, at these frequencies. Various other interesting scattering effects by homogeneous and inhomogeneous active scatterers will be discussed as well as a possible experimental verification of these phenomena.

B5-5 SCATTERING BY DIELECTRIC STEP DISCONTINUITIES FOR
1035 OBLIQUELY INCIDENT SURFACE WAVES: J. P. Hsu (on leave
from Kanagawa University, Japan), S. T. Peng, and
A. A. Oliner, MRI, Polytechnic Institute of New York,
Farmingdale, NY

Dielectric step discontinuities occur commonly in integrated optical circuits and in some recent millimeter wave integrated circuits. The basic structures on which these steps occur are dielectric layers on a substrate or on a metallic ground plane. Although this study is of interest in its own right, it was also undertaken because of its applicability to waveguiding structures since such steps form the sides of certain waveguides.

The scattering of a surface wave by a step discontinuity between two dielectric waveguides is an important basic electromagnetic boundary value problem, which in the past has been solved only for the case of normal incidence. In the general case of oblique incidence, the problem becomes a vector boundary value problem that requires the coupling of TE and TM modes, in contrast to the normal incidence case where the TE and TM waves can exist independently. We have obtained analytical solutions for the scattering of incident TE or TM waves when an arbitrary number of propagating modes may exist on each side of the discontinuity, and we have found numerical values for a variety of specific cases.

The results of these calculations show that a substantial amount of field is diffracted into other modes. For some modes, 10% to 20% represent typical values. We have also found that for TE mode incidence a Brewster angle effect appears, and we have paid particular attention to the evanescent field behavior of the various modes when total reflection occurs.

B5-6 SCATTERING FROM OBJECTS OVER REAL EARTH: H. S. Cabayan,
1100 J. N. Brittingham, F. J. Deadrick, and J. T. Okada,
Lawrence Livermore Laboratory, Livermore, CA

In this paper, a numerical approach is presented which deals with the problem of scattering from objects over lossy earth. The object maybe a composite of metals and dielectrics and the earth is characterized by its conductivity and dielectric constant. A region (R) around the object is defined which contains all inhomogeneities other than the earth. A finite difference approximation of the vector wave equation is defined throughout (R) and at all metal boundaries, the tangential electric field is set equal to zero. The appropriate boundary conditions over the external boundary (S) of (R) are found using appropriate boundary integral equations the kernels of wich are expressed in terms of Sommerfeld type integrals. In this manner, the finite difference equations can be terminated at (S) and the field quantities of interest inside (R) can be determined.

The Sommerfeld integrals are evaluated by three different methods depending on the relative positions of source points and field points. When the field point and source point are one wavelength and more above the interface, Norton's asymptotic formula will be used. When both points are within a hundredth of a wavelength from the interface, an analytical series representation will be used. For points in between, a bivariate interpolation scheme is used where the values of the integrals at the interpolation grid points are evaluated by numerical integration of the integrals.

B5-7 RADAR SCATTERING MEASUREMENTS OF CONES AND COMPUTATION
1125 OF TRANSIENT RESPONSE: E. K. Walton and J. D. Young,
The Ohio State University ElectroScience Laboratory,
Columbus, OH

The far zone scattered signal amplitude and phase for eight small cone and cone-like targets (sharp and spherically blunted) were measured using a 10-harmonic 20° bistatic radar system. As many as five of the first ten harmonics of 1.085 GHz were transmitted simultaneously. The received vector sum of the harmonics was measured (amplitude and phase) by a network analyzer and stored in a computer. Data were collected as the target moved a half wavelength at the fundamental, and individual data for each harmonic were extracted by Fourier analysis. Complementing the 10-harmonic data were data measured using a swept frequency system. In either system, empty pedestal (background) data were vectorally subtracted and sphere data were used for system calibration.

Data were collected for cones at aspect angles of 0, 10, 20, and 30 degrees for ka from 0.1 to beyond 4. The behavior of the data is compared to Rayleigh theory for the lower frequencies and GTD theory for the higher frequencies. These theories do not overlap and the data allow us to "fill the gap". The data were Fourier transformed to the time domain and the time response of the targets is discussed.

Commission B Session 5

B5-8 SCATTERING OF ARBITRARILY SHAPED PARTICLES IN FOCUSED
1150 BEAM: C. Yeh and S. Colak, Electrical Sciences and
Engineering Dept., University of California,
Los Angeles, CA

By strongly focusing a laser beam in a polydisperse ensemble medium, we have shown that it is possible to obtain the scattering characteristics of individual particles in such medium.

It is known that the scattering characteristics of an object from a focused beam field are considerably different than those from a plane wave field. This is particularly true when a strongly focused beam field is present. The purpose of this presentation is to describe a technique which can be used to provide accurate results for the problem of the scattering of arbitrarily shaped obstacles situated in a focused beam field. Detailed numerical examples will be given.

IMPAIRMENTS TO EARTH-SATELLITE TRANSMISSION

Tuesday A.M., 16 May, Room 1101

Chairman: L. C. Palmer, COMSAT

Laboratories, Clarksburg, MD

CI-1 DIGITAL TRANSMISSION PERFORMANCE OVER COMMUNICATIONS
0830 SATELLITES AS AFFECTED BY PROPAGATION PHENOMENA:
C. Devieux, Jr. and L. C. Palmer, COMSAT Laboratories,
Clarksburg, MD

The long-term and short-term bit-error rate (BER) performance of digital transmission in the TDMA mode of access over 6/4 GHz and 14/11 GHz frequency-reuse communications satellites is a function of the combined effect of propagation phenomena along the transmission path and transmission impairments dictated by earth station and satellite transponder characteristics.

This paper outlines the potential impact on long-term and short-term BER performance, evaluated with respect to accepted or proposed BER objectives and outage time objectives for PCM-telephony, of various propagation phenomena such as rain attenuation and depolarization and signal fading due to tropospheric and ionospheric scintillation. Various techniques which could be used to correct for performance degradations caused by these effects are discussed and implications for earth station equipment design requirements are reviewed.

The possible impact on TDMA synchronization and on modem synchronization circuits performance is also discussed especially during the occurrence of rain attenuation and scintillation events causing deep signal fades of short-duration. The possible implications on the design requirements for TDMA synchronization and modem synchronization circuits are discussed. Areas where more refined statistical characterization of propagation phenomena appears to be needed are outlined.

C1-2 SATELLITE SIGNAL LEVEL DISTRIBUTIONS FOR IONOSPHERIC
0900 SCINTILLATION: D. J. Kennedy, COMSAT Laboratories,
Clarksburg, MD

Historically, the statistics of ionospheric scintillation have been presented in a manner which is of limited use in predicting impact on digital transmission over satellite links. Specifically, the data are often reduced in terms of occurrence probabilities for given peak-to-peak (p-p) fluctuations while what is needed are instantaneous signal level distributions, average durations of specified fade depths, intervals between fades of a given depth, etc. Here the results of an effort to derive these statistics for 4 and 6 GHz paths are presented for a particular site which experiences significant scintillation activity (Tangua, Brazil). The measured p-p distribution at 6 GHz is used to first-derive the expected p-p distribution at 4 GHz. Then assuming a model of Rice-Nakagami fading, the instantaneous level distributions are derived for worst month and the year.

It is found for the worst month that 0.3 percent of the time the signal fades by 3.1 dB at 4 GHz and 1.6 dB at 6 GHz with respect to the median level. Annually, at the 0.1 percent outage level, the corresponding fade depths are 2.6 and 1.3 dB for 4 and 6 GHz respectively. At the same fade level with respect to the median, it is shown that at 6 GHz the outage based on instantaneous signal level is only 1/15 of that which would be estimated by the p-p distribution. The effect of a varying sunspot number has also been considered, although observations have not extended over a full eleven year cycle. It is estimated that, for the next solar sunspot peak in 1979-80, the dB values or margins may have to be increased by 0.5 to 1 dB at 6 GHz and 1 to 2 dB at 4 GHz relative to those given above to achieve the same levels of outage. Finally, recent studies of the duration and interval statistics with fade depth as a parameter are summarized.

C1-3 OPTIMUM SHAPE SURFACE ACOUSTIC WAVE BANDPASS FILTERS FOR
0930 SPECTRALLY EFFICIENT PSK MODEMS: N. G. Jones, Defense
Communications Agency, Reston, VA

As the demand for digital satellite service increases, the available bandwidth becomes increasingly congested. Frequency Division Multiple Access requires spectral control filtering at both the earth station transmitter and receiver for each user of a satellite to limit the transmitted bandwidth and provide for rejection of adjacent channel interference. However, the satellite power is also limited and techniques to reduce the bandwidth of satellite users should not result in a substantial increase in power to produce an acceptable bit error rate. Offset Phase Shift Keyed modems (operating at data rates up to 10 Mbps) of the Defense Satellite Communications System will use the filters which have been developed.

The filters which have been developed and tested are Surface Acoustic Wave (SAW) filters with an optimum bandpass characteristic for digital transmission. These optimum shape filters have been computer analyzed, compared to conventional filter types, manufactured and satisfactorily tested with multiple accesses in a satellite transponder. The SAW filter technology offers a nearly linear phase response (which is important for digital transmission), compact size and generally lower cost than conventional group delay equalized conventional filters. The optimized bandpass shape offers appreciably superior performance compared to conventional shapes such as Butterworth for digital transmission. Computer analysis results and test results for FDMA tests in a linear and non-linear satellite transponder will be presented.

C1-4 ADAPTIVE INTERFERENCE CANCELLATION FOR ELECTROMAGNETIC
1015 COMPATIBILITY IN MULTIPLE TRANSMIT-RECEIVE RADIO
COMMUNICATION SYSTEMS: C. L. Golliday, Jr., Naval
Research Laboratory, Washington, DC

In multiple transmit-receive radio communication systems, transmitters and receivers must often share a common platform such as a tower, ship, airplane, or spacecraft. The potential for severe electromagnetic interference is great due to the proximity of high-powered transmitters to sensitive receivers. Traditional methods of achieving electromagnetic compatibility (EMC) include RF filtering, physical separation between the transmit and receive antennas, and antenna pattern control.

Another method of achieving EMC is adaptive interference cancellation (AIC). In systems where separate transmit and receive antennas are employed, a sample of the radiated interference waveform is coupled from the output of the interfering transmitter and injected into the receiver. The sample is adaptively filtered to cancel interference that is coupled to the receiver through the receive antenna. The AIC technique provides transmit-to-receive antenna decoupling that can supplement or replace other EMC techniques. It is especially applicable to wideband communication systems where other EMC techniques (e.g., narrowband filtering) are unsuitable or difficult to implement. A shortcoming of the AIC technique is the possibility of desired signal cancellation if the desired signal "contaminates" the interference sample. This can happen because the transmit antenna also acts as a receive antenna. The problem can be avoided by careful design.

- C1-5 ON THE SIMILARITY BETWEEN VARIOUS LINEAR SYSTEM
1045 IDENTIFICATION TECHNIQUES: T. K. Sarkar, Gordon McKay
Laboratory, Harvard University, Cambridge, MA

This paper deals with the modeling of a linear system by poles and residues from a measured finite length, input-output record of the system. The objective is to illustrate that several different formulations for characterizing the impulse response of a system yield identical sets of equations.

[For detailed mathematical derivations, please see Scientific Report No. 2 on Air Force Contract F33615-77-C-2059, Air Force Weapons Laboratory, December 1977.]

- C1-6 NEUTRINO BEAM TELECOMMUNICATIONS: F. J. Kelly,
1115 H. Überall, A. W. Saenz, and N. Seeman, Naval Research
Laboratory, Washington, DC

It has been suggested that neutrino beams might be utilized for telecommunications even over global distances. A general description of such a link and some estimates of potential communication channel capacity will be given. Uncertainties regarding signal count rate and background noise will also be discussed. For example, the Tevatron (now under construction) should be able to cause 10^4 neutrino events per hour in a water detector of 10^6 m³ volume at a range of 10^3 km. Utilizing a storage ring at the transmitter and pulse position modulation, this neutrino event rate can support a communications rate of 8.1×10^3 bits per hour.

REMOTE SENSING OF THE ATMOSPHERE FROM SPACE

Tuesday A.M., 16 May, Room 1109

Chairman: I. Katz, Applied Physics Laboratory,
Johns Hopkins University, Laurel, MD

F2-1 AN ACTIVE MILLIMETER-WAVE TECHNIQUE FOR THE REMOTE
0900 MEASUREMENT OF ATMOSPHERIC PRESSURE AT THE EARTH'S
SURFACE: D. A. Flower, Jet Propulsion Laboratory,
Pasadena, CA; C. Gatley, H. W. Lightfoot, and G. E.
Peckham, Heriot-Watt University, Edinburgh, Scotland

The remote sensing of meteorological parameters with satellite instruments has been established as an economic method for data acquisition. Cloud cover, temperature profiles, water vapor and liquid water content of the atmosphere are routinely monitored from space while SEASAT A has instrumentation which will provide surface winds over the oceans. However, for measurements of pressure, which has historically been the basis of weather forecasting, we still rely on an inadequate network of ground based instruments. In this paper details are discussed of a design study for an active millimeter wave instrument to measure atmospheric pressure at the surface of the Earth from an orbiting satellite.

Pressure can be deduced from measurements of atmospheric transmissivity at several frequencies in the wings of the 60 GHz oxygen absorption band. Measurements must be made of the ratios of the amplitudes of signals reflected from the ocean surface for pairs of frequencies. By carefully selecting the operating frequencies the pressure can be determined without a knowledge of other meteorological parameters. Numerical simulations using a range of real atmospheres have been used to validate the frequency selection procedure. Atmospheric variability introduces an error, which when combined with an instrumental signal-to-noise error and an error associated with the statistics of sea surface reflectivity shows that the expected error in pressure measurement is between 1 and 2 mb if a reasonable surface coverage and resolution scheme is adopted. An assessment of the complete microwave system design indicates that the required instrumental stabilities, sensitivities and accuracies can be met with state-of-the-art components with the exception of the need for modest upgrading of the power output now available from millimeter wave sources. The development of these sources is in progress and should not delay the construction of an instrument for an early Spacelab flight to prove the Microwave Pressure Sounder as a technique for providing accurate global surface pressure fields from an orbiting satellite.

F2-2 A TWO SATELLITE TECHNIQUE FOR MEASURING ATMOSPHERIC
0930 SURFACE PRESSURE: A. D. Goldfinger, G. Bush, W. L.
Ebert, S. N. Foner, R. W. Hart, and I. Katz, Applied
Physics Laboratory, Johns Hopkins University, Laurel,
MD

The refractive path length effect on a radar signal passed through the troposphere and reflected from the sea surface is shown to yield an accurate estimate of the surface atmospheric pressure. By using two satellites, one as the transmitter and one as the receiver, it is possible to use signal paths that form a small grazing angle with the surface, thereby maximizing the amount of troposphere passed through and hence the magnitude of the effect. Sensitivity to errors in knowledge of geoidal height is also decreased.

In addition to the above instrumentation, the satellites also carry radar altimeters and nadir looking multi-frequency microwave radiometers to determine other needed quantities. The primary instruments measure the time delays both of signals reflected from the sea surface and those traveling directly from one satellite to the other.

A system optimization study shows that a two-satellite demonstration system operating at a surface grazing angle of 4.3° can measure surface pressure to an accuracy of about 4 mb. An operational constellation of satellites, due to reduced dependence on geoidal modeling, would operate at a surface grazing angle of 5.5° and be accurate to about 3 mb.

F2-3 RECOVERY OF REFRACTIVITY PROFILES AND PRESSURE AND
1000 TEMPERATURE DISTRIBUTIONS IN THE LOWER ATMOSPHERE FROM
SATELLITE-TO-SATELLITE RADIO OCCULTATION DATA: C. W.
Murray, Jr., NASA/Goddard Space Flight Center, Greenbelt,
MD

This paper demonstrates the feasibility of recovering lower atmospheric refractivity profiles and pressure and temperature distributions from satellite-to-satellite radio occultation data at S-band frequencies.

The tracking data (one-way range rate) is inverted by an integral transformation (Abel transform) to obtain a vertical refractivity profile above the point of closest approach of the ray connecting the satellites. The only restriction concerning the refractivity is that it is spherically symmetric. After accounting for ionospheric and water vapor effects; pressure and temperature are obtained from values of dry refractivity using the hydrostatic equation and perfect gas law.

Two methods are investigated for recovering atmospheric parameters. In the first method dry refractivity (which is proportional to density) is numerically integrated to obtain pressure. Temperature is then obtained from pressure and dry refractivity. In the second method the base temperature and lapse rate in an atmospheric layer are solved for by nonlinear least squares using values of dry refractivity. Pressure is then obtained from temperature and dry refractivity.

An error analysis is performed to assess the sensitivity of random and bias-type errors upon recovered parameters.

An example is given using occultation data obtained during satellite-to-satellite tracking of NIMBUS-6 via the geostationary ATS-6 satellite.

F2-4 AVERAGE RAINFALL DETERMINATION FROM A SCANNING BEAM
1045 SPACEBORNE METEOROLOGICAL RADAR: J. Eckerman, R.
Meneghini, and D. Atlas, NASA/Goddard Space Flight
Center, Greenbelt, MD

A simple spaceborne meteorological radar technique has been studied for the remote sensing of rain over land and sea. At attenuating wavelengths, the ratio of the return powers from the surface in the presence and absence of rain along the radar beam, yields an expression for the total two way attenuation. Using the standard k-R relationship and the measured value of attenuation, an estimate of the average rain rate can be obtained.

The performance of the technique has been assessed over a range of beamwidths, transmit powers, and wavelengths. The effects of frequency agility and the inhomogeneity of the surface scattering properties have been included in the model. The results are presented by plotting the error statistics of the rain rate estimate for rain rates between 5 mm/hr and 100 mm/hr. It has been shown that the lower frequencies, that exhibit higher signal to noise ratios, are more effective in predicting the more intense rain rates, whereas the lower rain rates are more accurately determined by employing higher frequencies where the error variance of the estimate is smaller.

F2-5 PULSED COHERENT LIDAR SYSTEM FOR SATELLITE-BASED WIND
1115 FIELD MEASUREMENT: R. M. Huffaker, P. A. Mandics,
T. R. Lawrence, and F. F. Hall, Jr., Dept. of Commerce,
NOAA, Environmental Research Laboratories, Wave
Propagation Laboratory, Boulder, CO

The accuracy and lead time of current numerical weather predictions are limited by the relatively wide separation of atmospheric measurements in space and time. Advancing laser technology has led NOAA, under a joint agreement with the USAF SAMSO-DMSP, to conduct a feasibility study for a satellite-borne coherent lidar system for global wind measurement. Pulsed CO₂ coherent lidar systems have achieved ranges of 10 km in the lower atmosphere, with laser pulse energies of approximately 30 mJ. The minimum system requirements considered in the study are to obtain wind field measurements with 1 km vertical and 300 km horizontal resolution from the surface to 15 km altitude while maintaining a measurement accuracy of $\pm 1 \text{ ms}^{-1}$ (speed) and $\pm 10^\circ$ (direction). The system will be compatible with the space shuttle vehicle requirements. A computer simulation of the pulsed coherent lidar satellite system has been developed and incorporates atmospheric propagation, backscatter, and refractive turbulence effects; global wind, aerosol, and cloud statistics; and all relevant engineering parameters in order to study the lidar system design questions. Space environment constraints are also being determined. No limiting problems have been identified to date. Detectable signal-to-noise ratios are predicted at CO₂ wavelengths for the 300-800 km altitudes and the 0° - 52° nadir angles required by the study.

TUESDAY AFTERNOON, 16 MAY, 1330-1645

Commission B Session 6

TRANSMISSION LINES

Tuesday P.M., 16 May, Room 0109

Chairman: R. E. Collin, Division of Electrical Science
and Applied Physics, Case Western Reserve University, Cleveland, OH

B6-1 RECENT THEORETICAL, NUMERICAL AND EXPERIMENTAL RESULTS
1330 FOR MULTICONDUCTOR TRANSMISSION-LINE NETWORKS: F. M.
 Tesche, T. K. Liu, and S. K. Chang, Science Applications,
 Inc., Berkeley, CA

As described in a previous URSI meeting (Amherst, 1976), we have developed a general multiconductor transmission-line model for analysis of the transient (EMP) response of systems. Recent improvements of this model include the distributed excitation of a multiconductor transmission-line network by an incident electromagnetic field.

In the present paper, a previous review of multiconductor transmission-line theory is presented, as well as a discussion of the treatment of large multiconductor networks. Experimental results for some sample multiconductor transmission-line networks (provided by Mission Research Corporation) will be compared with computational results using the multiconductor analysis.

- B6-2 TIME DOMAIN ANALYSIS OF MULTICONDUCTOR TRANSMISSION
1350 LINES WITH BRANCHES IN INHOMOGENEOUS MEDIA: A. K.
Agrawal, L. D. Scott, and H. M. Fowles, Mission
Research Corp., Albuquerque, NM

An effective method for computing the time domain response of lossless multiconductor transmission lines with branches in a cross-sectionally inhomogeneous dielectric media is presented. Lines of this type are characterized by multiple propagation modes having different velocities. The theory of wave propagation on lossless multiconductor transmission lines with inhomogeneous dielectrics is used to obtain the modal amplitudes on the uniform sections of the line. The scattering matrix for the junction is used to compute the transmitted and reflected waves in the different branches at the junction. Each mode arriving at the junction excites multiple modes in all branches. The method described in this paper identifies all propagation modes in all branches of the line and leads to the direct physical interpretation of the results. The method is general and can be applied to either partially or completely nondegenerate cases. Experimental results for a six-conductor transmission line having a single branch are found to be in good agreement with the results computed using the described method.

- B6-3 EXPERIMENTAL CHARACTERIZATION OF MULTICONDUCTOR
1410 TRANSMISSION LINES IN INHOMOGENEOUS MEDIA USING TIME
DOMAIN TECHNIQUES: A. K. Agrawal, H. M. Fowles, and
L. D. Scott, Mission Research Corp., Albuquerque, NM

An effective method for the time domain characterization of lossless multiconductor transmission lines with inhomogeneous dielectrics is presented. Lines of this type are characterized by multiple propagation modes with unequal velocities. Time domain reflectometry is used to obtain the characteristic impedance and the modal velocities of the line. The pulse or step function response of the line is used to obtain the modal amplitudes which in turn determine the velocity matrix. The appropriate multiconductor transmission line equations involving inhomogeneous dielectrics are solved to obtain the per unit length inductance and capacitance matrices in terms of the characteristic impedance and velocity matrices. The method is concise and complete and identifies the propagation modes in a way that permits direct physical interpretation of the results. The experimental results for a four-conductor transmission line are presented and are found to be in good agreement with independent frequency domain measurements within the accuracies of the measurements.

B6-4 ON ELECTROMAGNETIC FIELD EXCITATION OF UNSHIELDED
1430 MULTICONDUCTOR CABLES: C. E. Taylor, Mississippi State
University, Mississippi State, MS and J. P. Castillo,
Air Force Weapons Laboratory, Kirtland AFB, NM

The response of multiconductor cables to an electromagnetic illumination may be determined by using multiconductor transmission line theory. But this technique requires that the relative orientation of the wires within the cable remain fixed over the cable run or at least maintain some identifiable weave pattern. However, the typical cable bundle is not intended to be a multiconductor transmission line, and generally the relative orientation of wires varies considerably and without pattern.

This paper considers a few simple cable configurations and determines the response under different load conditions while examining the common mode current as related to the individual wire currents. To obtain the results three separate solution techniques are employed. Firstly, standard coupled circuit analysis is used with Faraday's law--the quasistatic formulation. Secondly, transmission line theory is used and thirdly, wire antenna theory is utilized to determine the wire currents. Inasmuch as transmission line theory neglects reradiation from the wire configuration a comparison of the aforementioned three results gives an indication of the accuracy and range of validity of the transmission line formulation.

B6-5 COUPLING BETWEEN TWO OPTICAL FIBERS THROUGH A COAXIAL
1505 DIELECTRIC SLEEVE: P. L. E. Uslenghi and A. -G. Kazkaz,
Communications Laboratory, Dept. of Information Engineering,
University of Illinois, Chicago, IL

A new method for head-on coupling of two optical fibers is described and analyzed in detail. It utilizes a dielectric tube, coaxial with both fibers, whose refractive index equals that of the fibers' core. A matching epoxy with refractive index equal to that of the fibers' cladding is inserted between the sleeve and the fibers. The proposed device is useful for single-mode fibers, and may be employed not only as a directional coupler but also as a mode selector. Unlike other fiber-joining techniques, our method is insensitive to the end preparation of the fibers and to the distance between ends, and is not very sensitive to the axial offset between the two fibers. The critical parameters which control the coupling are the wavelength, the refractive indexes of core and cladding, the coupling length between each fiber and the sleeve, and the difference between the inner radius of the sleeve and the radius of the core.

The analysis of the boundary-value problem for the proposed coupler is conducted by extending to cylindrical structures the strong-coupling method developed by Uslenghi and Kazkaz (abstracts for URSI Annual Meeting, Amherst, October 1976, p. 150) for two parallel rectangular waveguides. In the limit when both the coupling length and the distance between the inner surface of the sleeve and the outer surface of the core are large compared to the wavelength, our analysis coincides with the weak-coupling results obtained via the Miller-Marcatili approximation. This research was supported by the National Science Foundation under grant Eng77-06544.

B6-6 THEORY OF DISPERSION IN WIDE MICROSTRIP: D. C. Chang
1525 and E. F. Kuester, Electromagnetics Laboratory, Dept.
of Electrical Engineering, University of Colorado,
Boulder, CO

Previously, dispersion characteristics of open microstrip lines have only been obtained through purely numerical procedures, by a number of authors. In general, a set of coupled integral equations for the current distributions with complicated kernels must be solved. In the special case of a narrow (compared to substrate thickness) strip, several authors have presented analytical theories for the first or second order effects of frequency. The present paper will make less restrictive assumptions about strip width, but suppose that the substrate permittivity $\epsilon_r \gg 1$. It is then possible to obtain a solution under this approximation similar to that previously obtained by the authors for the narrow strip, but which now indicates that the transverse distributions of charge and of longitudinal current density are fundamentally different, and gives a closed form for the modal equation which again includes first and second order dispersion effects. Numerical results and comparisons with narrow-strip results will be presented.

- B6-7 INTEGRAL EQUATION SOLUTION FOR THE FIELDS IN THE APERTURE
1545 OF A PARALLEL PLATE WAVEGUIDE OPENING INTO A PLANE COVERED
BY A DIELECTRIC SLAB: R. D. Nevels and C. M. Butler,
University of Mississippi, University, MS

Transmission of electromagnetic waves through seams and apertures in waveguides and conducting screens covered by dielectric slabs has important applications in the area of communications and in the study of EMP penetration. In cases where the slit or aperture appears in a waveguide, measurements and approximations for input impedance are readily available. It is commonly recognized that some portion of the energy from fields that penetrate such apertures will be diverted into surface wave modes. The energy of the field coupled into these modes depends upon the electrical parameters and thickness of the dielectric slab and manifests itself in a degradation of the far field radiation pattern of the aperture.

In this paper we present an integral equation solution for the aperture electric field in the case of a parallel-plate guide opening into a ground plane covered by a dielectric slab, with TEM excitation in the guide and TE excitation in the exterior region. The integral equation contains an infinite series due to the presence of higher order waveguide modes in the aperture as well as a two-dimensional Sommerfeld integral term accounting for the presence of the slab. A solution is obtained for the integral equation by means of the method of moments. Results are given for the aperture field as a function of various parameters of the system. A comparison is also made of the far fields as a function of aperture width and slab thickness from the results of this paper and from the measured data of other authors.

B6-8 PROPAGATING MODES ON A BURIED LEAKY COAXIAL CABLE:
1605 W. S. Plate, D. C. Chang, and E. F. Kuester, Electro-
magnetics Laboratory, Dept. of Electrical Engineering,
University of Colorado, Boulder, CO

Recently, buried wires operating in the HF range (~ 100 MHz) have found important application as wave guiding structures in the design of groundwave radar detection systems for vehicle monitoring or perimeter surveillance. Leaky coaxial cables, which allow energy to couple continuously into the surrounding medium via a braid or periodic slots, can be used if they are placed in proximity to the earth's surface in order to enhance coverage and avoid excessive loss in the earth itself. We examine characteristics of discrete propagating modes on a buried leaky coaxial cable. Provided the transfer inductance of the braid is small, we found three distinct propagating modes for most of the cable depths. The first mode has a field structure closely associated with the TEM-mode of a coaxial line and referred to as a bifilar mode because of its almost equal but opposite current on the two conductors. The second mode has a field structure located mainly outside the cable in the earth region and is referred to as a monofilar mode. The third mode which exists only for certain cable depths has a field more spread out over the air-earth interface and is referred to as a surface-attached mode. Unlike the case of an elevated wire, no degeneracy of modes is observed for parameters of practical interest.

B6-9 THEORY OF NONUNIFORM TIME-VARYING TRANSMISSION LINES:
 1625 P. L. E. Uslenghi, Communications Laboratory, Dept. of
 Information Engineering, University of Illinois,
 Chicago, IL

A two-conductor transmission line whose constitutive parameters are functions of the distance x along the line and of the time t is considered. If $R(x,t)$ and $L(x,t)$ are respectively the series resistance and the series inductance per unit length, whilst $G(x,t)$ and $C(x,t)$ are respectively the shunt conductance and the shunt capacitance per unit length, then the voltage $v(x,t)$ and the current $i(x,t)$ obey the following generalized form of the telegrapher equations:

$$v_x = -(R + L_t)i - Li_t, \quad i_x = -(G + C_t)v - Cv_t$$

where the subscripts indicate partial derivatives. If no restrictions are imposed upon the functional forms of R , L , G and C , then the decoupling of this system leads to a rather complicated third-order partial differential equation for either voltage or current. There are, however, two particular cases in which such decoupling leads to second-order partial differential equations; these two cases are studied in detail.

The first case occurs when

$$R + L_t \equiv 0, \quad G + C_t \equiv 0,$$

whereas the second case occurs when

$$\begin{aligned} R(x,t) &= F(x)r(t), & L(x,t) &= F(x)l(t), \\ G(x,t) &= \Phi(x)g(t), & C(x,t) &= \Phi(x)c(t), \end{aligned}$$

where F and Φ are arbitrary functions of x , whereas r , l , g and c are arbitrary functions of time. In either case, $v(x,t)$ is known if $v(x,0)$, $v_t(x,0)$, $v(0,t)$, $v_x(0,t)$ are given and if the solution of a Volterra integral equation in two variables can be found; a dual analysis applies to the current.

Further developments as well as examples of the above theory are given, and applications are discussed. This research was supported by the Air Force Office of Scientific Research under grant AFOSR-77-3253.

SYSTEM ASPECTS OF ANTENNAS AND DUAL POLARIZATION TRANSMISSION

Tuesday P.M., 16 May, Room 1101

Chairman: W. F. Utlaut, Office of

Telecommunications, Boulder, CO

C2-1 SOME SYSTEM ASPECTS OF MULTIPLE BEAM COMMUNICATION
1330 SATELLITE ANTENNAS: A. Sinha, COMSAT Laboratories,
Clarksburg, MD

Increasing use of multiple beam satellite antennas and 'frequency reuse' is to be anticipated in the future in order to optimize the utilization of the allocated spectrum. Three types of beam multiplicity are envisioned: (1) Beams utilizing different frequency bands, (2) Spatially non-overlapping or disjoint beams with identical frequency bands and polarizations, and, (3) Beams with orthogonal polarizations. Multiple beams can be generated from a single antenna with the use of multiple feeds, the mutual coupling between the feeds significantly affecting the antenna pattern.

In this paper, an overview is presented of some of the systems considerations of multiple beam antennas for communications satellites. Factors relating to geographical locations to be covered and shaping of the beams, provision of interbeam connectivity, and the utilization efficiency of the available bandwidth in various transmission modes are discussed. For commercial satellites, these factors are intimately related to the geographical distribution and the communications requirements of the users in the network. Elements of general algorithms for beam formation based on the above factors and other systems constraints are presented. In particular, the impact of mutual coupling among the feeds of a multi-feed antenna on its performance characteristics (particularly in the far zone pattern of the cross-polarized field) is indicated. Methods to analyze mutual coupling and to minimize the resulting system degradation are suggested.

C2-2 IN-ORBIT VERIFICATION OF INTELSAT V ANTENNA POLARIZATION
1400 PERFORMANCE: W. J. English, INTELSAT, Washington, DC

The INTELSAT V satellite series employs frequency reuse by means of spatially isolated and dual-orthogonally polarized antenna beams at 4 and 6 GHz. Frequency reuse conserves spectrum in commercial communications satellite systems but requires exceptional polarization and sidelobe performance from the antenna systems.

This paper discusses the polarization, tracking and amplitude resolution capabilities which will be necessary in the earth station antenna system utilized for in-orbit verification tests of the INTELSAT V satellite antennas and the design difficulties encountered in realizing such a test antenna system. In addition, atmospheric and propagation effects which can limit the accuracy of measurement results are addressed.

Ground station test antenna polarization isolations greater than 40 dB are required in order to verify that the satellite antenna polarization performance is within 4 dB of its specified 32.75 dB value. The constraints which this type of requirement places on feed system hardware design, frequency bandwidth, tracking methods and optimal antenna geometries are discussed.

C2-3 THE EFFECT OF POLARIZATION DIVERSITY ON RECEIVING
1430 SYSTEMS: M. Lavi and W. A. Davis, Air Force Institute
of Technology, AFIT/ENG, Wright-Patterson AFB, OH

The effects of the polarization diversity of an electromagnetic wave upon reception has been considered extensively in the radio astronomy literature. However these studies have been limited to the case where the transmitted polarization state is time-varying and the receiver polarization state is kept fixed. This paper presents the effects of polarization diversity as employed by both the transmitter and receiver. The definition of the Stoke's parameters given in the radio astronomy literature is revised to enable its usage in a more general situation with both the transmitter and the receiver employing time-varying polarization diversity processes. In addition, the time average used for evaluating the likelihood of reception is replaced by the ensemble average of the polarization processes (equivalent for ergodic processes). Thus, the expected value of the received power is related to the autocorrelation of the received voltage or equivalently its power spectral density.

The system is modelled by two orthogonally-polarized, amplitude controlled, transmitting antennas connected to a common source through a power splitter and by a similar receiving system. The likelihood of reception is represented by the expected value of the received power which is given by the integral of the power spectral density at the receiver. It is shown that the likelihood of reception depends upon the spectral characteristics of the correlation between the transmitter and receiver polarization diversity processes. This spectral characteristic is additionally spread through convolution by the transmitter source spectrum. The resultant likelihood of reception is obtained by integrating the resultant spectrum over the bandwidth of the receiver and comparing to the polarization matched case.

C2-4 AN ADAPTIVE NETWORK FOR COMPENSATION OF UP-LINK AND
1515 DOWN-LINK RAIN DEPOLARIZATION: R. W. Gruner and
F. L. Frey, COMSAT Laboratories, Clarksburg, MD

An adaptive compensation network using cascaded quarter-wave and half-wave polarizers has been used for the correction of rain-induced depolarization. This correction is necessary during heavy rainstorms to maintain acceptable polarization performance in dual-polarized 4/6-GHz satellite communication links. A receiver detects the cross-polarized signal and in conjunction with a microprocessor produces error voltages to drive the down-link polarizers. This system maintained a 30-dB isolation in the presence of heavy rainfall that uncorrected would have degraded the isolation to 12-dB. An extension of this system is to compensate for up-link depolarization.

Measured up-link and down-link polarization isolation data will be shown and measurement techniques discussed. The measurements confirm that the differential phase shift of rain is proportional to frequency and that up-link and down-link depolarization is correlated. Therefore, the up-link polarizers can be positioned by the microprocessor using the positional information of the down-link polarizers. This will provide simultaneous correction on both the up- and down-links. A complete feed network providing this correction has been developed at COMSAT Labs.

- C2-5 THE PHASE OF CROSSPOLARIZED SIGNALS AND ITS EFFECT ON
1545 A CANCELLATION SYSTEM: W. P. Overstreet and C. W. Bostian, Electrical Engineering Dept., Virginia Polytechnic Institute and State University, Blacksburg, VA

Orthogonal polarization frequency reuse is a certainty in the future of satellite communications. At frequencies above 10 GHz the success of this technique depends upon perfecting a means of compensating for precipitation-induced crosspolarization. Adaptive cancellation techniques and restoration of orthogonality of signals appear to be viable solutions.

The proposed schemes for cancellation and for restoring the orthogonality of signals depend on the phase relationship of the signals received by the system. This paper investigates the phase relationship of the rain-generated crosspolarized signal relative to the copolarized signal. Theoretical results obtained from commonly accepted propagation models are presented. Experimental data from the Communications Technology Satellite beacon and from the Comstar beacons are presented and the correlation between theory and data is discussed. The system implications of phase variations are also discussed.

- C2-6 SPATIAL BEHAVIOR OF BROADBAND SIGNAL-MATCHED ARRAY
1615 ANTENNAS: F. I. Tseng, Electrical Engineering Dept., Rochester Institute of Technology, Rochester, NY and D. K. Cheng, Electrical and Computer Engineering Dept., Syracuse University, Syracuse, NY

In modern radar applications pulse compression is a technique for obtaining the resolution and accuracy of a short pulse and the detection capability of a long pulse. A matched filter is used to maximize the ratio of the output peak-signal to mean-noise power. However, the response to broadband signals incident on a signal-matched array designed for a single-frequency operation is not well understood and information on array characteristics in the transient state is generally not available. Because electromagnetic wave travels with a finite velocity the pattern characteristics of large arrays are not established instantaneously. This paper examines the space-time response of a matched-filter equipped Chebyshev array to both a pulse-compression signal and bandlimited white noise. Computed results show that in no case does the highest sidelobe level of the spatial pattern exceed the designed level. An expression for the expected (statistical average) pattern of an array for bandlimited white noise is derived and typical results are presented.

SCATTERING BY RANDOM MEDIA AND ROUGH SURFACES

Tuesday P.M., 16 May, Room 1109

Chairman: R. L. Lang, The George

Washington University, Washington, DC

F3-1
1330 MULTIPLE SCATTERING EFFECTS IN MICROWAVE PROPAGATION
THROUGH PRECIPITATION MEDIA: V. N. Bringi, V. K. Varadan,
V. V. Varadan, and T. A. Seliga, The Atmospheric Sciences
Program and Dept. of Engineering Mechanics, The Ohio State
University, Columbus, Ohio

A multiple scattering theory of electromagnetic waves in the atmosphere containing identical, randomly distributed hydrometeors using Waterman's T-matrix of a single scatterer and a statistical averaging procedure using Lax's "quasicrystalline" approximation is developed. Equations for the average amplitudes of the scattered and exciting fields are obtained and solved for the effective propagation constant of precipitation-filled media. Calculations of the effective propagation constants for rain and hail-filled space are given over a wide range of concentrations and ka-values extending from the Rayleigh to the resonance regions. For rain-filled media the scatterers are assumed to be identical, spherical and randomly distributed while for hail-filled space the scatterers are assumed to be identical, oblate spheroidal, randomly oriented and randomly distributed. Comparisons with the single scattering approximation are presented to determine whether multiple scattering effects are important in the cases studied. These results have important applications to terrestrial and satellite microwave communications links.

F3-2 WAVE FLUCTUATIONS IN RAIN AND TURBULENCE INCLUDING
1350 TRANSMITTER AND RECEIVER CHARACTERISTICS: A. Ishimaru,
 Electrical Engineering Dept., University of Washington,
 Seattle, WA

The fluctuations of a wave in turbulence, rain and other scatterers in the atmosphere are caused by the incoherent field which has certain angular spread (spectrum). Therefore, when the beamwidths of transmitting and receiving antennas are comparable to the angular spread, the fluctuation characteristics are greatly affected by the transmitter and receiver characteristics. Also, when a folded path is used, the reflector size needs to be taken into account in the fluctuation analysis. This paper presents a study of the effects of antenna beamwidths on amplitude and phase fluctuations, variances, and frequency spectra of a wave in turbulence and rain. For a weak fluctuation case, general fluctuations are given which include the effects of both turbulence and rain (and other scatterers). This is based on the modification of the Rytov solution to include the transmitter and receiver beamwidths. Both cw and pulse waves are considered and the relation with the aperture averaging effect is discussed. For a strong fluctuation case, expressions are given for spectra and variances including the effects of transmitter and receiver beamwidths.

- F3-3 THE MEAN GREEN'S DYADIC FOR A HALF-SPACE RANDOM MEDIUM -
1410 A NON-LINEAR APPROXIMATION: H. S. Tan, Electrical
Engineering Dept., University of Malaya, Kuala Lumpur,
Malaysia and A. K. Fung, Electrical Engineering Dept.,
University of Kansas, Lawrence, KA

In this paper we consider the vector problem of a source embedded in a half-space random medium, and derive a zeroth order solution for the mean Green's dyadic in the non-linear approximation. This is done by applying a two-variable expansion method to obtain a perturbation solution of the Dyson equation for the mean Green's dyadic. The final results of the dyadic are given in closed form as a corrected effective propagation constant, including terms of the order $k_a^2 \sigma^2 \ell^2$ where k_a is the wavenumber in the average medium, ℓ is the correlation length and σ^2 is the variance of the permittivity fluctuations. These results show a significant difference from those of the scalar problem considered by Tsang and Kong. Whereas the scalar solution gives different effective propagation constants for the component waves in the Green's function, the vector solution derived here contains only a single propagation constant for all components in the Green's dyadic. A brief discussion of the difference in these two solutions is given.

- F3-4 FREQUENCY CORRELATION OF BEAM WAVES PROPAGATING IN
1430 RANDOM MEDIA: S. T. Hong, IITRI / ECAC, North Severn,
Annapolis, MD

It has been shown in the literature that the core of the problem of pulses propagating in random media is to derive the two-frequency, two-position mutual coherence function Γ and to obtain its solutions at the different frequencies and the same positions (frequency correlation). In the past, Γ has been derived both for continuous random media such as atmospheric turbulences and for discrete random media such as rain, fog, cloud, etc.. However, the available solutions for Γ are mostly for incident plane waves.

This paper presents the analytical solution for frequency correlation based on the Rytov approximation, as a Gaussian incident wave is in weak fluctuation. The solution for Γ when a Gaussian beam wave is in very strong fluctuation will also be discussed.

- F3-5 BACKSCATTERED PULSE FROM TURBULENCE AND SCATTERERS:
1450 I. Sreenivasiah, Electrical Engineering, University of Colorado, Boulder, CO and A. Ishimaru, Electrical Engineering, University of Washington, Seattle, WA

The multiple scattering effects on the characteristics of backscattered waves may be important in the analysis of radar and lidar returns from a relatively dense distribution of scatterers such as heavy rain, snow, fog and strong turbulence. This paper presents a study of backscattered pulses from a slab of random medium. An expression for the two-frequency backscattered mutual coherence function is given as a volume integral of the product of the fourth moment of the field and the correlation function of the refractive index fluctuations. This is then simplified under the assumption that the field fluctuation is normally distributed. Differential equations for symmetric and asymmetric two-frequency mutual coherence functions are given and approximate solutions are obtained. When the difference frequency is zero, the results are shown to be similar to those obtained by de Wolf and Ito and Adachi. The Fourier transform of the two-frequency backscattered mutual coherence function yields the pulse intensity and the correlation function. Numerical results are shown for various optical distances and turbulence and scatterer sizes. If the sizes are much greater than a wavelength, the peak pulse intensity approaches twice the Born approximation results.

- F3-6 BEAM PROPAGATION IN FOCUSING MEDIA WITH RANDOM-AXIS
1525 MISALIGNMENTS: SECOND- AND HIGHER-ORDER MOMENTS:
I. M. Besieris, Dept. of Electrical Engineering,
Virginia Polytechnic Institute and State University,
Blacksburg, VA

A novel statistical technique which allows the asymptotic evaluation of second- and higher-order averaged observables related to the stochastic complex parabolic equation is applied to the problem of beam propagation in a focusing medium characterized by random-axis misalignments. Analytical and numerical results concerning on- and off-axis statistics (e.g., the variance of intensity fluctuations, modal power transfer, the probability distribution density of the log-irradiance, etc.) are presented, and comparisons are made with previously reported findings.

F3-7 WAVE PROPAGATION IN A RANDOM MEDIA WITH ANISOTROPIC
1545 IRREGULARITIES: R. Woo, Jet Propulsion Laboratory,
 CIT and F. C. Yang, Dikewood Corporation

In this paper we analyze the scintillations caused by anisotropic electron density irregularities in a planetary ionosphere during radio occultation. Using Rytov's approximation, we show that the power spectrum of the log-amplitude fluctuations depends to a large extent on the direction of the anisotropy and is, therefore, useful for measuring the orientation of the magnetic field in planetary ionospheres that have not yet been probed by direct measurements. We demonstrate this technique by applying it to the Pioneer 10 and 11 observations of Jupiter and obtaining the first measurements of magnetic field orientation in the ionosphere of Jupiter.

F3-8 SCATTERING OF PARTIALLY POLARIZED WAVES BY A PERIODIC
1605 STRUCTURE: A. A. Zvyagintsev, Electromagnetics
 Laboratory, Electrical Engineering Dept., University
 of Illinois, Urbana, IL

In this paper we have investigated the problem of scattering of partially polarized electromagnetic waves by a periodic structure. We have shown that both the elliptical angle and the orientation of the polarization ellipse can be determined by varying the geometrical properties of the periodic grating. We further show that the polarization of the reflected wave from the grating can be altered from that of the incident wave by an appropriate choice of the grating parameters and the incident frequency. As an example, we demonstrate how an elliptically polarized wave with an arbitrary ellipticity ratio can be transformed into a circularly polarized wave.

Also included in the paper is a discussion of the problem of scattering of random waves by a periodic surface. We describe a technique for computing the change in the coherence characteristics of a partially coherent incident field, as a consequence of its reflection from a periodic grating. We show how one can make profitable use of the coherence enhancement property of periodic structures when dealing with signals whose coherence characteristics have suffered degradation, as for instance, due to passage through a turbulent atmosphere.

F3-9 ROUGH SURFACE SCATTERING OF HORIZONTALLY POLARIZED WAVES:
1625 AND POLARIZATION DEPENDENCE OF BACKSCATTER CROSS SECTION
FULL WAVE SOLUTIONS: E. Bahar and G. G. Rajan, Electrical
Engineering Dept., University of Nebraska, Lincoln, NE

Full wave solutions for the horizontally polarized scattered radiation fields from rough surfaces are compared with geometrical optics solutions which are based on the local tangent plane approximations for the fields at the irregular boundary.

In the full wave solutions, we employ complete expansions for the fields and impose exact boundary conditions at the irregular interface between two semi-infinite media. Furthermore, for this problem the field expansions cannot be written in separable form and uniform convergence of the field expansions at the boundary cannot be assumed. Thus for the full wave solutions, Green's theorem is used to avoid interchanging the order of differentiation and integration of the field expansions [1]. The suitability of using the solutions based on the approximate impedance boundary condition is also examined.

The expressions for the backscatter cross section for both horizontally and vertically polarized waves are examined in detail and compared with earlier results based on perturbational approaches [2],[3]. Special attention is also given to reciprocity relationships in electromagnetic theory and to scattering at grazing angles. Solutions are presented in a form that can be readily used by engineers. They can easily be compared with earlier solutions to this problem and to the problem of rough surface scattering of vertically polarized waves. The full wave solutions can be readily applied to periodic and random rough surfaces.

This investigation of irregular ground effects on radio wave propagation is relevant to problems of communication, navigation and positioning as well as active remote sensing.

REFERENCES

- [1] Bahar, E. (1973a,b), Depolarization of Electromagnetic Waves Excited by Distribution of Electric and Magnetic Sources in Inhomogeneous Multi-layered Structures of Arbitrarily Varying Thickness--(a) Generalized Field Transforms, and (b) Full Wave Solutions, Journal of Mathematical Physics, Vol. 14, No. 11, November, pp. 1502-1509 and pp. 1510-1515.
- [2] Wright, J. W. (1966), Backscatter from Capillary Waves with Applications to Sea Clutter, IEEE Transactions on Antennas and Propagation, Vol. AP-14, pp. 749-754.
- [3] Barrick, D. E. and W. H. Peake (1968), A Review of Scattering From Surfaces with Different Roughness Scales, Radio Science, Vol. 8, pp. 865-868.

HF RADIO WAVE ABSORPTION AND HEATING EFFECTS

Tuesday P.M., 16 May, Room 0123

Chairman: A. J. Ferraro, Pennsylvania

State University, State College, PA

G1-1 RADIO WAVE ABSORPTION IN THE IONOSPHERE: P. L. Dyson,
1330 NASA/Goddard Space Flight Center, Greenbelt, MD and
J. A. Bennett, Monash University, Clayton, Australia

Appleton originally derived a relationship between the group path, phase path and the absorption of radio waves for the case of no magnetic field. Since then similar formulae applicable to quasi-longitudinal (QL) and quasi-transverse (QT) propagation in a static magnetic field have been derived. In many instances of radio propagation in the ionosphere the absorption is non-deviative (i.e. it occurs well below the reflection level) and if the QL approximation is appropriate the non-deviative absorption can be simply related to the electron density and collision frequency. Because of the simplicity of these formulae they have been used widely although their accuracy has not been assessed. In this paper we derive a general relationship between the phase path, group path and absorption which is not restricted to QL or QT propagation. The applicability of the usual QL and QT approximations is then assessed for both deviative and non-deviative absorption. It is found that in the case of non-deviative absorption the inaccuracy of the QL approximation is greatest at the same latitude as the peak in absorption reported in some studies. It thus appears that this mid-latitude peak is due to the approximation used to interpret the experimental observations rather than to a real peak in J_{Nvdh} .

New expressions for absorption are given which can be readily evaluated and are appropriate for use in ray tracing programs.

G1-2 IMPULSIVE, PERIODIC VARIATIONS IN IONOSPHERIC ABSORPTION
1400 OF COSMIC RADIO NOISE: T. J. Rosenberg, Institute for
Physical Science and Technology, University of Maryland,
College Park, MD; and L. J. Lanzerotti, C. G. MacLennan,
and C. Evans, Bell Laboratories, Murray Hill, NJ

The technique of monitoring cosmic radio noise by riometers has long been used for determining variations in ionospheric absorption at altitudes from ~ 70 to 100 km. Here we report on 30 MHz riometer data acquired at Siple Station, Antarctica (64.76°S geomagnetic latitude) which show impulsive, quasi-periodic variations of ~ 60 to 90 sec period in the level of cosmic noise absorption. An event typically will consist of 3 to 5 cycles of oscillation and can occur during disturbed or quiet geomagnetic conditions. The oscillations are not closely related to magnetic field fluctuations as measured on the ground at Siple or in the conjugate area. Conjugate x-ray data, available for one event, provides evidence that these absorption variations are caused by the impact on the ionosphere of a variable flux of energetic electrons from the magnetosphere. These absorption oscillations may be another manifestation of the process that produces short-term intensity and phase variations in fixed-frequency sub-ionospheric LF and VLF wave propagation. Further studies of this unique precipitation phenomenon will be conducted with appropriately sited riometer stations in a latitude array.

G1-3 ELECTRON DENSITY MODIFICATIONS IN THE D-REGION DURING
1430 HIGH POWER RADIO WAVE HEATING: A. A. Tomko and A. J.
Ferraro, The Pennsylvania State University, Ionosphere
Research Laboratory, University Park, PA

Plausible models of the electron temperature dependence of key ion chemistry parameters are used to estimate the size and time scale of electron density modifications in the D-region during high power radio wave heating. It is found that high power heating enhances the electron density in the upper D-region above ambient levels on a time scale of minutes in agreement with previous theoretical studies. However, the electron density in the lower D-region is reduced due to increased electron attachment to neutral particles in a few seconds or less. For CW heating over a period of minutes the depressed densities in the lower D-region begin to recover toward ambient. When the heating transmitter is switched off, the electron density in this region builds up rapidly (~ 5 s or less) to levels exceeding ambient and then decays toward ambient on a time scale of minutes or longer. This peculiar electron density variation may explain some of the unusual D-region heating effects observed at the Platteville HF Heating Facility.

G1-4 F-REGION FULL WAVE SOLUTIONS AND THEIR RELATIONSHIP TO
1515 HF RADIOWAVE HEATING: T. A. Seliga, Atmospheric Sciences
Program and Dept. of Electrical Engineering, The Ohio
State University, Columbus, OH

An important result of ionospheric high frequency (HF) heating experiments at Arecibo has been the observations of a strong narrow plasma line enhancement displaced below the HF wave and occurring in a very narrow height range. Consideration of classical magneto-ionic full wave solution theory is shown to provide a mechanism for transferring the electromagnetic heating wave energy into the appropriate narrow region in a form that is consistent with observations. The mechanism relies on coupling of the upgoing ordinary (O) wave energy into extraordinary (X) wave energy near the reflection region of the O-wave; such coupling should be enhanced during heating and dependent upon the angle of incidence of the heating wave. The X-wave under most conditions will travel to a higher height where it is reflected and transformed into a down-going X-wave which in the lossless case (i.e., no collisions) travels downward into a region of increasingly larger refractive index ($n \rightarrow \infty$). The height where this infinity occurs is just below the height where the plasma and wave frequencies are equal. Since this condition is a sink for electromagnetic X-mode energy, this is the region where the greatest plasma and other wave excitations should occur. The theory is illustrated by plots of the roots of the Booker Quartic and computer full wave solutions for conditions typical of Arecibo and Boulder.

G1-5 ON THE GEOMETRY OF SCATTER FROM FIELD-ALIGNED IONOSPHERIC
1545 IRREGULARITIES: V. Agy, Institute of Telecommunication
Sciences, Office of Telecommunications, Boulder, CO

A program has been written to give computer-produced plots of the points on the surface of the spherical earth reached by (UHF/VHF) radio waves from an arbitrarily located transmitter after they have undergone "specular scatter" from ionospheric irregularities aligned with the geomagnetic field. The field is synthesized from the 1960 Jensen-Cain coefficients.

Following a description of the geometry involved, a series of slides will be shown giving the geographic plots of returns scattered as if from heater-induced irregularities over Platteville. If your powers of visualization are good, there will be few surprises, especially, if you keep in mind the geometry first described in detail over 20 years ago by Leadbrand and Yabroff for the somewhat more special case of "auroral irregularities."

G1-6 SCATTER OF HF DUCTED RADIO WAVES BY IONOSPHERIC
1615 IRREGULARITIES: G. S. Sales, Rome Air Development
Center, Electromagnetic Sciences Division, Hanscom
AFB, MA

For a planned experimental measurement program scheduled for the Spring and Summer of 1978, an analytic study has been undertaken to determine the effectiveness of artificially generated ionospheric irregularities for the initiation and recovery of ionospherically ducted modes.

The experiments will use the RF Heating Facility of The Institute of Telecommunication Sciences at Platteville, CO. Transmitters at distances of 1 to 10 Mm will direct their HF swept frequency transmissions at the Platteville heater. A receiving site some 400 km south of the artificially generated irregularities will receive the scattered signals.

Assuming field aligned irregularities at altitudes varying from 130 to 280 km depending on the time of day, "specular" scatter calculations have been carried out to determine the intersection of the scattered energy with the ground. Three-dimensional ionospheric models and ray tracing were used to locate the ducting regions and the scattering pattern on the ground as a function of frequency and azimuth.

WEDNESDAY MORNING, 17 MAY, 0900-1200

Joint USNC/URSI - AP-S

PLENARY SESSION

Wednesday A.M., 17 May, Room 1105

Chairman: E. A. Wolff, NASA/Goddard

Space Flight Center, Greenbelt, MD

- 0900 WELCOME: G. Hyde, COMSAT Laboratories, Clarksburg, MD
1. BEYOND TELECOMMUNICATIONS SCIENCE: ECONOMIC AND SOCIAL
0915 IMPACTS: J. M. Richardson, Director, Office of Telecommuni-
cations, U.S. Dept. of Commerce, Washington, DC
2. SATELLITE POWER SYSTEMS CONCEPT--DEVELOPMENT AND EVALUATION:
0945 F. A. Koomanoff, Chief, Environmental and Resource Assessment
Programs, Solar Technology, Dept. of Energy, Washington, DC
3. THE GRAVITATIONAL ANTENNA: J. Weber, Dept. of Physics,
1045 University of Maryland, College Park, MD
4. MATHEMATICAL ASPECTS OF ATHLETICS: J. B. Keller, Courant
1115 Institute of Mathematical Sciences, New York, NY

WEDNESDAY AFTERNOON, 17 MAY, 1330-1710

Commission B Session 7

ANTENNAS

Wednesday P.M., 17 May, Room 0109

Chairman: W. Wasytkiwsy, Institute

for Defense Analyses, Arlington, VA

B7-1 THEORETICAL AND EXPERIMENTAL STUDIES OF MICROSTRIP ANTENNAS:
1330 Y. T. Lo, D. Solomon, and W. F. Richards, Electromagnetics
Laboratory, Dept. of Electrical Engineering, University of
Illinois, Urbana, IL

Microstrip antennas are inherently narrow band devices with low efficiency. On the other hand, they have many unique and attractive properties: they are low in profile, light in weight, compact and conformable in structure, and easy to fabricate and to be integrated with solid-state devices. They are superior to the conventional flush-mount antennas since they are truly "thin" antennas, requiring no cavity backing. There seems to be little doubt that they will find many applications as more compact efficient solid state sources, amplifiers, and self-matching networks are developed to compensate for the shortcomings.

In this investigation a simple and useful theory, based on the cavity model, has been developed to analyze and predict the fundamental behavior of microstrip antennas of various basic shapes. In general, there is a good agreement between the theory and experiment.

From this theory, the general behavior of the radiation pattern can be predicted by simply noting the relative modal field directions along the edges of the antenna. For numerical results, the computation is simple and straightforward. A microstrip antenna can be fed in many different ways. The input impedance at the feed can be computed from the modal field expansion. In particular, the real part of the impedance can be computed from the power radiated and lost in the cavity while the reactive part can be obtained from the stored energy associated with the cavity field. The impedance varies rapidly with frequency. As the frequency sweeps through the resonant value for a particular mode, the susceptance changes the sign

and the conductance passes through a minimum. Thus, the resonant admittance is a stationary point and for frequencies in the neighborhood of resonance the admittance locus follows approximately a constant conductance circle in the Smith chart plot (except for multiple resonances). Since the real power can easily be computed, the admittance locus is determined immediately.

The theory predicts that the input impedance varies with the feed location if the feed is applied along the edge with nonuniform field distribution. This is verified experimentally. Therefore, by simply locating the feed properly, the antenna can be matched to the feeder over a wide impedance range.

Most radiation takes place along the edge with uniform field distribution. Thus, the longer the edge is, the higher the efficiency and the wider the bandwidth. Parasitic elements of proper dimensions have the function to broaden the resonant frequency region or to cause multiple resonances near to each other. In some symmetrical geometries, the degenerate resonate frequency can split into two close values if the symmetry is perturbed slightly. This can also cause multiple resonances, resulting in an unusual behavior in the impedance.

B7-2 RADIATION AND MUTUAL COUPLING BY PRINTED MICROSTRIP ANTENNAS:
1350 N. K. Uzunoglu and J. G. Fikioris, Dept. of Electrical
Engineering, National Technical University of Athens, Athens,
Greece; and N. G. Alexopoulos, Dept. of Electrical Sciences
and Engineering, University of California, Los Angeles, CA

Radiation from center driven horizontal dipoles printed on a dielectric layer of thickness B which is mounted on a perfect conductor surface is considered.

The dyadic Green's function $\underline{G}(\underline{r}, \underline{r}')$ for a unit current excitation on the dielectric-air interface is obtained by Sommerfeld's method but a two dimensional plane wave representation is used instead of cylindrical wave functions. In order to obtain the far field for a known antenna current "stationary phase integration" approximation is used. The far field for an array of printed antennas is obtained as a product of the free space array factor and a term dependent to dielectric constant and thickness. The mutual coupling and input impedances for an array are obtained by using the well known variational principle expressions. The trial functions used for the current distributions are based on the quasi-static TEM field description of the microstrip transmission lines. The evaluation of the impedances involves two dimensional improper integrals. An efficient numerical technique is developed by treating separately the surface wave singularities.

Numerical results are being computed and results will be presented for several antenna array coupling geometries.

B7-3 ELECTROMAGNETIC PENETRATION INTO THE END OF A FINITE COAXIAL
1410 THIN CYLINDER: L. W. Rispin and D. C. Chang, Electromagnetics
Laboratory, Dept. of Electrical Engineering, University of
Colorado, Boulder, CO

The system analyzed is that of a finite-length thin cylinder ($kb \ll 1$) which contains an internal coaxial line and is illuminated by a uniform plane wave of arbitrary incidence. Internally the one end of the coaxial line's inner conductor is recessed a short distance from the cylinder end, while the opposite end is terminated with a load. The outer cylinder (antenna) to circular waveguide transition and the circular waveguide to coaxial line transition are characterized by current scattering parameters which are derived from the results of a Wiener-Hopf analysis of each junction. Combining these characterizations with the simple formula for current on a receiving antenna of Chang, Lee, and Rispin [1], the current and power in the load have been formulated for a uniform plane wave incident upon the cylinder at an arbitrary incident angle. Acceptable agreement has been found between this analytical approach and related experimental investigations. Noteworthy from both approaches is that the maximum load current does not necessarily occur when the open end of the coaxial line is directly illuminated,

[1] Chang, D.C., S.W. Lee, and L.W. Rispin, "Simple expressions for current on a thin cylindrical receiving antenna," Tech. Rept. #20, Univ. of Colorado, Boulder, Colorado, Dec. 1976 and supplement to this report Sept. 1977.

B7-4 GROUNDWAVE PROPAGATION AND RADIATION PATTERNS OF A VERTICAL
1430 ELECTRICAL DIPOLE OVER A RADIALLY VARYING SURFACE IMPEDANCE
PLANE: C. S. Teng and R. J. King, Dept. of Electrical and
Computer Engineering, University of Wisconsin, Madison, WI

EM propagation over and radiation from radially varying surface impedance planes is studied by numerical methods using integral formulations of the compensation theorem. The source is taken to be a vertical electric dipole (VED) situated either on or above the plane. The arbitrary surface impedance profile on the plane is assumed known and only varies radially.

The numerical approach first involves solving a reduced one-dimensional integral equation for the field on the perturbed surface and then performing the two-dimensional integration to find the field above the plane, as well as the radiation pattern. This integral formulation can be applied to many classes of problems. Radial wire ground systems and land-sloping beach-sea propagation at HF are used to illustrate the possible applications. Chief attention is given to determine the effect of various surface impedance profiles on the radiation pattern.

It is shown that with suitable combinations of VED height, electric properties of the ground beneath VED, and the length (typically less than $5-7.5 \lambda_0$) and number of radial wires, the low angle radiation can be improved somewhat. The sloping beach is found to have little impact on the radiation pattern compared to that for an abrupt coastline at HF.

B7-5 A COMPUTER PROGRAM FOR ANTENNAS IN THE IMMEDIATE VICINITY
1505 OF EARTH SURFACE: C.-L. Chen and W. L. Weeks, School of
Electrical Engineering, Purdue University, West Lafayette, IN

There are three major steps in the application of the method of moments to wire antenna structures in order to calculate their current distributions, immittances and radiated fields. The steps are: the division of the wires into segments, the calculation of self and mutual impedances of the wire segments and the inversion of the impedance matrix or matrices derived from the impedance matrix. The second step depends critically on the environment surrounding the antenna system. The complexity of the impedance calculation increases considerably in the presence of lossy earth, since the Sommerfeld integrals are involved. The Sommerfeld integrals are slow to converge when the wire segments are very close to the earth surface. The numerical difficulty will be traced. A method to alleviate the problem as well as its theoretical justification will be presented. A general purpose program (WF-LLL2B) previously written by Lytle and Lager was so modified. The modified program was used to investigate the effect of thin wire ground screens on the radiation of HF antenna systems with particular emphasis on the enhancement of the low angle radiation by the ground screens. Results on the enhancement and front-to-back ratio of antenna systems with ground screens of fork, cross and Y shapes over a typical ground will be presented.

B7-6 OFFSET PARABOLOID FIELD COMPUTATIONS USING AN EFFICIENT
1525 SERIES EXPANSION: Y. Rahmat-Samii, R. Mittra (consultant),
V. Galindo-Israel, and R. Norman, Jet Propulsion Laboratory,
CIT, Pasadena, CA

Offset parabolas find applications as communication satellite antennas where aperture blockage and scattering from supporting structures preclude the use of symmetric, front-fed reflectors. The blockage of these structures causes degradation in sidelobe levels, polarization characteristics, gain, and other performance parameters. The lack of symmetry in the geometry of the offset reflector and the feed system makes the task of accurate computation of the secondary pattern a very time-consuming process. In a recent paper Galindo-Israel and Mittra [AP-S Sept., 1977] described a series method for the efficient pattern computation of symmetric parabolic reflectors. In a subsequent communication [Mittra and Galindo-Israel, 1977 AP-S Symposium], they have indicated the analytical steps for generalizing the series approach for application to offset geometries. In this paper we report the results of a study of the series technique as it applies to the offset parabola and present extensive numerical results to demonstrate its usefulness with regard to rapid convergence properties, computational efficiency and other unique features of the technique. Numerical results exhibiting the systematic degradation of the vector secondary pattern as a function of feed displacement, the effect of f/D on gain and sidelobe level versus beam scan, and the analytic and numerical existence of an optimum scan plane is demonstrated. Finally, the generalization of the method to non-parabolic offset reflectors (applicable to offset dual shaped reflectors) is illustrated by computing the radiation patterns of distorted parabolas that are found to exhibit extensive pattern degradation even with relatively minor changes in their surface properties.

B7-7 HOW NOT TO SEARCH FOR A SPECULAR POINT IN GEOMETRICAL OPTICAL
1545 ANALYSIS OF NUMERICALLY SPECIFIED SURFACES: R. Mittra and
 A. Rushdi, Electromagnetics Laboratory, Electrical Engineering
 Dept., University of Illinois, Urbana, IL

In the conventional geometrical optical analysis of smooth surfaces, it is customary to search for a specular point on the surface of the scatterer for each given combination of source and observation points. In many situations, only a numerical description of the surface is available rather than an analytical expression which lends itself more readily to a determination of the specular point. The numerically prescribed form for the surface may be locally interpolated, e.g., say, using a sixteen-point grid, that leads to a 16×16 matrix equation. This matrix must then be inverted for the interpolation coefficients each time a specular point is to be calculated.

In this paper, we investigate an alternative approach that circumvents the step of deriving the specular point and obtains the scattered field in a more direct manner. Basically, the method begins by computing the reflected rays off the surface at the points where its coordinates, as well as the partial derivatives (or equivalently the direction of the normal), are numerically specified. Next, a cluster of three adjacent rays are chosen to define a "mean ray" and the divergence factor associated with this mean ray. Finally, the field at a given observation point is derived by associating this point with the nearest mean ray, determining its position relative to such a ray, and making use of the divergence factor of the mean ray. The paper presents the detailed procedure for computing the mean rays and the geometrical optics reflected field from a numerically described smooth surface for an arbitrary location for the point of observation. It also presents a discussion on the scope and limitations of such a method, and points out its advantages and disadvantages vis-à-vis the conventional specular point approach.

B7-8 DETERMINATION OF NEAR-ZONE FIELDS OVER LIMITED ANGULAR
1605 SECTORS USING WAVENUMBER BANDPASS FILTERING: E. C. Burdette
(Engineering Experiment Station) and J. D. Norgard, School
of Electrical Engineering, Georgia Institute of Technology,
Atlanta, GA

In the Plane Wave Spectrum (PWS) method for the computation of antenna near-zone fields, integration over all visible wavenumbers is not always required to adequately describe the near field of a radiating structure. By bandpass filtering the PWS spectral samples in wavenumber space, a method of antenna analysis is developed which is significantly faster than the original PWS method. Once the near field on a plane in front of the antenna is known, wavenumber bandpass filtering may be employed to minimize the number of spectral samples required to accurately compute the near-field of an antenna over a particular angular sector at another near-field distance by utilizing only those spectral components which make significant contributions to the field.

A "wavenumber bandpass filtering" criterion is developed for determining the number of spectral samples required to describe the antenna near field in a particular angular sector and for determining the location of the sector in wavenumber space. This technique has been verified by comparing near-zone radiation patterns computed from wavenumber bandpass filtered spectral data to (1) near-zone patterns computed from unfiltered spectral data and (2) near-zone patterns computed using aperture integration techniques. For each case, a comparison of data requirements and computation time has been performed. The results show that the use of such a criterion for either measured or theoretical near-field distributions is particularly useful for determining the local field incident upon a scatterer located in the near field of a radiating structure or for identifying potential radiation hazards occurring in limited near-field sectors of radar antennas.

B7-9 THE LOG PERIODIC ANTENNA AND DATA PROCESSING FOR TIME DOMAIN
1625 SCATTERING MEASUREMENTS: S. K. Chaudhuri and Y. L. Chow,
Dept. of Electrical Engineering, University of Waterloo,
Ontario, Canada

The base band radar measures the time domain scattering of targets by short unmodulated pulses. A major difficulty encountered is that most antennas, including the broadband ones, cannot radiate short pulses directionally and without distortion. A method is proposed below to circumvent this difficulty.

The log-periodic antenna has the directivity, and the bandwidth to reasonably accommodate the unmodulated short pulse. The pulse distortion comes from its phase dispersion at different frequencies. This antenna phase dispersion can be compensated anywhere in the transmitting/receiving system of the radar. Instead of having the compensation at the transmitting phase at high power as proposed by Miller [1], we propose to have the compensation at the receiving phase at low power. In fact it can be done by data processing the received signal through, say, a mini-computer with Fourier transformation. Such processing is well known in radio astronomy.

To verify the feasibility of the method, we computed the following wave forms: (1) The pulse to be transmitted, (2) The distorted pulse radiated by the antenna, (3) The time domain waves scattered by simple targets such as a sphere, (4) The signal after further distortion by the receiving antenna and (5) The recovered pulse responses of the targets after phase compensation. These computed wave forms will be presented.

- [1] E.K. Miller and J.A. Landt: IEEE Transactions, AP-25, No. 5
Sept. 1977, pp. 621-626.

Commission F Session 4

APPLICATIONS OF PROPAGATION MODELING FOR 30/20 GHz SYSTEMS ENGINEERING

Wednesday P.M., 17 May, Room 1109

Chairman: J. Reilly, Defense

Communications Agency, Reston, VA

F4-1 30/20 GHz SYSTEMS OVERVIEW: J. Reilly, DCA, Reston, VA
1330

This paper provides a general introduction to system designs and concepts relevant to the development of an operational 30/20 GHz military satellite communications system. It characterizes MILSATCOM user requirements. It points out potentials of 30/20 GHz for meeting these requirements. It identifies system engineering conclusions on propagation effects and relates these conclusions to system design impacts. It discusses some system parameters, constraints, and trade-offs, as currently perceived.

F4-2 PROPAGATION REQUIREMENTS FOR 30/20 GHz SYSTEM DESIGN:
1400 P. Brandinger, CSC, Falls Church, VA

The growth of satellite communication systems to 30/20 GHz requires the engineering application and extrapolation of currently available propagation data to worldwide site specific locations. Propagation models have been developed to resolve limited subsets of the overall problem but a unified analytic approach is required to provide useful system engineering information. Currently available data from rain-gauge, radiometer, radar and satellite beacons is useful but generally limited in time and site specific in nature. The current need is to improve the extrapolation in space and time of available site specific data.

The outages due to rain attenuation at 30/20 GHz may be alleviated by either frequency, dual site or angle diversity. The use of path correlation statistics is necessary to identify the required site separation (for dual site diversity) and the available diversity gain. Angle diversity uses the limited volumetric extent of rain cells to provide reduced path correlations from one site to one of two satellites in view. The impact of amplitude and phase scintillation, angle of arrival fluctuations and phase smear (due to scattering by rain) is necessary to evaluate at operational elevation angles to determine the effect on system performance.

F4-3 ACCURACY OF PROPAGATION MODELLING REQUIRED FOR OPERATIONAL
1430 SYSTEMS: R. K. Crane, Environmental Research and Technology,
Inc., Lexington, MA

A number of prediction models are now available for the estimation of propagation effects at 20 and 30 GHz. These models depend on the use of experimental data obtained over limited time periods at a limited number of locations, frequencies, and propagation path geometries. The data used to generate these models have not been selected to represent a wide range of climate regions and are not representative of the possible range of effects that can occur at the very small percentages of the time of interest for system design. Predictions based upon the use of these models may be in error but error estimates are not currently part of most prediction models.

Data are now available to assess the possible errors in prediction methods and to establish duration requirements on observations to be used in refining propagation models. For instance, between 10 and 15 years of observations are required to obtain an estimate of the total attenuation to be expected to occur for .001 percent (5 minutes) of the year with an error of less than 10 percent.

F4-4 SYSTEM IMPLICATIONS OF 30/20 GHz PROPAGATION MODELLING:
1515 J. Dudzinsky, RAND Corp., Santa Monica, CA

A model is developed for the statistical distribution of atmospheric attenuation, sky noise temperature, and total link degradation due to atmospheric effects as a function of frequency (20 to 300 GHz) and elevation angle. The attenuation model is based on (1) weather statistics in the Rand Weather Data Bank (RAWDAB), in combination with measured attenuation by molecular constituents and Deirmendjian's calculated values of attenuation by particulate (fog and rain) components, and (2) measured values of attenuation using suntrackers, beacon trackers, and radiometers. Atmospheric constituents such as rain degrade link performance in two ways: they attenuate the signal and they increase system noise by adding a sky noise contribution. The additional sky noise effect is most significant at the lower frequencies (20 GHz) where, in the examples treated, it added roughly 4 dB of degradation with uncooled receivers and 8 dB with cooled receivers.

The model is applied to hypothetical communication links, permitting the estimation of the statistical distribution of weather outages, as a function of data rate and other system parameters. The model was developed for Washington, D.C. (a region with relatively high rainfall) but could be extended to any location in the world where weather data are available. The performance estimates were made for the downlink, which is usually the limiting case. We found that performance degrades rapidly as the elevation angle at the user falls below 30 deg, especially at frequencies above 30 GHz. Hence, for communications systems which must operate during rain, the higher the frequency the more important it is to avoid elevation angles below 30 deg. The estimated annual throughput increases monotonically with frequency up to about 152 GHz for elevation angles of 30 deg and above.

F4-5 WORST-MONTH PERFORMANCE SPECIFICATIONS AND PROPAGATION
1545 PREDICTION: F. Altman, CSC, Arlington, VA

The C.C.I.R. Recommendations 233 and 393 on maximum circuit noise power permitted in any month have led to the concept of the worst month in the year, which has been useful for transmission at frequencies below 10 GHz. At higher frequencies, however, noise is controlled by rainfall, which is highly variable from year to year, so that the concept of a worst month by name may be misleading. After a review of U. S. rainfall data, both intense (exceeded 0.1% of W. M.) and hourly (exceeded 1.0% of W. M.), the following conclusions are reached:

- a) The ratio of time with rainfall rate above some threshold in an average year to that in an average worst month is generally less than four (Report 563), when calculated correctly for 0.1% of W. M. or less;
- b) From hydrological methods using extreme values it is shown that the time above threshold in the worst month of 20 years (0.2 probability in 5 years) is expected to be about twice that of the average worst month in a);
- c) A rational basis for design of rainfall-limited circuits may be achieved by permitting N noise power in P percent of any month in Y years, a worst worst month. Further rainfall studies are required to develop a climatology useful where sufficient instantaneous and hourly data are unavailable.

F4-6 PROPAGATION MODELING FOR SYSTEM DESIGN: R. E. Castle
1615 and C. W. Bostian, Electrical Engineering Dept.,
Virginia Polytechnic Institute and State University,
Blacksburg, VA

The usefulness of a propagation model for system design is dependent on its accuracy and the amount and type of data it requires. This paper will examine some currently available models and their usefulness in system design at 20/30 GHz. Rainfall statistics, compiled over varying periods of time, will be used to predict attenuation and depolarization levels which will be compared to measured attenuation and depolarization levels. Estimates of model accuracy and the amount and type of rainfall data needed by current models will be made and their impact on system design discussed.

Commission G Session 2

RADIO PROPAGATION AND DIAGNOSTICS

Wednesday P.M., 17 May, Room 0123

Chairman: D. M. Towle, MIT

Lincoln Laboratory, Lexington, MA

G2-1 LOW FREQUENCY RADIO EXPERIMENTS: F. J. Kelly, J. A.
1330 Murray, D. J. Baker, and F. J. Rhoads, Naval Research
 Laboratory, Washington, DC

Low frequency radio propagation experiments were conducted to provide comprehensive propagation data from U. S. Navy transmitting stations using NRL's RP-3A aircraft as a collection platform. Data were recorded while flying on radials toward and away from stations. Both daytime and nighttime propagation conditions were investigated. During the flights, signal strength and noise levels were recorded on magnetic tape continuously on several frequencies. Identical receivers were located on the ground near each transmitter site to measure and record the actual radiated signal. Rubidium and cesium clocks at the ground sites and on the aircraft synchronized the recordings within a few microseconds for later analysis. From this data both the field strength versus distance and the transfer function of the channel have been obtained.

G2-2 SPORADIC E RECEPTION AT 25 AND 35 MHz: A. S. Ratner,
1355 Laboratory for Physical Sciences, College Park, MD

The signal strengths of two beacon transmitters at approximately 25 and 35 MHz have been measured at a distance of 2100 km, nearly the maximum range for one-hop sporadic E propagation. The dynamic range of the system provides 45 and 50 db between estimated free space signal levels and median noise levels at 25 and 35 MHz, respectively. The variations in signal levels caused by changes in sporadic E layer height due to the variation of antenna gain with elevation angle have been minimized by the appropriate selection of antenna heights. On a monthly basis, the diurnal variations in reception probability at the two frequencies were significantly different. For the period May through September 1977, a linear regression analysis of the median signal strengths (in dbm) during those half-hour periods when both signals were received, showed a correlation coefficient of +0.56 (with 95% confidence limits of +.06 and -.09) and a slope (change in 35 MHz signal relative to 25 MHz change) of $+0.50 \pm 0.06$.

G2-3 THE NOAA SEL HF RADAR SYSTEM: R. N. Grubb, US Dept.
1420 of Commerce, NOAA, Environmental Research Laboratories,
Space Environment Laboratory, Boulder, CO

The Space Environment Laboratory of the National Oceanic and Atmospheric Administration has developed a new general purpose computer based system for pulsed RF measurements of the ionosphere in the 100 kHz-30 MHz frequency range. This is a development of the earlier Dynasonde concept to permit full digital signal processing of returned echoes, monopulse measurement of polarization and direction of arrival, and a considerably enhanced data processing and display capability. The system philosophy adopted is discussed and some details of the implementation and performance of the instrument are given. A number of instruments are now being produced for various institutions which will form the basis of a coordinated research program over the next ten years.

Commission G Session 2

G2-4 DOPPLER TECHNIQUE USED IN AIRBORNE IONOSPHERIC SOUNDING OF
1445 HIGH-LATITUDE IONOSPHERE: J. Buchau, Air Force Geophysics
Laboratory, Hanscom AFB, MA and K. Bibl and B. W. Reinisch,
University of Lowell, Center for Atmospheric Research,
Lowell, MA

A Digisonde 128, onboard a USAF research aircraft, was modified to include spectral integration. Spectral analysis is performed in real time, separately for each frequency/range bin. The spectrum is limited to a maximum of 18 lines arranged symmetrically around zero Doppler shift. Recorded are the amplitude value and the Doppler bin number of the strongest line in each frequency/range bin of the ionogram.

A test flight was conducted on 4/5 November 1977 from Pease AFB, NH into the auroral region. The flight provided a cross-section of ionospheric conditions through the midlatitude F-layer, the F-layer trough and the auroral oval. The ionograms collected demonstrate the usefulness of Doppler information for the identification of the complex high-latitude ionograms.

Doppler ionograms recorded onboard the moving aircraft permit one to distinguish between overhead and various oblique traces and give a general idea about the location of oblique reflectors. This information is important to the description of the complex structure of the high latitude/auroral ionosphere.

G2-5 CHARACTERISTICS OF OBLIQUE HF REFLECTIONS FROM THE POLEWARD
1530 BOUNDARY OF THE NIGHT-TIME IONOSPHERIC TROUGH: R. W. Jenkins,
E. L. Hagg, and L. E. Montbriand, Communications Research
Centre, Ottawa, Canada

Measurements of the direction and doppler shifts of HF signals reflected from the poleward edge of the trough, obtained under both quiet and moderately active conditions, are used to describe the detailed behaviour of the F-layer in that vicinity.

The data were obtained using the Canadian Department of Communications 4000-foot aperture HFDF receiving array near Ottawa to record CW signals transmitted from a specially outfitted USAF Ionospheric Physics Laboratory aircraft flying over the western Atlantic, in the vicinity of the night-time trough. These data were combined with aircraft positions and path lengths scaled from oblique ionograms recorded on the aircraft, to uniquely determine the location, orientation, and velocities of the ionospheric reflecting surfaces.

Reflections from the poleward edge of the trough were observed on both the ionograms and CW recordings, on two occasions. On the first, geomagnetic conditions were quiet; the auroral electrojet magnetic index AE remained below 50 γ . The locations derived for the reflecting surface lay between the southern edges of the Q=0 and Q=1 Feldstein auroral ovals. The near-instantaneous velocities of the reflecting surface derived from doppler measurements were a few tens of m/s and agreed with the large-scale time-averaged motion of the trough edge derived from the measured orientations and time-changes in position. On the second occasion, moderate geomagnetic activity was present; AE reached 500 γ at times. The locations derived for the reflecting surface lay close to the southern edge of the Q=3 oval. The reflecting surface was much more disturbed than previously. There was a wide spread in doppler-derived velocities present for each of the measurements. The near-instantaneous velocities of the trough-edge reflector(s) varied between 150 and 870 m/s equatorward over the measurements period, while the time-averaged motions of the trough-edge derived from changes in position remained near zero.

G2-6 IONOSPHERIC SCINTILLATIONS AT THE CREST ZONE OF THE
1555 EQUATORIAL ANOMALY: Y.-N. Huang, Telecommunication
Laboratories, Taiwan, Republic of China

The ionospheric scintillation data obtained at Lunping Observatory (25.00°N , 121.17°E geographic; 13.8°N , 189.5°E geomagnetic) during January to June, 1976 by receiving 136.44 MHz beacon signal from INTELSAT 2F3 geostationary satellite with an AFCRL polarimeter were used to study the ionospheric scintillation activity at geographic latitude 22.7°N near to the crest zone of the so called equatorial anomaly of F2 layer. Unusually large scintillation activity was found. Seasonally, the activity was largest in summer and smallest in winter. The scintillation occurred not only at night but also at daytime. At nighttime in summer, the monthly mean scintillation index (range from third peak to third null) reached a value as large as 10 dB. At daytime in summer, the monthly mean scintillation index was larger than 5 dB. The diurnal pattern of the percentage occurrence of scintillations was very similar to that of the percentage occurrence of sporadic E greater than 5 MHz. The nighttime scintillation was found to be closely related with the occurrence of spread F; and the daytime scintillation with the occurrence of sporadic E. It was found that the geomagnetic activity seemed to decrease the scintillation activity at nighttime; and to increase scintillation activity at daytime.

G2-7 VHF AND UHF RADAR MEASUREMENTS OF IONOSPHERIC IRREGULARITIES:
1620 D. M. Towle, MIT Lincoln Laboratory, Lexington, MA

A series of measurements of the behavior of small-scale sized ionospheric irregularities were made using the Lincoln Laboratory ALTAIR radar at Kwajalein, in the Marshall Islands (9.5° N. Latitude, 167.5° E. Longitude) during August, 1977.

Backscatter echoes were recorded at radar frequencies of 155 MHz and 415 MHz in the altitude region from 250 Km to 750 Km. A stepwise scan was used to obtain cross-sectional maps of the irregularity echoes at a rate of 5 minutes per frame. The scan covered a sector 120° wide, in azimuth, centered around magnetic North such that the radar beam was aligned orthogonal to the geomagnetic field lines passing through the peak plasma density F-region. Altitude distributions of the irregularities were determined with resolutions as fine as 38M and 15M at VHF and UHF respectively. Changes in the irregularity patches appearing in the maps from scan to scan were used to deduce the vertical and the horizontal motion of the patches as well as their temporal changes. Radial motion of the individual echoes relative to the radar site was also indicated by the doppler frequency of the coherent echo signals. The relative strength of the VHF and the UHF echoes from different regions was measured.

In addition to the recording of the backscatter echoes, propagation effects on radar signals transmitted through the irregularity regions were made by active tracking of satellites orbiting above these regions. This set of measurements provided concurrent data on the horizontal extent and the strength of the scintillation regions. The range delay of the VHF signal relative to the UHF signal was also measured to indicate the total electron content of the ionosphere in these regions.

G2-8 ATMOSPHERIC PROPAGATION EFFECTS ON THE PERFORMANCE OF
1645 SYNTHETIC-APERTURE RADARS: W. D. Brown, Sandia Laboratories,
 Albuquerque, NM

The effects of hydrometeors, tropospheric turbulence, and the electron density irregularities in the ionosphere on SAR performance are described. Attenuation and back-scattering by hydrometeors create significant problems for most SAR systems only at frequencies above 10 GHz. The phase errors induced by turbulence in the troposphere can be important at low elevation angles. An analysis of the scintillation data from 500 passes of the Wideband Satellite shows that propagation through electron density irregularities in the ionosphere can produce appreciable performance degradations for a significant fraction of the time for the SEASAR synthetic-aperture radar.

THURSDAY MORNING, 18 MAY, 0830-1200

Commission F Session 5

PROPAGATION EXPERIMENTS USING THE

19 AND 28 GHz BEACONS ON COMSTAR SATELLITES

Thursday A.M., 18 May, Room 1109

Chairman: D. C. Cox, Bell

Laboratories, Holmdel, NJ

F5-1 RADAR AND DISDROMETER PREDICTED RAIN ATTENUATION OF THE
0830 28 GHz COMSTAR BEACON SIGNAL: J. Goldhirsh, Applied
Physics Laboratory, Johns Hopkins University, Laurel, MD

A program to measure the rain attenuation of the COMSTAR beacon signal at 28.56 GHz has been in continuous operation since March of 1977 at Wallops Island, Virginia. During the summer of 1977, simultaneous radar and disdrometer measurements were also made and used for predicting path attenuation. The best fit values of a and b of the relation $k = a Z^b$ were deduced for each rain period from the raindrop size measurements; where k is the attenuation coefficient [db/km] and Z is the reflectivity factor [mm^6/m^3]. The measured k - Z relations and the simultaneous radar reflectivity measurements along the beacon path were injected into a computer program for estimating the path attenuation. Predicted attenuations when compared with the directly measured ones showed generally good correlation on a case by case basis and very good agreement statistically.

The results demonstrate the utility of using radar in conjunction with disdrometer measurements for predicting fade events and long term fade distributions associated with earth-satellite telecommunications.

F5-2 A MM-WAVE PROPAGATION EXPERIMENT IN GEORGIA AND ILLINOIS
0855 UTILIZING COMSTAR BEACON SIGNALS: H. J. Bergmann,
A.M.T.S., Bell Telephone Laboratories, Holmdel, NJ

Radio propagation measurements involving the 19 and 28 GHz beacon signals transmitted from the COMSTAR Satellite have been in progress almost twenty months at Bell Laboratories field locations near Atlanta, Georgia and Chicago, Illinois. In addition to the monitoring of beacon signals, measurement of 13 GHz attenuation along the same line of sight was estimated with radiometer signals derived from the same antenna. Statistical results from individual operating sites will be presented along with fade performance improvement obtained through diversity operation; in both Illinois and Georgia, site diversity measurements were made using a 20 mile baseline. In addition, promising early results are shown for a configuration which was implemented in Georgia to measure the diversity improvement offered by co-located antennas addressing satellites spaced significantly in their stationary orbits.

F5-3 COMSTAR BEACON MEASUREMENTS AT CRAWFORD HILL: ATTENUATION
0920 STATISTICS AND DEPOLARIZATION: D. C. Cox and H. W. Arnold,
Bell Laboratories, Crawford Hill Laboratory, Holmdel, NJ

A precision 7m diameter antenna and receiving electronics at Crawford Hill, New Jersey have been measuring attenuations, depolarizations and differential phases of 19 and 28 GHz COMSTAR beacon signals since January 1977. This experiment uses the beacon in synchronous orbit at 95°W longitude. In clear air, the copolarized signal to noise ratios are 60 dB and the crosspolarization discrimination is greater than 35 dB. The 19 GHz beacon is switched between two orthogonal polarizations. All co- and cross-polarized received signal amplitudes and phases are measured. The complete 19 GHz transmission matrix for the propagation medium can be constructed from these measurements. From this matrix, attenuation and depolarization of the medium can be calculated for any incident polarization. These calculations do not depend on any assumptions about the medium and are based only on the measured amplitudes and phases. Examples of 19 GHz depolarization and attenuation as functions of polarization angle will be presented. These examples are from measurements of rain and ice events. Similar calculations cannot be made at 28 GHz without involving assumptions about the medium because only one polarization is transmitted from the beacon at this frequency.

Attenuation statistics will be presented for the 19 and 28 GHz measurements described above; the statistics are for a path elevation of 38.6° and azimuth of 210.5°. These statistics will be compared with 19 GHz statistics from a colocated experiment having an elevation of 18.5° and an azimuth of 244.7°. This second experiment measures 19 GHz attenuation using a 3.7 meter diameter antenna and the COMSTAR beacon at 128°W longitude.

F5-4 EXPERIENCE WITH COMSTAR BEACON RECEIVING TRIAD IN TAMPA,
0945 FLORIDA: S. C. Bloch, University of South Florida,
Tampa, FL and D. Davidson and D. D. Tang, GTE Laboratories,
Incorporated, Waltham, MA

The COMSTAR beacon receiving terminals in Tampa form a triad with baselines of about 13 km length. The main terminal at the University of South Florida records co-polar and cross-polar signals on 19 GHz and only co-polar carrier on 29 GHz. The outlying terminals record only the 19-GHz vertically polarized signal to determine diversity effectiveness in this Gulf Coast area, where in summer frequent, almost daily, intense rain cells pass through boresight regions. The results to be reported were derived from the D-2 COMSTAR transmissions (longitude 95°W) received at a high elevation angle.

F5-5 MEASUREMENTS OF COMSTAR 29 AND 19 GHz BEACON SIGNALS AT
1025 CLARKSBURG, MD: G. Hyde, F. Tseng, and J. M. Harris,
COMSAT Laboratories, Clarksburg, MD

Measurements at 29 and 19 GHz have been conducted at COMSAT Laboratories, Clarksburg, Maryland of the signals from the COMSTAR 29/19 GHz beacons on board the COMSTAR D1 and D2 satellites. Measurements on the D1 beacon, at an elevation angle of 28°, were conducted from July, 1976 to August, 1977. Measurements on the D2 beacon, at an elevation angle of 41°, were initiated in August of 1977 and are continuing. Additional measurements were made using an 11.7 GHz radiometric terminal to measure sky temperature variation along the same paths and a tipping bucket rain gauge to measure point rainfall at the site. Cumulative distributions of attenuation at 29 and 19 GHz will be presented for the approximately one year of D1 beacon measurements and about 6 months of D2 beacon measurements, and at 11.7 GHz (as derived from the radiometric data). Comparison will be made of the attenuation in the 19 GHz vertically and horizontally polarized signal channels. The diurnal distributions of the attenuation data will be presented. Cumulative distribution of the rain-rate will be presented. Selected event data on 19 GHz depolarization in the presence and absence of significant attenuation, and on 29 GHz differential phase will be offered. Finally, frequency scaling and attenuation/rain-rate models will be discussed.

F5-6 PRELIMINARY OBSERVED STATISTICS FROM COMSTAR D1 RADIO BEACON
1050 AT 19 AND 28 GHz: K. C. Allen, H. B. Janes, R. H. Ott,
D. Smith, and M. C. Thompson, Jr., US Dept. of Commerce,
Office of Telecommunications, Institute for Telecommunication
Sciences, Boulder, CO

Initial long and short term time statistics are presented for the amplitude, phase and depolarization collected during the first quarter of 1978 on the COMSTAR D1 beacon at 19.04 and 28.56 GHz at an elevation angle of 38.7° and an azimuth of 213.1° corresponding to the receiver site at the Radio Building in Boulder, Colorado. The propagation measurements are supported by a LIDAR looking at the common scattering volume for determining the mean height and scattering constituents producing the observed amplitude, phase and depolarized signal variations. In addition, temperature, refractive index, and rain rate are recorded for a 740 m folded path operating at 28.8 GHz in the immediate vicinity of the receiving paraboloidal antenna. The LIDAR and 28.8 GHz terrestrial propagation data are used to interpret the signal behavior during periods where weather fronts move through the path. In particular, scattering from ice crystals occurring in cumulus clouds and the phenomenon of ice depolarization are explored.

Histograms, cumulative distributions, cross and auto correlations and temporal spectra statistics are presented for the amplitude of the 28 GHz co and cross polarized signal, and the four combinations of transmit and receive polarizations on the 19 GHz signal as well as statistics on the amplitude differences between the 19 and 28 GHz signal. For example, cumulative distributions on the 28 GHz amplitude before, during and after an ice crystal event indicate nearly Gaussian statistics with a variation in the variance indicative of the strength of the event.

F5-7 PRELIMINARY RESULTS OF COMSTAR 19/29 GHz MEASUREMENTS
1115 AT HANSCOM AFB, MA: L. E. Telford and E. E. Altshuler,
Rome Air Development Center, Hanscom AFB, MA

This paper describes the Rome Air Development Center experimental receiving site for reception of the COMSTAR 19/29 GHz millimeter wave beacon and presents preliminary propagation results obtained at the Prospect Hill site near Hanscom AFB, Massachusetts. The present receiver configuration measures the 19 GHz attenuation of the vertical polarized component, 29 GHz attenuation of the carrier and two sidebands and the relative phase between the 29 GHz carrier and its associated sidebands. The antenna is 5.5 meters in diameter and has a unique stepper motor digital drive system. The receiver was specifically designed to track the diurnal beacon frequency changes. Data collection is by a microprocessor controlled data acquisition system and real-time antenna pointing is provided by a scientific calculator. Available attenuation statistics and analysis will cover the period from 1 January 1978 until the present so the results will consequently be very preliminary.

F5-8 RESULTS OF COMSTAR 19 AND 28 GHz ATTENUATION AND
1140 DEPOLARIZATION MEASUREMENTS AT BLACKSBURG, VA:
C. W. Bostian, W. L. Stutzman, E. A. Manus, P. H. Wiley,
S. R. Kauffman, R. E. Marshall, W. P. Overstreet, and
R. R. Persinger, Electrical Engineering Dept., Virginia
Polytechnic Institute and State University, Blacksburg, VA

This paper summarizes the results of 11 months of dual-frequency attenuation and depolarization measurements with the COMSTAR D-2 beacons. It discusses signal behavior during individual storms and presents data on the statistical relationships between rain rate, attenuation, and polarization isolation. Effective path lengths, techniques for frequency-scaling attenuation and depolarization, and the adequacy of existing theoretical models are examined.

REMOTE SENSING OF EARTH'S SURFACE AND SUBSURFACE

Thursday A.M., 18 May, Room 0109

Chairman: R. J. King, Dept. of Electrical
and Computer Engineering, University of Wisconsin, WI

F6-1 RADAR PROBING OF GEOLOGIC MATERIAL: A. P. Annan and J. L.
0830 Davis, Geological Survey of Canada, Ottawa, Canada

Electromagnetic methods which operate in the frequency range of 1 to 1000 MHz are relatively new geophysical techniques for probing geologic materials. Geologic information which has important geotechnical applications often lies at depths of less than 100 m. The high frequency electrical properties of some geologic materials permit penetrations approaching these depths. As a result, very high resolution radar systems can be employed to delineate geologic structure. The principle design parameters for such radar systems are the centre frequency, the bandwidth, and the antenna fidelity. The maximum penetration depth and resolution are determined by these system parameters. The choice of these parameters must be based on the electrical properties of the geologic environment and the target geometry. Optimum penetration and resolution are generally obtained by minimizing the centre frequency and maximizing the bandwidth. Criteria for the choice of the appropriate system parameters are developed in terms of the electrical properties of geologic material. Field examples of radar soundings are presented which illustrate these criteria.

F6-2 RESISTIVITY ANOMALIES FROM LOCALIZED VOIDS UNDER IRREGULAR
0855 TERRAIN: R. J. Spiegel, V. R. Sturdivant, and T. E. Owen,
Southwest Research Institute, San Antonio, TX

In applying earth resistivity methods to the problem of locating and delineating subsurface cavities and other geologic structures, surface elevation variations along the surveyed terrain introduce distortions in the soundings, which, if not properly compensated, will mask the resistivity perturbations characterizing the subsurface targets of interest. The analysis presented in this paper is aimed at characterizing such terrain variations in the detection of relatively small three-dimensional subsurface targets such as caves, sinks, and tunnels in otherwise homogeneous earth materials. The analytical approach involves, first, the development of a suitable earth resistivity model for localized three-dimensional subsurface anomalies in a homogeneous halfspace. The approach taken was to divide the anomaly into multiple rectangular surface patches and utilize moment method procedures to calculate the surface charge induced on the patches as a result of current being injected into the ground at the earth's surface. The induced surface charge forms the basis for calculating the secondary electric fields and surface potentials representing the anomaly response. Second, terrain surface variations along the survey traverse are approximated by piece-wise linear line segments which are intentionally warped into a flat halfspace by a Schwarz-Christoffel mapping process to permit use of the target anomaly halfspace model. In addition, the subsurface geologic anomaly in the real terrain is also accordingly warped in size, shape, and location when transformed to its halfspace model representation. The technique is illustrated by several numerical examples.

F6-3 REMOTE SENSING OF A BURIED SCATTERING LAYER: J. A. Kong,
0920 L. Tsang, and B. Djermakoye, Research Laboratory of
Electronics, Massachusetts Institute of Technology,
Cambridge, MA

In the applications of microwave remote sensing, practical and useful theoretical models are essential to data interpretation. For low conductivity earth media such as the desert and ice and snow covered areas, the factors affecting radiometric measurements are absorption, layering, and scattering. Recently radiative transfer theory has been applied to the study of microwave thermal emission from scattering media. In this report we solve the problem of remote sensing of a scattering layer buried under a dielectric layer and bounded by a half-space homogeneous medium below. This three-layer model easily reduces to a bounded scattering layer with no top layer or to a half-space scattering medium studied in the literature.

We assume the scattering effect is due to discrete scatterers modelled with spheres. Mie scattering phase functions are used and incorporated into the radiative transfer equations. In addition to the thermal emission from the three-layer medium, we also account for an incident sky radiation. The results are plotted as functions of frequencies and viewing angles.

In the absence of the top layer or when the top layer is a homogeneous dielectric with permittivity close to the background permittivity of the scattering medium, the brightness temperature as a function of frequency oscillates and decreases. When the top layer is a dispersive dielectric with a high permittivity such as water, the brightness temperature increases with frequency. We apply such characteristics to the interpretation of the diurnal change of observed brightness temperatures for a snow field. The radiative transfer theory with the scattering layer modelled as a random medium will also be applied to the interpretation of snow data.

F6-4 ELECTROMAGNETIC MODELING OF TRANSMISSIONS THROUGH AN
0945 IN-SITU GASIFIED COAL SEAM: J. J. Holmes, Naval Surface
Weapons Center, White Oak Laboratory, Silver Spring, MD
and C. A. Balanis, Dept. of Electrical Engineering, West
Virginia University, Morgantown, WV

The development of an efficient underground coal gasification process may become an important step in achieving energy self-sufficiency. To realize the benefits of the underground coal gasification process, an electromagnetic monitoring system must be developed to convey information about the status of the gasification process. As an aid in the design of an electromagnetic system for the measurement of the overall width of the gasified section of the underground (in situ) coal gasification process, an analytical model has been developed that will predict the electromagnetic field transmitted through the gasified portion of the coal seam. The gasified and ambient (ungasified) coal media have been modeled electrically as being lossy, surrounded above and below by relatively high conducting overburden and underburden. Vertical electric and horizontal magnetic dipoles have been investigated, utilizing a geometrical optics formulation. Indications, from the frequency responses of the transmission monitoring scheme, are that the system is capable of measuring the width of the modeled In Situ gasification process with reasonable accuracy.

F6-5 THE DIELECTRIC CONSTANT OF SALINE SOILS AT L-BAND:
1025 K. R. Carver and R. P. Jedlicka, Physical Science
Laboratory, New Mexico State University, Las Cruces, NM

The complex dielectric constants of saline soils from New Mexico, Utah, and South Dakota have been measured at 1.5 GHz as a function of gravimetric soil moisture. The New Mexico soil is gypsum ($\text{CaSO}_4 \cdot 2\text{H}_2\text{O}$) taken from the White Sands deposit; the Utah soils are from the Great Salt Lake and the South Dakota soils are associated with saline seeps. In all cases, the soil salinities are much higher than those of other soils for which measured dielectric constants have been reported in the literature. As expected, the imaginary part of the measured dielectric constant is commensurately higher. For example, the dielectric constant of gypsum is $3.63 - j 0.86$, $5.00 - j 1.67$, $5.78 - j 2.50$, $7.84 - j 2.18$, and $10.42 - j 3.80$ at gravimetric soil moisture levels of 5%, 10%, 15%, 20%, and 25% respectively. Measurements were made using a reflectometer-network analyzer technique which is well suited to this type of soil.

In addition, a mixing model is presented which can take measured dielectric constants at one frequency (in this case, L-Band) and extrapolate to other frequencies (e.g., X-Band). This combination of experimental and theoretical approaches is significant in explaining microwave remote sensing signatures of terrain with elevated salinity levels.

F6-6 MICROWAVE REMOTE SENSING OF SNOW PACK CHARACTERISTICS:
1050 J. C. Shiue, NASA/Goddard Space Flight Center; J. A. Kong,
Massachusetts Institute of Technology; H. A. Boyne,
National Bureau of Standards, Boulder, CO; A. T. Chang,
NASA/Goddard Space Flight Center; D. A. Ellerbruch,
National Bureau of Standards, Boulder, CO; and L. Tsang,
Massachusetts Institute of Technology, Cambridge, MA

Recently there have been extensive theoretical and experimental studies on microwave remote sensing of snow fields. The characteristics of a snow pack reveal many interesting aspects that are useful and important in the study of remote sensing of other earth material. Theoretical models applicable to snow include (1) radiative transfer theory with a random medium model that ignores coherent effect, (2) modified radiative transfer theory with random medium model that incorporates partial coherent effects and (3) radiative transfer theory with discrete scatterer models by employing Mie scattering phase functions.

In this paper we report brightness temperature measurements of snow packs with four radiometers operating at frequencies 5 GHz, 10.7 GHz, 18 GHz, and 37 GHz. The measured experimental results are interpreted with the various theoretical models. Observations are made on naturally formed snow pack as a function of time. When there is no falling snow over period of day and the pack is at a constant depth, the diurnal changes show distinctive features during morning and afternoon. Plotted as a function of frequency, the brightness temperature decreases in the morning and increases in the afternoon. These diurnal characteristics have been interpreted with three layer scattering models using the radiative transfer theories.

Artificially packed snow are also made to observe the brightness temperature changes as functions of depth, frequency, and angle of observation. To examine the effect of interference resulted from coherence, both natural and artificial snow packs are made on top of aluminum plates. The scattering effects are clearly more pronounced for old snow as opposed to new snow. The dependence of scattering strength as a function of wavelength and scatterer sizes is examined. Studies are also made in the estimation of equivalent liquid water content of the snow pile from these passive radiometric measurements.

F6-7 OIL EXPLORATION AND THE USE OF DIELECTRIC MIXTURE THEORIES:
1115 G. S. Huchital, Schlumberger-Doll Research Center,
Ridgefield, CT

As the search for oil becomes more difficult, sophisticated techniques are applied in order to locate economically producible hydrocarbons.

A recent addition to the types of devices used to locate hydrocarbons in a borehole drilled in the earth is an electromagnetic measurement system operating in the microwave region.¹⁻³ This device measures the propagation velocity and attenuation of a 1.1 GHz wave. From these measurements, the dielectric constant and conductivity of the rock formation can be determined. The question to which this paper will address itself is how to interpret the measured bulk dielectric constant and conductivity in terms of the sedimentary rock, water, and oil mixture; that is, how much oil is present in the host rock.

The model used for this study is based on some work by Taylor.⁴

Taylor's theories related the bulk dielectric constant of a material to the dielectric constants of the constitutive components and the shape of the inclusions within the host material.

This paper investigates the effect of the shape of inclusions on the bulk dielectric constant of a mixture.

The results of this study show that a simple model of sedimentary rocks can be used in conjunction with a measure of bulk dielectric constant to accurately predict rock-water-oil distribution.

References:

1. Calvert, T.J., Rau, R.N. and Wells, L.E.: "Electromagnetic Propagation... A New Dimension in Logging", presented at the 47th Annual California Regional Meeting of the Society of Petroleum Engineers of the AIME, April, 1977.
2. Calvert, T.J.: "Microwave Logging Apparatus Having Dual Processing Channels", U.S. Patent No. 3,849,721, November 19, 1974.
3. Rau, R.N.: "Method and Apparatus Utilizing Microwave Electromagnetic Energy for Investigating Earth Formation", U.S. Patent No. 3,944,910, March 16, 1976.
4. Taylor, L.S.: "Dielectric Properties of Mixtures", IEEE Trans. AP-13, No. 6, November 1965.

WAVES IN PLASMAS

Thursday A.M., 18 May, Room 0123

Chairman: R. W. Fredricks, Plasma Physics Group,

TRW Defense and Space Systems, Redondo Beach, CA

H1-1 TEMPORAL CORRELATION PROPERTIES IN SHORT ELECTROMAGNETIC
0830 PULSES IN THE WHISTLER MODE: S. C. Bloch, Physics Dept.,
 University of South Florida, Tampa, FL

Results are presented of a computer study of the propagation of short electromagnetic pulses in the whistler mode, with emphasis on analysis of the temporal cross correlation function. The original pulses, linearly polarized with rectangular modulation envelopes coherent with the carrier, are cross correlated with the x or y components of the received circularly polarized pulses. Correlation velocities and maxima of the cross correlation functions are computed for ranges of electron plasma frequency, cyclotron frequency, collision frequency, path length, and pulse width.

H1-2 WHISTLER MODE PULSE PROPAGATION IN A MAGNETOPLASMA:
0850 D. C. D. Chang and R. A. Helliwell, Radioscience
 Laboratory, Stanford University, Stanford, CA

Pulse distortion due to propagation in a dispersive medium becomes important in studies of VLF wave-particle interaction (WPI) processes by injecting RF pulses into the magnetosphere from the ground. Whistler mode (WM) propagation of RF pulses through a homogeneous magnetoplasma as well as through a duct in the magnetosphere has been investigated by using the FFT technique. This technique works in both homogeneous and slowly varying media. As far as we know this is the first time that the distortion of a VLF pulse propagating in the magnetosphere has been calculated. Even though we have not used the group velocity concept in our simulation, our results show that the center of a WM pulse does indeed travel with the group velocity (within a measurement error of 1%).

In a homogeneous medium at frequencies below $f_H/4$ the high frequency components arrive prior to the main body of the pulse while the low frequency components lag behind. This sequence is reversed when the carrier is above $f_H/4$. The distortion increases as the frequency departs from $f_H/4$.

In the magnetosphere it is found that the frequency of minimum distortion is the nose frequency f_N , as expected. When the carrier frequency is below f_N , the high frequency components of a pulse always arrive first at the monitor stations along the path and the distortions increase as the carrier departs from f_N . Above f_N , on the other hand, there is always a location along the path where the pulse distortion is minimum.

HI-3 PROPAGATION OF UNSTABLE WAVES DURING THE RELAXATION OF
0910 A VELOCITY ANISOTROPY: Y. Kiwamoto, NASA/Goddard Space
Flight Center, Laboratory for Planetary Atmospheres,
Greenbelt, MD

Electrostatic waves observed by OGO-5, ISIS and other satellites are considered to be driven by anisotropic deformations of the electron velocity distribution. They are often assumed to persist outside of the region of the original strong anisotropy, which may be transient. This assumption is made implicitly in many discussions of electrostatic - electromagnetic wave mode conversion processes in order to explain the electromagnetic wave emissions from Jupiter and the earth. It should be noted, however, that the propagation direction of the electrostatic waves may change after the relaxation and the damping rate is sensitive to the propagation direction.

Here we analyze the propagation characteristics of electron cyclotron harmonic waves during the relaxation of a bi-Maxwellian velocity distribution. The dominant propagation direction changes from around 60° to 80° with respect to the magnetic field. In a linear analysis, the peak of the frequency spectrum shifts toward a narrow pass-band allowed in the final dispersion relation. A nonlinear analysis of long persisting electrostatic waves stimulated by ISIS satellite will also be presented taking these effects into consideration.

HI-4 NONLINEAR MECHANISM FOR MAINTAINING THE $3/2 f_H$ ELECTRON
0930 CYCLOTRON HARMONIC WAVE INITIATED BY TOPSIDE SOUNDERS:
 R. F. Benson and Y. Kiwamoto, NASA/Goddard Space Flight
 Center, Laboratory for Planetary Atmospheres, Greenbelt, MD

The Alouette and ISIS topside sounders radiate a considerable amount of energy in the form of electrostatic waves. At a number of characteristic frequencies of the medium these stimulated electrostatic waves can have near-zero group velocity leading to strong signals (plasma resonances) that persist for many milliseconds after the transmission of the 100 μ sec stimulating pulse. One of the most prominent resonances, however, corresponds to a dispersion condition where the wave group velocity is more than 10 times the satellite velocity. This resonance, the so-called diffuse resonance observed between f_H and $2f_H$ where f_H is the electron cyclotron frequency, requires a local energy source which persists long after the sounder stimulated wave has escaped. Oya (Phys. Fluids, 14, 2487, 1971) proposed a sounder-stimulated plasma wave instability and a nonlinear mechanism based on the 3 wave decay process to explain the diffuse resonance. We will present theoretical and observational difficulties with this model and will propose an alternative explanation based on nonlinear Landau damping of the sounder stimulated $2f_H$ wave. Observations will be presented which support the proposed mechanism.

H1-5 NONLINEAR INTERACTION BETWEEN HIGH-POWER HF RADIATION
1005 AND THE IONOSPHERIC PLASMA: K. J. Harker, Institute
for Plasma Research, Stanford University, Stanford, CA

Getmantsev et al.¹ have reported a wave-wave interaction experiment in which a modulated high-power signal was transmitted at 5.75 MHz. Using a sensitive receiver located 180 km to the north, a signal was observed at the modulation frequency, which ranged from 1 to 7 kHz.

We report a theory to explain these experimental results based on parametric mixing interaction in a cold, inhomogeneous, and collisionless plasma. The mechanism on which the theory is based is the nonlinear interaction between two components of the modulated signal to produce a whistler which then propagates to the ground where it is detected. The strength of the received signal is calculated and compared to the experimentally observed values.

1. G.G. Getmantsev, N.A. Zuikov, D.S. Kotik, L.F. Mironenko, N.A. Mityakov, V.O. Rapoport, Yu.A. Sazonov, V.Yu. Trakhtengerts, and V.Ya. Eidman, JETP Lett., 20, 101 (1974).

H1-6 DIRECT AND CROSS-POLARIZED SCATTER FROM A TURBULENT
1025 LABORATORY PLASMA: D. E. Tremain, K. A. Graf, and
H. Guthart, SRI International, Inc., Menlo Park, CA

A study has been conducted to examine the depolarizing backscatter characteristics of turbulent plasmas at high electron densities. Data are presented from a turbulent-plasma scattering experiment that is concerned with depolarization of an incident microwave signal. The plasma is a turbulent column produced in a flame chamber. Calculations based on a modified first-Born approximation agree well with the direct polarized data. Calculations which assume that reflection from an overdense core is the dominant mechanism responsible for depolarization agree well with the cross-polarized data at high electron densities and small aspect angles.

H1-7 AN ANALYSIS OF THE EFFECTS OF SCATTERING OF TERRESTRIAL
1045 KILOMETRIC RADIATION OF PLASMA INHOMOGENEITIES IN THE
MAGNETOSHEATH: J. K. Alexander and M. L. Kaiser, Laboratory
for Extraterrestrial Physics, Goddard Space Flight Center,
Greenbelt, MD

Observations of terrestrial kilometric radiation obtained from the Radio-Astronomy-Explorer-2 spacecraft during lunar occultations of the Earth are sometimes characterized by the reception of strong terrestrial signals at frequencies below ~ 250 kHz even when the Earth is more than 10° below the lunar horizon. On some occasions the kilometer wave radiation must be coming to the spacecraft from a region at a geocentric distance of $\geq 38 R_E$ corresponding to a far greater altitude than the generally accepted location of the "auroral" radio source at $R \sim 2-3 R_E$. We present evidence based on analysis of the occurrence morphology and direction of arrival measurements for these events that suggests they are the result of strong scattering of the low frequency radiation by plasma inhomogeneities in the terrestrial magnetosheath. The frequency range over which these events occur varies directly with the solar wind plasma frequency, presumably because the plasma density in the scattering region (the magnetosheath) tracks the variations of the solar wind density. We can use the apparent magnitude of the scattering to estimate limits to the scale size and amplitude of the plasma inhomogeneities and to speculate on their origin.

- H1-8 PLASMA WAVES ASSOCIATED WITH SOLAR WIND BEAM-PLASMA
 1105 INTERACTIONS: P. Rodriguez, M. L. Kaiser, and D. H. Fairfield, Laboratory for Extraterrestrial Physics, Goddard Space Flight Center, Greenbelt, MD

The earth's bow shock is known to emit suprathermal electrons ($E \sim 1$ KeV) into the solar wind when the interplanetary magnetic field intersects the bow shock surface. These energetic electron beams generate electron plasma oscillations at the electron plasma frequency f_{pe} (~ 30 kHz) which are routinely detected by the plasma wave and radio wave experiments on the IMP-6 spacecraft. In addition, lower frequency electrostatic and electromagnetic waves are detected near and below $2 f_{pi}$, where f_{pi} is the nominal proton plasma frequency ($= f_{pe}/43$), and these waves are apparently Whistlers and ion acoustic or Buneman waves. We have studied the wave spectrum over the range 20 Hz - 200 kHz for all local times in the solar wind to determine the characteristic wave spectrum of the beam-plasma interaction. We have also determined that significant modifications in the wave spectrum occur when up-streaming energetic protons are suspected to be present in the solar wind.

- H1-9 RADIO MEASUREMENTS OF MAGNETOSHEATH ELECTRON DENSITIES AND
 1125 DENSITY FLUCTUATIONS: M. L. Kaiser, P. Rodriguez, D. H. Fairfield, and J. K. Alexander, Laboratory for Extraterrestrial Physics, Goddard Space Flight Center, Greenbelt, MD

Satellite-borne radio astronomy experiments have detected strong line emissions near the electron plasma frequency in the earth's magnetosheath. From these observations which are free of spacecraft sheath effects, we can determine the electron density and the scale size of electron density fluctuations at positions near the equatorial plane in the magnetosheath. We will show examples of periods when the electron density along the flanks of the magnetosheath exceed 200 cm^{-3} . Electron density fluctuations and associated magnetic field fluctuations of 50-100% are observed over time intervals as short as 10-20 sec. If these fluctuations are frozen within the convecting magnetosheath they correspond to scale sizes of a few thousand kilometers.

THURSDAY AFTERNOON, 18 MAY, 1330-1640

Commission F Session 7

PROPAGATION EFFECTS IN COMMUNICATIONS

Thursday P.M., 18 May, Room 1109

Chairman: L. J. Ippolito, NASA/Goddard

Space Flight Center, Greenbelt, MD

F7-1 ATTENUATION STATISTICS AT 11.7 GHz - LONG TERM MEASUREMENT
1330 AND PREDICTION TECHNIQUES: L. J. Ippolito, NASA/Goddard
 Space Flight Center, Greenbelt, MD

The Goddard Space Flight Center of the National Aeronautics and Space Administration is performing an experiment with the Communications Technology Satellite, CTS, designed to measure and characterize the radio propagation phenomena important to earth/space applications in the 12/14 GHz frequency bands. Rain attenuation statistics developed at Greenbelt (GSFC) and Rosman, North Carolina for the first sixteen months of CTS measurements are presented. The correlation of measured rain rate with signal attenuation is evaluated and compared with theoretical models.

Worst month statistics developed for the two locations show a wide variability, ranging from 16 minutes to 36 minutes outage at the 10 dB level, and from 1-1/2 minutes to 11 minutes at a 20 dB level. Attenuation events at Greenbelt have exceeded 30 dB on several occasions, resulting in a total of five minutes in excess of 30 dB. Long term attenuation measurements at Rosman and Greenbelt have shown that for a one hour per year allowable outage due to rain, power margins of 7.3 dB and 8.5 dB would be required, respectively. In general, the attenuation observed at 11.7 GHz has been statistically as expected, however, individual events with very high attenuation levels, particularly during thunderstorm activity, have been observed.

The paper concludes with an assessment of the impact of the propagation and link characterization measurements on the design and performance of 12/14 GHz space communications systems.

- F7-2 CTS 11.7 GHz ANGLE-OF-ARRIVAL MEASUREMENTS: D. M. Theobold
1355 and D. B. Hodge, The Ohio State University ElectroScience
Laboratory, Columbus, OH

The Ohio State University's participation in the CTS Communications Link Characterization Experiment was developed in an effort to measure the long term propagation characteristics of a microwave earth-space path. A receiver utilizing a four element self-phased array antenna was implemented to provide amplitude and differential phase measurements of the incident signal. This system is used to provide continuous measurement of angle-of-arrival fluctuations, as well as attenuation and amplitude scintillation characteristics, induced as a result of propagation through rainfall and the turbulent troposphere.

Measurements of differential phase between the four antenna elements, the amplitude of each of the elements, and the coherent sum amplitude of the array are recorded on digital tape. The effect of the diurnal motion of the satellite is processed out of the differential phase and amplitude data, allowing statistical analysis of the propagation effects to be performed. Long term probability distribution functions are found for the four amplitude and coherent sum signals. Probability distribution functions of angle-of-arrival are also derived from the differential phase data. Variance statistics of amplitude and angle-of-arrival fluctuations are calculated and presented in the form of probability density functions. Examples of the correlation between angle-of-arrival fluctuation and amplitude fading during precipitation events will be presented.

- F7-3 RESULTS OF CTS 11.7 GHz ATTENUATION AND DEPOLARIZATION
1420 MEASUREMENTS AT BLACKSBURG, VA: C. W. Bostian, W. L.
Stutzman, E. A. Manus, P. H. Wiley, S. R. Kauffman,
R. E. Marshall, W. P. Overstreet, and R. R. Persinger,
Electrical Engineering Dept., Virginia Polytechnic
Institute and State University, Blacksburg, VA

This paper summarizes the results of two years of rain attenuation and depolarization measurements with the CTS 11.7 GHz beacon. It discusses signal behavior during individual storms and presents data on the statistical relationships between rain rate, attenuation, and depolarization isolation. The dependence of effective path length on rain rate and local terrain is explored.

F7-4 A RAIN PROPAGATION PREDICTION MODEL FOR EARTH-SPACE
1445 MILLIMETER WAVE SIGNALS: R. R. Persinger and W. L.
Stutzman, Virginia Polytechnic Institute and State
University, Dept. of Electrical Engineering,
Blacksburg, VA

Millimeter wave signals along a satellite-earth path experience attenuation, depolarization, and phase shift due to rain. In this paper a model is presented which permits calculation of these effects for a given rain condition and specified transmit/receive antenna parameters.

Calculation of the propagation effects of rain are based on the concepts of the propagation constant model. The rain path is divided into subintervals which may have different rain parameters. This path subdivision provides a means to approximate an actual rain in a piecewise sense. The rain rate, fraction of oblate spheroidal shaped rain drops, and mean canting angle can be specified for each subinterval. The path model also includes distributions of rain drop shapes, sizes, and canting angles. These distributions are included directly and are a result of the theoretical derivations.

Wave-antenna interaction effects are also computed. The transmit antenna used to generate the wave incident on the rain medium and the antenna receiving the altered wave exiting the rain can have any polarization state. This permits a careful examination of antenna effects on experimental data.

The results of the theoretical model for the CTS (11.07 GHz) and COMSTAR (19.04 and 28.56 GHz) satellite paths and comparisons to experimental results will be presented.

F7-5 CROSSPOLARIZATION EFFECTS DUE TO ICE CRYSTALS AT 12.5
1525 AND 15 GHz: H. K. Burke and R. K. Crane, Environmental
 Research and Technology, Inc., Concord, MA

A model for calculating the magnitude of crosspolarization effects due to ice crystals both in the linear and circular senses is developed. The ice crystals are treated as prolated spheroids. Different axial ratios are used to deduce shape factors for polarizabilities along major and minor axes. Variations in the relative orientation of the ice crystals with respect to the propagation path and the equivalent liquid water content are also included.

Results are in reasonable agreement with available measurements. For example, assuming (1) a constant elevation angle of 25° for the ice crystals, (2) axial ratios between 2 and 5, (3) their equivalent liquid water content of 0.2 gm/m^3 , (4) thickness of the medium of 2 km and (5) an aspect angle of the propagation path of 15° , the cross polarized signal discrimination (XPD) values are between -27 and -21 dB for the linear case and between -25 and -19 dB for the circular case. Reducing the liquid water content to 0.05 gm/m^3 decreases XPD to between -39 and -33 dB for the linear case and between -37 and -31 dB for the circular case. The cross-polarization effects are always worse for the circular case than the linear as expected.

F7-6 THE DEPOLARIZING PROPERTIES OF SOLID HYDROMETEORS AT
1550 INTERMEDIATE HEIGHTS: G. C. McCormick and A. Hendry,
Division of Electrical Engineering, National Research
Council of Canada, Ottawa, Canada

Depolarization along a satellite path caused by rain is well known. More recently there has been discussion of an "anomalous depolarization" produced by solid particles oriented by the strong electric field in the upper parts of thunderstorm cells. It is the purpose of this paper to identify a depolarization taking place at lower altitudes, namely, from the 0° isotherm to a height of approximately 6 km. Data from polarization diversity radar observations of thunderstorm cells in the period 1972-1977 have been analyzed. The observed depolarizations are less spectacular than those taking place at greater heights, and are apparently caused by solid particles having a mean orientation which is exclusively horizontal. While the depolarization produced by these particles is different from that due to those at higher altitudes, there is no evidence that the particles themselves are different.

F7-7 RADIOMETRIC MEASUREMENTS OF SKY NOISE TEMPERATURE AT 11.6
1615 GHz: D. V. Rogers, COMSAT Laboratories, Clarksburg, MD

COMSAT Laboratories, on behalf of INTELSAT, is engaged in a program to collect, at various locations around the world, atmospheric data that can be used to model and predict propagation effects in the 11/14 and 20/30 GHz bands. The primary goal of this effort is to determine the statistics of precipitation-induced signal attenuation along earth-space paths for the above frequency bands. Radiometric measurements of sky noise temperature at frequencies of 11.6 and/or 20/30 GHz are collected, along with tipping bucket raingage data, for several climate types. In addition, deployment of radiometers in diversity configurations is planned for early 1978. The current status of this program is summarized, and recent results of rain and 11.6 GHz radiometer measurements are presented for several locations around the world. These data are analyzed from the standpoint of climate type, and the experimental cumulative distributions are compared with theoretical predictions of rain and attenuation statistics, as derived from the Rice-Holmberg model.

FRIDAY MORNING, 19 MAY, 0830-1200

Commission F Session 8

RADIOMETRIC SENSING

Friday A.M., 19 May, Room 1109

Chairman: C. I. Beard, Naval

Research Laboratory, Washington, DC

F8-1 MEASUREMENTS OF INTEGRATED ATMOSPHERIC ABSORPTION BY A
0830 DUAL-CHANNEL MICROWAVE RADIOMETER: F. O. Guiraud, NOAA,
Environmental Research Laboratories, Wave Propagation
Laboratory, Boulder, CO

A dual-channel all-weather ground-based microwave radiometer has been developed for the continuous measurement of total integrated atmospheric water vapor and cloud liquid. The system comprises two radiometers: a vapor channel at 20.6 GHz and a liquid channel at 31.65 GHz. Initial measurements for the calibration of this instrument indicate that the absorption coefficients of both water vapor and oxygen that are presently used for computation of brightness temperatures at these frequencies are too low. Samples of elevation scans of brightness temperatures taken on clear days near Denver, CO., are presented and compared with theoretical calculations based on temperature and water-vapor content measured by radiosonde. Measured absorption coefficients to date are 10-20% higher than presently accepted values.

F8-2 AN EXPERIMENTAL INVESTIGATION OF SELF-EMISSION FROM
0900 MICROWAVE RADIOMETERS: K. R. Carver, Physical Science
Laboratory, New Mexico State University, Las Cruces, NM

Microwave radiometers are customarily described as receiving devices used to detect thermal radiation from earth's surface or atmosphere. However, in a radiometer with an uncooled front end, the noise power generated by the first stage (e.g., a mixer) causes an incoherent wave to be transmitted, so that the radiometer functions as a weak radar. Furthermore, this self-emission noise can contribute to the apparent nadir brightness temperature from quasi-specular earth surfaces with low emissivities, and has been qualitatively noted in various microwave remote sensing experimental investigations.

This paper describes two separate controlled experiments designed to describe the range and angular dependence of the self-emission noise term. The first of these was conducted in April, 1977 at the University of Kansas, using a 10.69 GHz radiometer with a scalar horn; the beam was pointed down toward a large aluminum plate and the dependence of the apparent brightness temperature on both range and angle from nadir was noted. The second experiment, conducted in October, 1978 at New Mexico State University also used a 10.69 GHz radiometer with a standard gain horn and was pointed toward a larger flat conducting plate. In both cases, the apparent temperature varied inversely as the square root of range distance, from a nadir angle of 0° ; the self-emission term fell off very rapidly with nadir angle. A theoretical study of this self-emission range dependence is in progress.

F8-3 DETERMINATION OF VERTICAL TEMPERATURE AND HUMIDITY
0930 PROFILES OF THE ATMOSPHERE BY A COMBINATION OF
RADIOMETRIC AND ACTIVE GROUND-BASED REMOTE SENSORS:
E. R. Westwater, NOAA, Environmental Research Labora-
tories, Wave Propagation Laboratory, Boulder, CO

Ground-based microwave radiometric techniques have heretofore yielded smoothed, but useful, replicas of vertical temperature and humidity profiles. Conversely, returns from active sounders, such the acoustic sounder or the FM-CW radar, have shown a high-degree of atmospheric structure, but the received signals are not simply related to the temperature and humidity distributions. However, in many cases, the height of nocturnal temperature inversions, and the base height of elevated inversions can be deduced accurately (usually to well within 100 m) from the active returns.

It is plausible that a combination of the active information, which yields information about the height of significant points of the profiles, and the radiometric technique, which yields gross information on the absolute profiles, could significantly improve profile recovery. We demonstrate this by first presenting an inversion method that combines active and passive information. Next, we evaluate the theoretical accuracy of the combined system. Finally, we show temperature and humidity profile retrievals, determined from experimental radiometric data and hypothetical height information, and compare these with profiles derived from passive information alone.

F8-4 POWER SPECTRA OF ATMOSPHERIC RADIANCE: P. Ciotti,
1015 D. Solimini, and P. Basili, Universita de Roma, Italy

Ground-based radiometric observations have proved to be effective means for remotely determining both the static and the dynamic thermal vertical structure of the lower troposphere. Since the meteorological parameters are random fields, the atmospheric radiance measured by a ground-based radiometer fluctuates in time randomly, and, under suitable conditions, these fluctuations result essentially from atmospheric temperature fluctuations.

In this experiment the downgoing radiance has been measured for various elevation angles in several bands of the infrared in which the atmosphere exhibits different absorptions. The low-frequency power spectrum of the fluctuating radiance has been computed by a fast Fourier transformation of both records of the radiometer output and its real-time autocorrelation. The Fourier power spectra of the suitably windowed data apparently show different patterns according to the degree of dynamic stability of the lower tropospheric layers. Under unstable conditions, individual spectra exhibit nearly "frozen" Kolmogorov shape with usually steeper slopes, while with stable conditions intermittent sharp periodicity frequently appears. To investigate the latter case, maximum - entropy spectrum analysis has been used, because of its ability to evaluate the parameters of multiple sinusoids embedded in a flat spectrum time series. From the obtained results, the sensitivity of the radiometer output to the varying dynamic state of the low troposphere has become apparent.

F8-5 FURTHER WORK ON THE INFRARED DETECTION OF SURFACE CURRENT
1045 AND CHARGE DISTRIBUTIONS: R. W. Burton and W. C. Russell,
Dept. of Electrical Engineering, Naval Postgraduate School,
Monterey, CA

A method has been developed for rapid measurement of the magnitudes of charge and surface current distributions using an infrared scanner. Thermal distributions due to I^2R heating are detected and displayed on a color TV-type monitor. Not all surfaces and materials are sufficiently emissive in the infrared region, particularly among the metals. The effectiveness of surface preparations intended to enhance the infrared emissivity of these metals is presented. The feasibility of utilizing these methods with practical metallic models is explored. Flat-plate scatterers and electrically thick cylinders ($ka = 1$) are investigated and the results compared with measurement and theory.

F8-6 SATELLITE PASSIVE MICROWAVE IMAGING SYSTEM DESIGN:
1115 J. L. King, NASA/Goddard Space Flight Center,
 Greenbelt, MD

Many tradeoffs are required in the design of high resolution (1-20 km) passive microwave imaging systems for satellites. The satellite orbit, sensor swath width, resolution antenna system, scan type, calibration accuracy, temperature sensitivity, and selection of channels required to perform the required measurements are only a partial list of the major design considerations. Both low and geosynchronous orbit systems are needed to provide the wide variety of passive microwave measurements which are capable of producing significant meteorological, oceanographic, and earth resource data. Spatial resolution and time between measurements must be traded off in deciding between single or multiple low orbiting satellites or geosynchronous satellites.

A brief background in previously flown passive microwave instruments will be presented along with some of the more significant results giving references for detailed information. A brief discussion of the rationale behind the channel selection process will also be presented with user agency inputs of requirements for measurements of various parameters. This will be used to establish a baseline system requirement for a post 1980 multichannel microwave radiometer system for weather and climate, oceanography, and earth resources applications.

The system design tradeoffs will be discussed related to the spacecraft orbit, the radiometer receiver sensitivity, antenna type (mechanical scan, electrical scan, or pushbroom) and scan geometry. The antenna system design of arrays, reflectors, and multichannel feed approaches will be discussed in terms of performance parameters such as beam efficiency, losses, and bandwidth. A new concept for improving the radiometer temperature sensitivity in bandwidth limited large phase arrays will be described for a 100 meter aperture array. Radiometer receiver designs currently in use will be also discussed in terms of achievable temperature resolutions and calibration accuracies. A 4-100 GHz seven channel 3-20 km resolution Advanced Scanning Multichannel Microwave Radiometer for low orbit satellite systems will then be presented.

PROPAGATION AND SCATTERING APPLICATIONS

Friday A.M., 19 May, Room 0109

Chairman: R. K. Crane, Environmental

Research and Technology, Inc., Lexington, MA

F9-1 REMOTE SENSING OF THE ATMOSPHERE USING COMBINED EXPERI-
0830 MENTAL TECHNIQUES - SYMBIOTIC ASPECTS: G. M. Lerfald
and V. E. Derr, NOAA, Environmental Research Laboratories,
Wave Propagation Laboratory, Boulder, CO

Scattering and absorption of electromagnetic energy by the constituents of the atmosphere are the basis of most remote sensing methods developed for use in the atmosphere. An experimental and analysis program which combines several techniques is described.

The techniques employed include a large backscatter lidar system with dual polarization or dual wavelength capabilities, a microwave (24 GHz) backscatter radar with polarization sensitivity, infrared radiometry, several channels of solar photometry, a solar aureole radiometer (near-forward scattering of solar radiation), all sky photography, and acoustic sounder. The parameters measured include the precipitable water vapor, the total columnar ozone in the atmosphere, aerosol loading, aerosol size distribution, glaciation in clouds, cloud type and geometry, size distribution of cloud particles and the spectral absorption and scattering of visible and infrared radiation in the atmosphere.

Emphasis is given in the paper to the advantages of combining the experimental techniques to improve the accuracy or extend the range of the remote sensing methods. Among the specific advantages described are the overlapping ranges (range of cloud thicknesses) of infrared lidar and microwave radar, the combination of angular scattering measurements and spectral extinction measurements to determine size distributions of aerosols and cloud particles, and the usefulness of some of the less quantitative data, such as time lapse all-sky photography, when data analyses are performed.

F9-2 RAY TRACING OF ISOLATED TORNADO-ORIGINATED GRAVITY WAVES
0855 DETECTED AT F-REGION IONOSPHERE: R. J. Hung, The
 University of Alabama, Huntsville, AL and R. E. Smith,
 NASA/Marshall Space Flight Center, Huntsville, AL

The ionosphere is capable of sustaining a large number of wave phenomena, waves propagating downward from the magnetosphere, waves propagating upward from the neutral lower atmosphere, etc. This paper is dealing with the ray tracing of atmosphere waves, observed in ionosphere, which were propagating upward from the troposphere during the activity of isolated tornadic storms. These atmospheric waves are observed on ground-based ionospheric sounding records as perturbations in ionization.

The experimental facility employed in this study is the high frequency radio wave Doppler array system which consists of three sites with nine transmitters operating at nominal frequencies of 4.0125, 4.759 and 5.734 MHz. with receivers located at NASA/Marshall Space Flight Center, Alabama.

Based on the data observed from the Doppler sounder array, power spectral density is subjected to obtain the wave period of waves associated with storms. Also, the direction of the wave vector and phase velocity of waves generated are obtained from cross-correlation analysis.

Ray tracing computation has been attempted to trace back the location of the wave source from the observed atmospheric waves at ionospheric height. By considering the data on the atmosphere and wind profiles, the location of wave sources can be computed.

Five events of waves associated with isolated tornadic storms will be presented. The results based on ray tracing indicates that the waves were excited near the location where the tornado touched down more than one hour later.

The characteristics of waves propagated in inhomogeneous medium will be discussed. The possible wave excitation mechanism based on the model of enhance overshooting turrets will also be presented.

F9-3 MEASUREMENTS OF THE 1.5 GHz MARISAT SIGNALS AT LOW ELEVATION
0920 ANGLES: F. T. Tseng and D. J. Fang, COMSAT Laboratories,
 Clarksburg, MD

MARISAT signal degradation such as fading and scintillation, observed at low elevation angles, are believed to be caused by a combination of tropospheric scattering effects and sea surface multipath reflections. In order to get a general characterization of the degradation, measurements were made on board of SS Mobil Aero en route from Boston to Beaumont, Texas. Significant results indicate that as elevation angle decreased from 10° to 5° , the mean C/N dropped about 3 dB from its nominal value, and the instantaneous value of the C/N fluctuated markedly.

F9-4 OBSERVATIONS OF TROPOSPHERIC SCINTILLATION ALONG LOW ELEVATION
0945 ANGLE 6/4 GHz EARTH-SPACE PATHS: D. J. Kennedy and J. M.
Harris, COMSAT Laboratories, Clarksburg, MD

A series of observations to gather long term statistics of tropospheric induced scintillation on CW signals over low elevation angle 6/4 GHz earth-space paths is described. The data were collected for a period of nine months over paths from a geostationary satellite (60° E longitude) to Goonhilly U.K. (~6.5° elevation angle) and Yamaguchi Japan (~7° elevation angle). Signal level recordings were made concurrently at Goonhilly and Bahrain and included four links, two of which exhibited uplink scintillation at 6 GHz, one having downlink scintillation at 4 GHz, and one having both up and downlink scintillation (Yamaguchi to Goonhilly). The scintillation activity shows a strong diurnal and seasonal dependence which correlates well with ground based meteorological data of wind velocity, wet bulb depression and acoustic sounder echoes. For the Goonhilly path the magnitude of the scintillations for 0.01 percent of the time was approximately 4.5 dB peak-to-peak at both 4 GHz and 6 GHz. 3 dB or greater scintillations occurred about 0.3 percent of the time. Amplitude fluctuations which may have been satellite induced were also observed.

F9-5 MILLIMETER WAVE PROPAGATION IN OCEAN FOGS AND MISTS:
1025 K. L. Koester and L. H. Kosowsky, Norden Division of
United Technologies Corporation, Norwalk, CT

The proposed utilization of millimeter wave radar systems for surveillance and tracking of targets over the ocean has necessitated a close examination of factors affecting propagation. In previous work, the propagation of millimeter waves in pure water clouds and inland fog was investigated in detail. The dielectric constant of pure water was determined and the predicted attenuation factors were obtained for clouds and fogs.

In order to compute the attenuation factors of ocean fogs and mists, the dielectric properties of salt water were incorporated into the attenuation calculations. The Debye formula, with appropriate constants, was used to determine the dielectric properties of saline water at 70 and 94 GHz. The attenuation coefficient of fogs comprised only of saline water was derived for these frequencies. It should be noted that the attenuation coefficient is dependent on temperature and the salinity of the water comprising the fog.

A salt water fog with a liquid water content of 0.12 g/m^3 (corresponding to an approximate optical visibility of 100 meters) was analyzed. It was found that at 70 GHz, the attenuation coefficient is 0.42 dB/km at 0°C and 0.22 dB/km at 40°C . At 94 GHz, the attenuation coefficients are 0.61 and 0.38 dB/km at 0°C and 40°C , respectively.

F9-6 MAPPING OF LINE-OF-SIGHT-FADING ZONES: C. Fengler, Dept.
1050 of Electrical Engineering, McGill University, Montreal,
Canada

A map divided in zones of different line-of-sight fading characteristics was developed for North America. It was derived from topographic and meteorological features. An example of an open-scale map for one area is presented. The limitations of this approach are discussed.

- F9-7 THE INTERACTION BETWEEN A ONE-DIMENSIONAL COMPOSITE OCEAN
1105 SURFACE AND A FLAT PLATE MODEL OF A SHIP: D. Ryan,
J. Huang, and W. H. Peake, The Ohio State University
ElectroScience Laboratory, Columbus, OH

The fields received, transmitted or scattered by a ship at sea are greatly complicated by the interaction between the structure of the ship and the sea surface. Here a one-dimensional composite model for the sea surface (with gravity waves modelled by a large scale sine wave, and capillaries modelled by small trapezoids) is augmented by a flat plate with variable roll angle as the model for the ship. Four principal scattering mechanisms which contribute to the radar signature of this complex target have been identified, viz the direct backscatter from the large scale waves, Bragg scatter from the trapezoids, forward multipath from the transmitter to surface to plate to receiver, and edge diffraction from the plate. A variety of techniques (physical optics, GTD, perturbation theory) has been used to find the contribution to the back-scattered field from each of these mechanisms, and to determine, e.g. the position and number of the multipath reflection points. A number of signatures for several encounter geometries and antenna polarizations were calculated, and were found to be in good agreement with measured signatures.

- F9-8 BISTATIC RADAR CROSS SECTION OF SHIP TARGETS: G. W. Ewell
1120 and S. P. Zehner, Georgia Institute of Technology,
Engineering Experiment Station, Atlanta, GA

The bistatic radar cross section of complex targets constitutes a formidable analytical problem, and little experimental data are available describing bistatic radar reflectivity. This paper presents a set of experimental data describing simultaneous bistatic (BRCS) and monostatic (MRCS) radar cross section of freighters taken with a moderately high resolution X-band radar system, for both horizontal and vertical polarizations over a range of bistatic angles from 0.7 to 54 degrees.

F9-9 PREDICTING AVERAGE VALUE SCATTERING FROM SMOOTH, CORRUGATED
 1140 OR DIELECTRIC SURFACES AT RADAR OR LASER FREQUENCIES:
 N. A. Howell, Technology Service Corporation, Santa Monica, CA

UNIVERSAL CURVE METHOD: The purpose of this paper is to demonstrate a technique of calculating average value radar cross section (RCS)[1] for lumpy dielectric and corrugated surfaces (such as building materials), both at radar and laser frequencies. A "lumpy flat plate" is a plate with electrically significant lumps but where there is essentially no angular dispersion of the normal vectors from various parts of the surface. For a square flat plate or a randomly oriented "lump" on a lumpy plate, the RCS is proportional to λ^{-2} . Increasing the frequency raises the peak but squeezes the sidelobes in closer to the mainlobe. Increasing the size of the plate raises the peak proportional to the area² but also squeezes the sidelobes in closer to the main beam. The result is that the average value RCS is independent of frequency and equals the area of the plate times a universal curve "U", described below:

Angle from normal	0.0	2.	4.	10.	23.7	40.	90.
σ_0 = RCS/area(db)	45.4	21.4	15.1	7.2	0.	-4.2	-8.2

DIELECTRIC SURFACES: For flat surfaces, reflection coefficients can be obtained for plane waves polarized perpendicular to and parallel with the plane of incidence. These reflection coefficients are calculated for reflection to the specular angle. It is the sidelobes from the specular reflection that cause the monostatic return. Hayes and Dyer[2] have compiled much data on the σ_0 from asphalt and concrete vs aspect angle at frequencies of 40-90 GHz. Since the universal curve was derived from a one sq.m. flat plate illuminated by a uniform plane wave, the value for σ_0 calculated was adjusted to allow for the tapered illumination used. Using a mean dielectric constant of 5 to compute the reflection coefficients[3], the results all fall within the 10-db range of measured data and within 3 db of the mid-value (± 2 db typical).

LASER SCATTERING: Since the technique is independent of frequency, it should also apply to scattering of laser beams, provided the conditions remain the same. The major differences are that at laser frequencies, there is a significant Lambertian (diffuse) scattering component due to microscopic surface roughness and materials are quite often lossy. Beard, Maxwell and Ulrich[4] have made extensive measurements of the bidirectional reflectance at laser frequencies. For three dissimilar targets - sandblasted galvanized steel, olive drab paint on aluminum and Oregon white oak - Lambertian and non-Lambertian reflection coefficients were chosen empirically to derive curves. Agreement with experimental curves was generally within 1 db for all materials.

PEBBLY OR CORRUGATED SURFACE SCATTERING: Many surfaces are "pebbly" and while being approximately lumpy planes, do not have some angular dispersion. A "new universal curve" can be created by combining universal curves at the statistical distribution of normals about the average normal. This method described above has been applied to a compound corrugated metal surface measured by Harry H. Porter to simulate

ocean waves[5]. First a "new universal curve" was made using the distribution of normals from the sine wave. Then this curve was used as the "universal curve" to generate the "final new universal curve", using the distribution of normals caused by the small trapezoidal corrugations (about 3 cm). Self-shadowing effects were considered by limiting the statistical distribution of normals to those on visible parts of surface. The agreement with experiment at both S and C bands is reasonably good (5 db) considering that the trapezoidal surface facets are narrower than a wavelength.

CONCLUSION: The techniques described above provide a quick way to approximate the average value scattering from pebbly or dielectric surfaces at laser, as well as radar frequencies.

ACKNOWLEDGEMENTS AND REFERENCES: Technical development in this paper was performed in conjunction with the DARPA Continuous Terminal Homing Program. The author wishes to thank Mark Rosen for his help in cataloging and analyzing the experimental data.

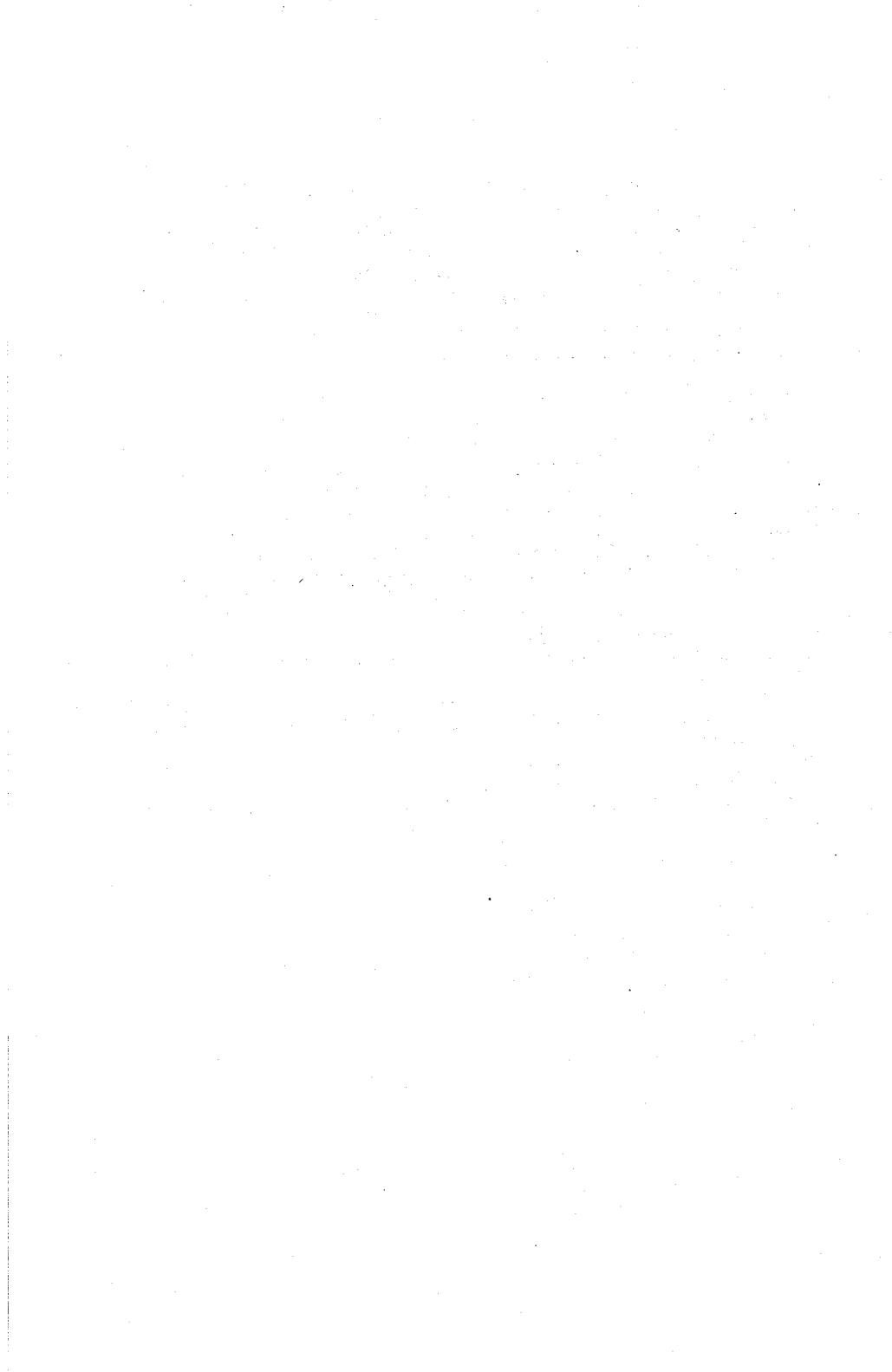
[1] Howell, N. A., "Calculating Average Radar Cross Sections of Flat Plates and Lumpy Flat Plates", 1977 IEEE-GAP Symposium Digest.

[2] Hayes, R. D. and Dyer, F. B., "Land Clutter Characteristics for Computer Modeling of Fire Control Radar Systems", AD912490, Georgia Institute of Technology, May 1973.

[3] Porter, R.A., Radiometric Technology, Inc., Wakefield, Mass., private communication, 1977.

[4] Beard, J. L., Maxwell, J. R. and Ulrich, J. P., Target Signature Analysis Center Data Compilation, 11th Supplement, Vol II, Bidirectional Reflectance, 1972.

[5] Porter, H. H., "A Modified Moment Method Calculation of the Electromagnetic Field Scattered by a Cylindrical Period Surface", Ohio State University Electrosciences Lab Report 4428-1, Dec. 1976.



INDEX

Agrawal, A. K.	61
Agy, V.	83
Ahn, A.	32
Alexander, J. K.	127, 128
Alexopoulos, N. G.	45, 88
Allen, K. C.	112
Altman, F.	100
Altshuler, E. E.	113
Annan, A. P.	114
Arnold, H. W.	110
Atlas, D.	58
Bahar, E.	2, 78
Balanis, C. A.	117
Baker, D. J.	101
Barber, P. W.	45
Barcilon, V.	33
Barrick, D. E.	40, 41
Barry, J.	11
Basili, P.	137
Bennett, C. L.	29
Bennett, J. A.	79
Benson, R. F.	125
Bergmann, H. J.	109
Berntsen, S.	8
Besieris, I. M.	76
Bibl, K.	103
Blaker, H.	34
Blejer, J.	23
Bloch, S. C.	111, 122
Boerner, W. M.	20, 29
Bojarski, N. N.	27
Bostian, C. W.	72, 100, 113, 130
Bowers, L. Q.	1
Boyne, H. A.	119
Brandinger, P.	97
Bringi, V. N.	5, 73
Brittingham, J. N.	24, 25, 47
Brown, W. D.	107
Buchau, J.	103
Burdette, E. C.	94
Burke, H. K.	132
Burton, R. W.	138
Bush, G.	56
Butler, C. M.	21, 65
Cabayan, H. S.	47
Carver, K. R.	118, 135
Castillo, J. P.	62
Castle, R. E.	100
Chang, D. C.	64, 66, 89
Chang, D. C. D.	123

Chang, A. T.	119
Chang, S. K.	60
Chaudhuri, S. K.	95
Chen, C.-L.	91
Cheng, D. K.	72
Chow, Y. L.	95
Ciotti, P.	137
Coffey, E. L.	31
Colak, S.	49
Cook, R. B.	26
Cox, D. C.	110
Crane, R. K.	98, 132
Crow, T. T.	12
Das, Y.	29
Davis, J. L.	114
Davis, W. A.	70
Davidson, D.	111
Deadrack, F. J.	14, 47
Devieux, C., Jr.	50
Derr, V. E.	140
DeHass, T.	34
Djermakoye, D.	116
Dougherty, H. T.	34
Dudzinsky, J.	99
Durney, C. H.	7
Dyer, F. B.	42
Dyson, P. L.	79
Eaton, E. L.	34
Ebert, W. L.	56
Eckerman, J.	58
Ekelman, E. P., Jr.	22
Ellerbruch, D. A.	119
English, W. J.	69
Evans, C.	80
Ewell, G. W.	145
Fairfield, D. H.	128
Fang, D. J.	142
Fengler, C.	144
Ferraro, A. J.	81
Fikioris, J. G.	88
Flower, D. A.	55
Follin, J. W., Jr.	18
Foner, S. N.	56
Fosque, H.	34
Fowles, H. M.	61
Frey, F. L.	71
Fukunishi, H.	20
Fung, A. K.	75
Galindo-Israel, V.	92
Gandhi, O. P.	7

Gatley, C.	55
Goddard, W. R.	20
Goldfinger, A. D.	56
Goldhirsh, J.	108
Golliday, C. L., Jr.	53
Graf, K. A.	126
Gray, E. P.	18
Grubb, R. N.	102
Gruner, R. W.	71
Guiraud, F. O.	134
Guthart, H.	126
Hagg, E. L.	104
Hagmann, M. J.	7
Hall, F. F., Jr.	59
Harker, K. J.	126
Harrington, R. F.	44
Harris, J. M.	143, 111
Hart, R. W.	56
Helliwell, R. A.	123
Hendry, A.	133
Hodge, D. B.	130
Holmes, J. J.	117
Hong, S. T.	75
Horst, M. M.	42
Howell, N. A.	146
Hsu, J. P.	46
Huang, J.	145
Huang, Y.-N.	105
Huchital, G. S.	120
Huffaker, R. M.	59
Hung, R. J.	141
Hyde, G.	111
Ippolito, L. J.	129
Ishimaru, A.	74, 76
Jain, V. K.	31
Janes, H. B.	112
Jedlicka, R. P.	118
Jenkins, R. W.	104
Johnson, R. L.	19
Jones, N. G.	52
Jones, R. K.	6
Jones, W. L.	37
Jordan, A. K.	32
Kahn, W. K.	3
Kaiser, M. L.	127, 128
Katz, I.	56
Kauffman, S. R.	113, 130
Kazkaz, A.-G.	63
Keller, J. B.	85
Kelly, F. J.	54, 101

Sinha, A.	68
Smith, D.	112
Smith, G. S.	4, 5
Smith, R. E.	141
Solimini, D.	137
Solomon, D.	86
Spiegel, R. J.	115
Sreenivasiah, I.	76
Stafsudd, O. M.	45
Stone, W. R.	28
Sturdivant, V. R.	115
Stutzman, W. L.	113, 130, 131
Swift, C. T.	38
Tai, C. T.	10
Tan, H. S.	75
Tang, D. D.	111
Taylor, C. D.	12, 13
Taylor, C. E.	62
Telford, L. E.	113
Teng, C. S.	90
Tesche, F. M.	60
Theobald, D. M.	130
Thiele, G. A.	22
Thompson, M. C., Jr.	112
Tomko, A. A.	81
Towle, D. M.	106
Tremain, D. E.	126
Tsang, L.	116, 119
Tseng, F.-I.	72
Tseng, F. T.	111, 142
Tuley, M. T.	42
Überall, H.	54
Uliana, E. A.	39
Uslenghi, P. L. E.	63, 67
Utlaut, W. F.	34
Uzunoglu, N. K.	45, 88
Valenzuela, G. R.	36
Varadan, V. K.	73
Varadan, V. V.	73
Villaseca, E. H.	1
Walsh, E. J.	39, 40
Walton, E. K.	48
Wang, D. Y.	45
Weber, J.	85
Weeks, W. L.	91
Weiner, D. D.	31
Weppler, H. E.	34
Westwater, E. R.	136
Wiley, P. H.	113, 130
Wilton, D. R.	21

Woo, R.	77
Woodford, D. A.	20
Wright, J. W.	36, 37
Yang, F.-C.	77
Yeh, C.	49
Yoshimo, T.	20
Young, J. D.	48
Yu, K.	18
Zehner, S. P.	145
Zvyagintsev, A. A.	77

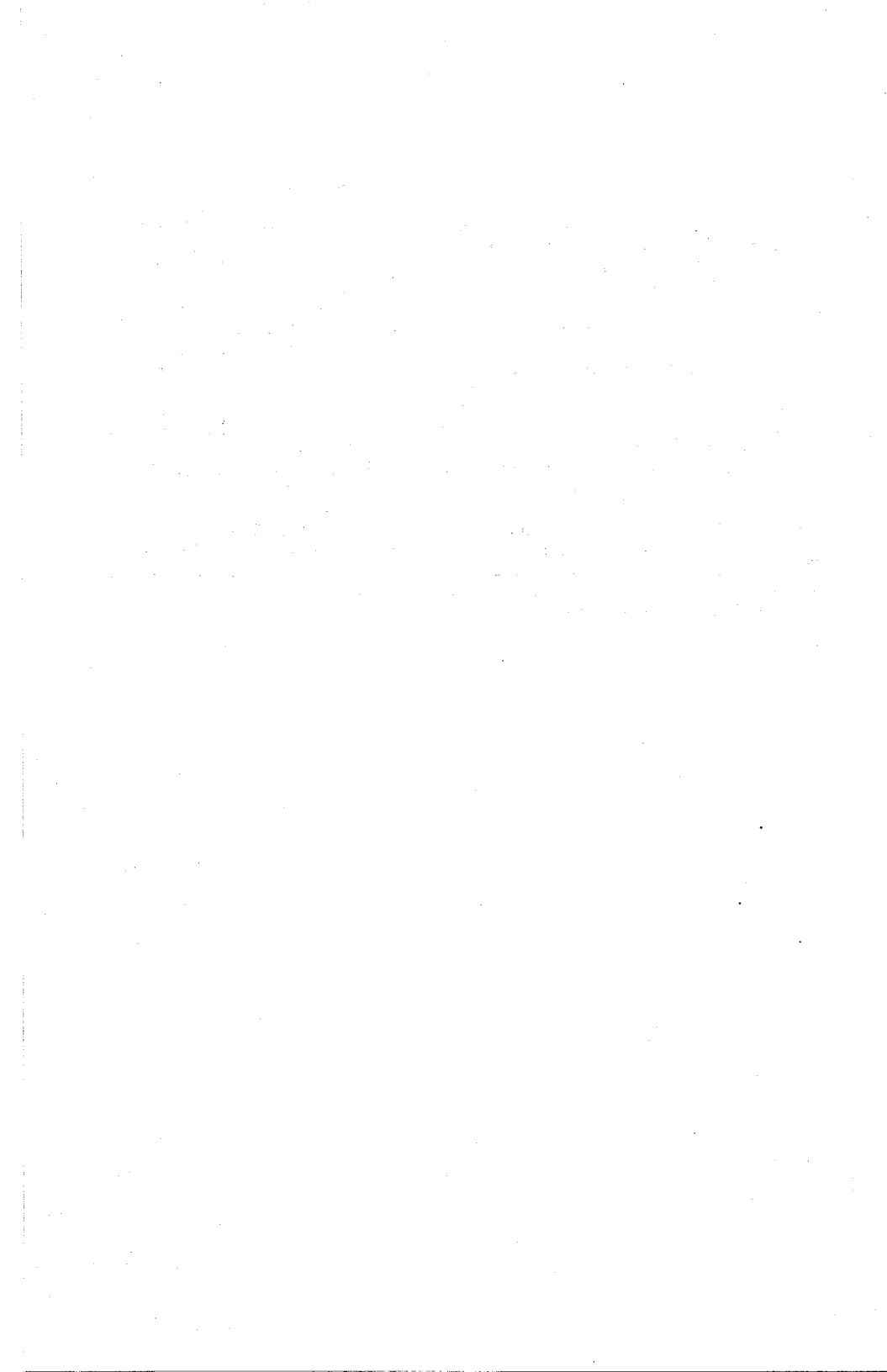
FUTURE MEETINGS SPONSORED BY USNC/URSI:

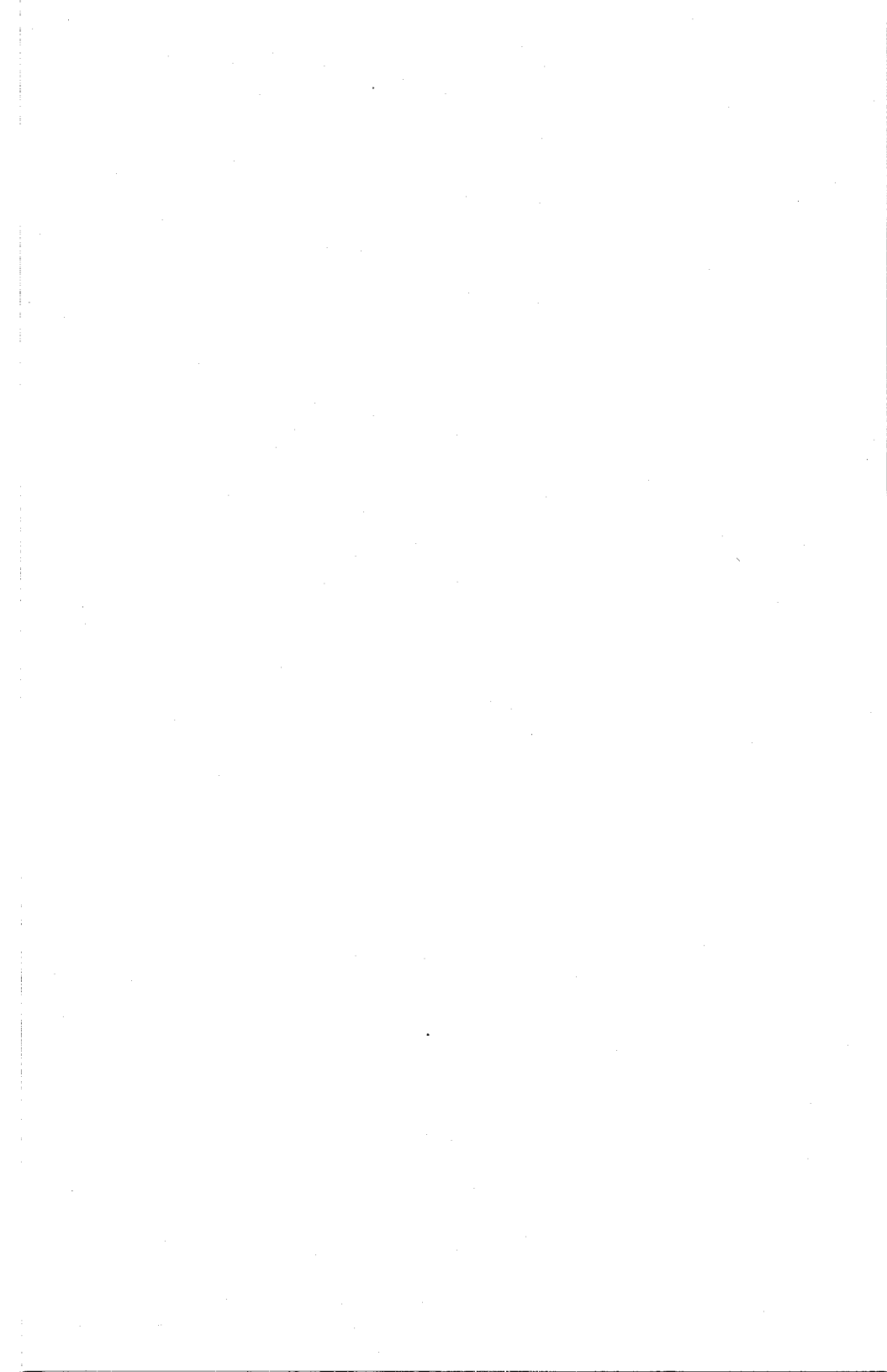
National Radio Science Meeting - Boulder, CO, 5-10 November 1978 in cooperation with various groups and societies of the IEEE (contact Prof. S. W. Maley - Electrical Engrg. Dept., University of Colorado, Boulder, CO 80309).

National Radio Science Meeting - Seattle, WA, 18-21 June 1979 to be held jointly with AP-S/IEEE (contact Prof. A. Ishimaru - Dept. of Electrical Engrg., FT-10, University of Washington, Seattle, WA 98195).

Canadian/American Radio Science Meeting - Quebec City, 2-6 June 1980 to be co-sponsored by CNC/URSI and held jointly with AP-S/IEEE (contact J. A. Cummins - Université Laval, Département de Génie Electrique, Faculté des Sciences et de Génie, Cité Universitaire, Québec G1K 7P4, Canada).

The USNC/URSI will also be sending a delegation to the URSI General Assembly to be held in Helsinki, Finland from 31 July to 10 August 1978. With the exception of business sessions, this will be an open meeting (contact C. M. Minnis - Secretary-General of URSI, Rue de Nieuwenhove 81, B-1180 Brussels, Belgium).





WEDNESDAY, 17 MAY

	<u>Room</u>
<u>0900-1200</u>	
Joint USNC/URSI - AP-S Plenary Session	1105
<u>1300-1700</u>	
B-7 Antennas	0109
F-4 Applications of Propagation Modeling for 20/30 GHz Systems Engineering	1109
G-2 Radio Propagation and Diagnostics	0123
<u>1700</u>	
Commission G Business Meeting	0123

THURSDAY, 18 MAY

<u>0830-1200</u>	
F-5 Propagation Experiments Using the 19 and 28 GHz Beacons on COMSTAR Satellites	1109
F-6 Remote Sensing of Earth's Surface and Subsurface	0109
H-1 Waves in Plasma	0123
<u>1330-1700</u>	
F-7 Propagation Effects in Communications	1109

FRIDAY, 19 MAY

<u>0830-1200</u>	
F-8 Radiometric Sensing	1109
F-9 Propagation and Scattering Applications (Joint with AP-S)	0109

